

FOSIL

DOE/PC/89785--T4
(DE95005936)

THE SINGLE ELECTRON TRANSFER CHEMISTRY OF COALS
Final Report

By
John W. Larsen
Robert A. Flowers II

Work Performed Under Contract No. FG22-89PC89785

For
U.S. Department of Energy
Pittsburgh Energy Technology Center
Pittsburgh, Pennsylvania

By
Lehigh University
Bethlehem, Pennsylvania

DISCLAIMER

This report was prepared as an account of work sponsored by an agency of the United States Government. Neither the United States Government nor any agency thereof, nor any of their employees, makes any warranty, express or implied, or assumes any legal liability or responsibility for the accuracy, completeness, or usefulness of any information, apparatus, product, or process disclosed, or represents that its use would not infringe privately owned rights. Reference herein to any specific commercial product, process, or service by trade name, trademark, manufacturer, or otherwise does not necessarily constitute or imply its endorsement, recommendation, or favoring by the United States Government or any agency thereof. The views and opinions of authors expressed herein do not necessarily state or reflect those of the United States Government or any agency thereof.

This report has been reproduced directly from the best available copy.

Available to DOE and DOE contractors from the Office of Scientific and Technical Information, P.O. Box 62, Oak Ridge, TN 37831; prices available from (615) 576-8401.

Available to the public from the U.S. Department of Commerce, Technology Administration, National Technical Information Service, Springfield, VA 22161, (703) 487-4650.

DISCLAIMER

Portions of this document may be illegible in electronic image products. Images are produced from the best available original document.

DE-FG22-89PC89785

The Single Electron Transfer Chemistry of Coals

Final Report

John W. Larsen and Robert A. Flowers II

Department of Chemistry
Lehigh University
6 E. Packer Avenue
Bethlehem, Pennsylvania 18015

Report of work on DE-FG22-89PC89785
Prepared for the United States Department of Energy

*Book 77
Sheet 1*

TABLE OF CONTENTS

CHAPTER	PAGE
Abstract	1
I. INTRODUCTION	3
Part I. The Reactivity of Native Radicals in Argonne Premium coals.	9
II. BACKGROUND	10
III. EXPERIMENTAL PROCEDURES.	23
A. Vapor Swelling of Argonne Premium Coal Samples With 4-Vinylpyridine.	23
B. Deposition of N,N'-diphenyl-p-phenylenediamine in Argonne Premium Coals.	25
C. DRIFT Determinations of 4-Vinylpyridine Swollen and Dried Coals.	26
D. EPR Determinations of 4-Vinylpyridine, and DPPD Treated Coals.	27
IV. RESULTS AND DISCUSSION	28
A. Determination of the Reactivity of Native Free Radicals in Argonne Premium Coals With 4-Vinylpyridine.	28
1. Gravimetric Vapor Swelling Measurements	29
2. Diffuse Reflectance FTIR (DRIFT) Spectroscopy.	34

CHAPTER	PAGE
IV. (Continued)	
3. Electron Paramagnetic Resonance Spectroscopy (EPR).	42
B. Determination of the Reactivity of Native Free Radicals In Argonne Premium Coals With N,N'-Diphenyl-p-phenylenediamine (DPPD).	47
1. Swelling of Argonne Premium Coals With DPPD.	47
2. Electron Paramagnetic Resonance Spectroscopy (EPR).	49
Part II. The Single Electron Donating Ability Of Coal and Its Relation to the Solid Structure of Coal.	53
V. BACKGROUND	54
VI. EXPERIMENTAL PROCEDURES.	69
A. Deposition of TCNQ and TCNE on Argonne Premium Coals.	69
B. Demineralization Procedure.	70
C. Preparation of Aromatic-TCNQ and TCNE Complexes.	71
D. DRIFT Determinations of Argonne Premium Coals Containing TCNQ and TCNE.	72

CHAPTER	PAGE
VI. (Continued)	
E. FTIR Measurements of Aromatic-TCNQ and TCNE Complexes in Solution.	72
F. FTIR Measurements of Aromatic-TCNQ and TCNE Complexes in the Solid State.	73
G. EPR Determinations of TCNQ and TCNE Treated Coals.	73
VII. RESULTS AND DISCUSSION	74
Characterization Of The Single Electron Donor Capability Of Coal.	75
A. Diffuse Reflectance Infrared Spectra of Whole Coals With TCNQ and TCNE.	76
B. Diffuse Reflectance Infrared Spectra of Pyridine Coal Residues and Extracts With TCNQ and TCNE.	103
C. Absorbance Infrared Spectra of Aromatic Compounds With TCNQ and TCNE in Solution and in the Solid State.	123
D. Electron Paramagnetic Resonance Spectra of Coals Containing TCNQ.	135
VIII. Summary and Conclusions.	149
LIST OF REFERENCES	152

List of Tables

TABLE		PAGE
I.	Weight Percent Elemental Analyses (dmmf) of Argonne Premium Coal Samples.	24
II.	Pyridine Extraction Data for Argonne Premium Coals.	31
III.	Gravimetric Swelling Factors of the Argonne Premium Coals and Biobeads With 4-vinylpyridine.	32
IV.	Retention of 4-vinylpyridine by Coals and Biobeads Heated to 100°C Under Vacuum.	33
V.	The Radical Densities (spins/gram) for the Pyridine Residues and the Residues Containing 4-vinylpyridine.	45
VI.	The Amount of Chlorobenzene Retained in 500 mg Argonne Coal Samples which were Swollen with 0.02 M DPPD in Chlorobenzene.	48
VII.	Comparison of the Radical Spin Densities of Pyridine Residues Before and After Treatment with DPPD.	50
VIII.	Bond Stretching Frequencies (cm^{-1}) for TCNE and its Radical Anion.	65
IX.	Percent Aromatic Carbon and Aromatic Carbons per Cluster Obtained by Pugmire and Coworkers.	90

TABLE	PAGE
X. Amount of Pyridine Contained (in grams and moles) in Argonne Premium Coals With a 100% Loading of TCNQ (based on PNA's) Compared to the Number of Moles of TCNQ	102
XI. Fractal Dimensionalities of Argonne Illinois #6 and Pittsburgh #8 Coals Compared to Their Pyridine Residues.	104
XII. Model Aromatic Compounds Complexed With TCNQ.	126
XIII. Model Aromatic Compounds Complexed With TCNE.	128
XIV. Electron Spin Concentrations of Solid TCNQ Complexes.	138
XV. EPR Spin Densities (Measured and Calculated) of Coals Containing TCNQ.	140

LIST OF FIGURES

FIGURE	PAGE
1. Shinn Model of Coal Structure.	6
2. A Schematic Reproduction of the EPR Absorption.	13
3. Functional Dependencies of the EPR g Values of Vitraains From Selected Coals.	16
4. Harrick Praying Mantis Accessory for Diffuse Reflectance Infrared Spectroscopy.	36
5. Absorbance Spectrum of 4-vinylpyridine.	38
6. DRIFT Spectrum of Poly(4-vinylpyridine).	39
7. Difference Spectrum of Illinois #6 Coal Containing 4-vinylpyridine - Illinois #6 Coal.	40
8. Difference Spectrum of Wyodak Coal Containing 4-vinylpyridine - Wyodak Coal.	41
9. (a) EPR Spectrum of Illinois #6 Pyridine Residue; (b) EPR Spectrum of Illinois #6 Containing 4-vinylpyridine.	43
10. (a) EPR Spectrum of Wyodak Subbituminous pyridine residue; (b) EPR Spectrum of the Same Coal Containing DPPD.	52
11. Orbital Energies and Transitions in a Charge- Transfer Complex Formed by Donor A and Acceptor B.	58

FIGURE	PAGE
12. Possible Shapes of Potential Wells for a One Dimensional Treatment of Donor-Acceptor Compounds.	59
13. Orbital (band) Diagram for Some Small Cyclic Compounds and a Large Ring.	62
14. Nitrile Stretching Frequency of TCNQ for 19 Salts.	63
15. (a) DRIFT Spectrum of TCNQ; (b) DRIFT Spectrum of TCNE.	78
16. (a) DRIFT Spectrum of Illinois #6 Coal; (b) DRIFT Spectrum of Illinois #6 Coal Containing 20 mg of TCNQ/gram of Coal.	79
17. (a) DRIFT Spectrum of Beulah-Zap Lignite; (b) DRIFT Spectrum of Beulah-Zap Lignite Containing 20 mg of TCNQ/gram of Coal.	81
18. (a) DRIFT Spectrum of Wyodak Coal; (b) DRIFT Spectrum of Wyodak Coal Containing 20 mg of TCNQ/gram of Coal.	82
19. (a) DRIFT Spectrum of Blind Canyon Coal; (b) DRIFT Spectrum of Blind Canyon Coal Containing 20 mg of TCNQ/gram of Coal.	83
20. (a) DRIFT Spectrum of Pittsburgh #8 Coal; (b) DRIFT Spectrum of Pittsburgh #8 Coal Containing 20 mg of TCNQ/gram of Coal.	84

FIGURE	PAGE
21. (a) DRIFT Spectrum of Lewiston-Stockton Coal; (b) DRIFT Spectrum of Lewiston-Stockton Coal Containing 20 mg of TCNQ/gram of Coal.	85
22. (a) DRIFT Spectrum of Upper Freeport Coal; (b) DRIFT Spectrum of Upper Freeport Coal Containing 20 mg of TCNQ/gram of Coal.	86
23. DRIFT Spectrum of a Demineralized Pittsburgh #8 Coal Containing 20 mg of TCNQ/gram of Coal.	87
24. DRIFT Spectrum of Illinois #6 Coal Containing 20 mg of TCNE/gram of Coal.	88
25. DRIFT Spectrum of Beulah-Zap Lignite Containing 100 mg of TCNQ/gram of Coal.	91
26. (a) DRIFT Spectrum of Illinois #6 Coal With a 100% Loading of TCNQ (based on PNA's); (b) DRIFT Spectrum of Illinois #6 Coal With a 100% Loading of TCNE (based on PNA's).	93
27. (a) DRIFT Spectrum of Beulah-Zap Lignite With a 100% Loading of TCNQ (based on PNA's); (b) DRIFT Spectrum of Beulah-Zap Lignite With a 100% Loading of TCNE (based on PNA's).	94
28. (a) DRIFT Spectrum of Pittsburgh #8 Coal With a 100% Loading of TCNQ (based on PNA's); (b) DRIFT Spectrum of Pittsburgh #8 Coal With a 100% Loading of TCNE (based on PNA's).	95

FIGURE	PAGE
29. (a) DRIFT Spectrum of Lewiston-Stockton Coal With a 100% Loading of TCNQ (based on PNA's); (b) DRIFT Spectrum of Lewiston-Stockton Coal With a 100% Loading of TCNE (based on PNA's).	96
30. (a) DRIFT Spectrum of Upper Freeport Coal With a 100% Loading of TCNQ (based on PNA's); (b) DRIFT Spectrum of Upper Freeport Coal With a 100% Loading of TCNE (based on PNA's).	98
31. (a) DRIFT Spectrum of Pocahontas #3 Coal With a 100% Loading of TCNQ (based on PNA's); (b) DRIFT Spectrum of Pocahontas #3 Coal With a 100% Loading of TCNE (based on PNA's).	99
32. Differential Scanning Calorimetry (dsc) Thermogram Comparing the Heat Capacity (Cp) of Pittsburgh #8 Coal and a Pittsburgh #8 Pyridine Residue.	106
33. DRIFT Spectrum of an Illinois #6 Pyridine Residue With a 10% Loading of TCNQ (based on PNA's).	108
34. DRIFT Spectrum of an Illinois #6 Pyridine Residue With a 50% Loading of TCNQ (based on PNA's).	109
35. DRIFT Spectrum of an Illinois #6 Pyridine Residue With a 100% Loading of TCNQ (based on PNA's).	110
36. DRIFT Spectrum of an Illinois #6 Pyridine Extract With a 50% Loading of TCNQ (based on PNA's)	111

FIGURE	PAGE
37. DRIFT Spectrum of an Illinois #6 Pyridine Extract With a 100% Loading of TCNQ (based on PNA's).	112
38. DRIFT Spectrum of an Illinois #6 Pyridine Residue With a 10% Loading of TCNE (based on PNA's).	114
39. DRIFT Spectrum of an Illinois #6 Pyridine Residue With a 50% Loading of TCNE (based on PNA's).	115
40. DRIFT Spectrum of an Illinois #6 Pyridine Residue With a 100% Loading of TCNE (based on PNA's).	116
41. DRIFT Spectrum of an Illinois #6 Pyridine Extract With a 10% Loading of TCNE (based on PNA's).	117
42. DRIFT Spectrum of an Illinois #6 Pyridine Extract With a 50% Loading of TCNE (based on PNA's).	118
43. DRIFT Spectrum of an Illinois #6 Pyridine Extract With a 100% Loading of TCNE (based on PNA's).	119
44. DRIFT Spectrum of a Pittsburgh #8 Pyridine Extract With a 50% Loading of TCNQ (based on PNA's).	120
45. DRIFT Spectrum of a Pittsburgh #8 Pyridine Extract With a 50% Loading of TCNE (based on PNA's).	121
46. Solid State FTIR Absorbance Spectrum of a 1-1 Complex of Fluoranthene and TCNQ.	130
47. ^1H NMR Spectrum of the Reaction Product of 9- Methylantracene and TCNE.	132

FIGURE	PAGE
48. (a) DRIFT Spectrum of 2,3-Dihydroxynaphthalene; (b) DRIFT Spectrum of the 1-1 Complex of 2,3-Dihydroxynaphthalene and TCNE.	133
49. EPR Spectrum of Beulah-Zap Lignite.	143
50. EPR Spectrum of Beulah-Zap Lignite Containing a 3% Loading of TCNQ (based on PNA's).	144
51. EPR Spectrum of Beulah-Zap Lignite Containing a 20% Loading of TCNQ (based on PNA's).	145
52. EPR Spectrum of Beulah-Zap Lignite Containing a 100% Loading of TCNQ (based on PNA's).	146
53. EPR Spectrum of Lewiston-Stockton Coal Containing a 3% Loading of TCNQ (based on PNA's).	147
54. EPR Spectrum of Lewiston-Stockton Coal Containing a 100% Loading of TCNQ (based on PNA's).	148

*Beulah-Zap
Lignite*

Abstract

The solid residues from pyridine Soxhlet extractions of Pocahontas #3, Upper Freeport, Pittsburgh #8, Illinois #6 and Wyodak coals were exposed to 4-vinylpyridine vapors and swelled. All of the 4-vinylpyridine could not be removed under vacuum at 100°C. Diffuse reflectance FTIR demonstrates the presence of poly-(4-vinylpyridine) in the Illinois #6 and Wyodak coals. EPR spectra display the loss of inertinite radicals in Upper Freeport, Illinois #6 and Wyodak residues after exposure to 4-vinylpyridine. There is little change in the vitrinite radical density or environment. While the coincidence of inertinite radical disappearance and polymerization does not demonstrate the radicals caused polymerization, it is a reasonable supposition.

The molecule N,N'-Diphenyl-p-phenylene diamine (DPPD) reacts with carbon radicals to give hydrocarbons and an imine product. The solid residues from pyridine Soxhlet extractions of Pocahontas #3, Upper Freeport, Pittsburgh #8, Illinois #6 and Wyodak coals were exposed to DPPD dissolved in chlorobenzene. Diffuse reflectance FTIR failed to detect the imine product from radical reaction with DPPD. EPR spectra display the loss of inertinite radicals in Upper Freeport and Wyodak residues. This part

of the project was unsuccessful.

7,7,8,8-Tetracyanoquinodimethane (TCNQ) and Tetracyanoethylene (TCNE) were deposited into coals in pyridine. FTIR indicates complete conversion of TCNQ to a material with a singly occupied LUMO. In TCNE the LUMO is about 30% occupied. TCNQ and TCNE were deposited into the pyridine extracts and residues of Illinois #6 and Pittsburgh #8 coals. Only a small amount of the TCNQ and TCNE displayed nitrile shifts in the IR spectrum of a material with an occupied LUMO. Studies on model PNA's showed that individual molecules will not form the TCNQ radical anion. EPR radical population studies on coals containing TCNQ were inconsistent with a high population of the TCNQ radical anion.

It has been concluded that TCNQ must be part of the aromatic stacks in coal and the TCNQ LUMO is part of an extended band. Furthermore, this behavior is a bulk property of the coal dependent on its solid structure which cannot be modelled using individual molecules.

Chapter I

Introduction

Coal is a widespread and widely differing heterogeneous material that contains both organic and mineral matter. The mineral matter occurs as discrete mineral species and mineral phases of various particle sizes. A small amount of the mineral matter in coal is complexed to organic functionalities such as carboxylates and porphyrins. The organic portion of coal is derived from plant materials and is mainly composed of polymeric aromatic species whose structures are variable and non-repetitive.¹

Coal originates from decomposed plant material. Through a series of complex chemical reactions humic acid is initially formed. Under the appropriate geological conditions the humic acid is subsequently converted into peat, lignite, subbituminous coal, bituminous coal and anthracite. During this evolutionary process, carbon content increases and oxygen and hydrogen contents decrease. This process is known as coalification.

Coals consist of microscopic organic substituents called macerals. The macerals form the combustible part of coal and are classified by an international system which is described in van Krevelen's book "Coal"². There are a number of macerals in coal and they can be separated

into three main categories: Vitrinites, Liptinites and Inertinites. These macerals differ in origin and composition. Vitrinites are derived from plant cell wall material and make up 50-90% of most North American coals. Liptinites are derived from the waxy part of plants and make up 5-15% of most North American coals. Inertinites are derived from degraded plant tissue and comprise 5-40% of North American coals.³

Various types of functional groups have been identified in coal through IR spectroscopy, NMR and chromatographic analysis of coal derived liquids. Oxygen occurs mostly as phenolic groups or ether groups. Some ketones and aldehydic carbonyls have been observed.⁴ Oxygen is also present to a lesser amount in the form of carboxylic acids and esters. Nitrogen occurs as a part of heterocyclic rings and sulfur appears in forms similar to oxygen.^{5,6,7,8,9}

On a molecular level coal is generally believed to be a three dimensionally crosslinked network^{10,11,12,13} which contains extractable materials which are non-covalently bound to the network. The network is also bound to itself through non-covalent bonds. An important feature of the three dimensionally crosslinked network is the presence of hydrogen bonds that act to link topologically distant but spatially close segments of the network chains. Because

of the presence of aromatic and polar functional groups in coal, dispersion, dipole-dipole, and dipole-induced-dipole forces may also contribute to noncovalent binding in the coal network. Figure 1 contains a molecular picture of coal proposed by Shinn¹⁴. This structure is not meant to specify a particular coal molecule, but to give a feeling for the different types of molecular units and linkages found in coals.

Coal is known to contain free radicals. The radicals are mainly associated with the organic phase in coal.¹⁵ The radical intensities observed by EPR are related to the radical densities. The radical densities in coal display a near exponential increase of free radical concentration with increasing carbon content up to 94% carbon.^{1,16,17,18,19} It is assumed that these radicals arise from chemical reactions or degradations and are stabilized by resonance in the aromatic system in coal.

Coal is the most abundant fossil fuel in the United States²⁰ and is a relatively cheap source of energy. Presently, the United States derives most of its energy from petroleum and natural gas. In the future, recovery of these fluid fuels will become more difficult and eventually their supplies will be exhausted. Coal offers an alternative source of energy.

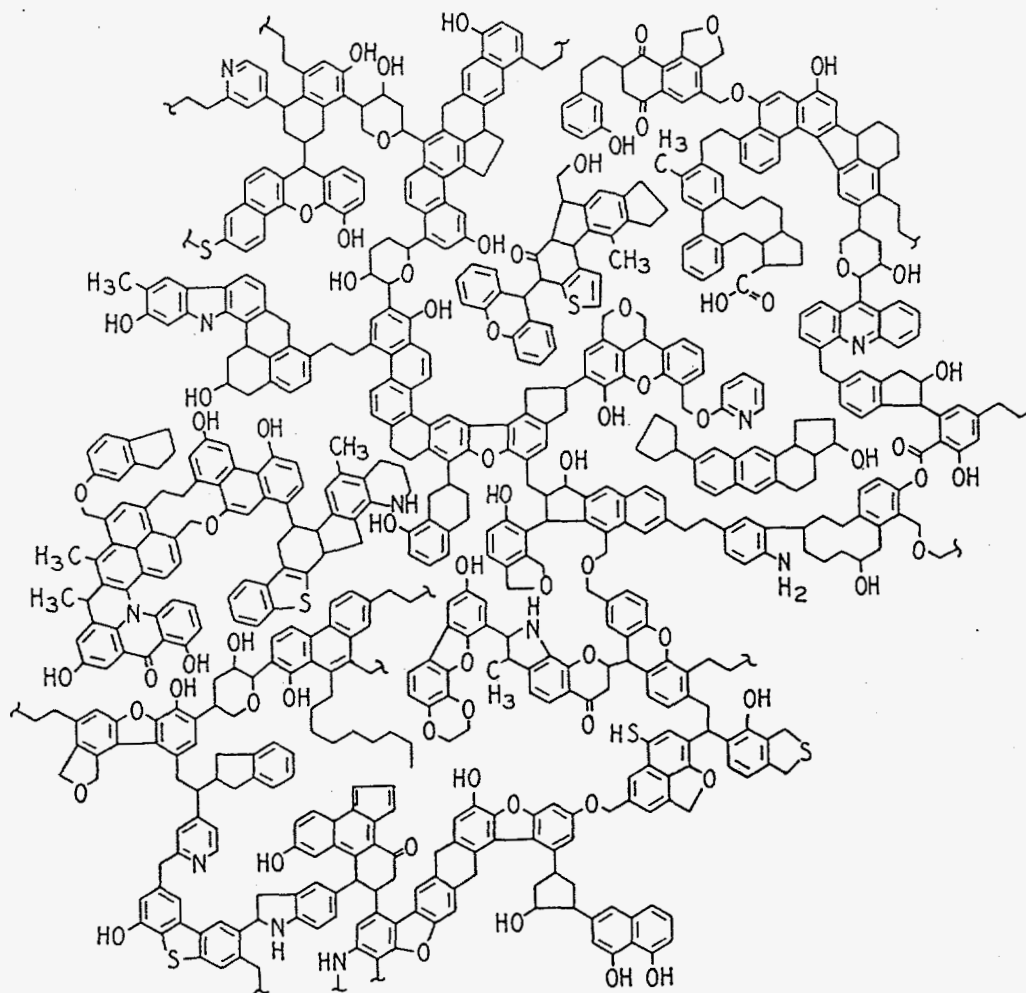


Figure 1. Shinn Model of Coal Structure.

* Shinn, J.H., *Fuel*, 1984, 63, 1187.

A major focus of the DOE and other governmental agencies is the development of efficient coal conversion processes. Many of these processes are difficult to optimize because the physical and chemical nature of coal is not fully understood. It is known that coal is much more reactive than is predicted by current structures.^{14, 21} Either the structures are wrong or unsuspected reaction pathways are occurring.

This dissertation addresses the fundamental question of the single electron donor properties of coal. One aspect of this chemistry is the ability of coals to initiate chemical reactions using the unshared electrons from its naturally occurring radicals. The consequences of the radicals in coal serving as initiators in chemical reactions is easy to visualize. The unpaired spins in coal may play a significant role in initiating chain reactions which occur during coal conversion. With this in mind it is necessary to characterize the number and, if possible, the type of reactive radicals in coal.

Another perhaps more important aspect of this chemistry is the ability of coals to donate an electron in a charge transfer process producing a radical cation in the donor and a radical anion in the acceptor. It is well known that the formation of a charge transfer complex is the first step in a wide variety of organic reactions,²²

especially those involving aromatic systems as donors.

23,24 Coal is known to contain many substituted aromatics. It is possible that the aromatics in coal form complexes which undergo single electron transfer reactions. An understanding of these single electron processes may enable coal scientists to optimize conversion processes making them more cost efficient.

Part I

The Reactivity of Native Radicals in Argonne Premium
Coals.

Chapter II

Background

Since the independent discovery of free radicals in coal by Uebersfeld²⁵ and Ingram²⁶ in 1954, radicals in coal and coal components have been receiving much attention in an attempt to understand both their structure and their role in the chemical processes that take place during coal conversion. Radicals are also a very important analytical probe because they can provide information on some of the chemical species in coal.^{27,28}

Electron Paramagnetic resonance (EPR) and electron nuclear double resonance (ENDOR) spectrometries are the most frequently applied techniques to elucidate the nature of free radicals in coal and its components. The ENDOR technique is becoming increasingly popular in free radical studies because the resulting spectra are generally highly resolved as compared to EPR spectra.²⁹

The discovery of free radicals led directly to the question of the origin of free radicals in coal. Retcofsky et al³⁰ examined various coal and ash samples employing EPR. They found that the main contribution to the spin density in coal came from the organic matter.³¹ ENDOR was also employed to study the coal and ash signals. The paramagnetic species were again shown to be organic in nature.³² The possibility of charge transfer

interactions, especially in the case of coal^{33,34} and petroleum-derived asphaltenes^{35a,b} was considered. The role of charge-transfer complexes in coal derived asphaltenes is minor.³¹ Free radicals exhibit EPR intensities that obey Curie law ($I=CT^{-1}$) while unshared electrons produced via charge transfer do not. Retcofsky studied the vitrains from nine coals studying their EPR intensities and found that they exhibit Curie Law down to liquid Helium temperatures.³⁶

There are a variety of factors which influence the stability of radicals. Aliphatic radicals are energetic and highly reactive. A radical on a large aromatic ring system is stabilized to some extent and would be expected to be less reactive. Thermal and chemical stabilities of organic free radicals are governed by two main factors: resonance and steric hindrance.³⁷ Radicals may be stable in coals for two similar reasons: 1) They may lack the molecular mobility which allow their recombination, or, 2) they are delocalized to an extent which makes them inherently stable. Work in our laboratory with rearranged coals suggest that the radical stability is due to delocalization.³⁸

The EPR spectrum contains a number of pieces of information which give insight about the environment of the radicals in coal. This information is the width and

shape of, the g value, and the intensity of the absorption lines in the EPR spectrum.

The intensity of the EPR signal is related to the number of unpaired spins which is referred to as the radical density. Computer programs are available which compare the intensity of the signal obtained experimentally with that of a standard with a known spin density. The intensity of the experimentally obtained EPR absorption is then integrated to give a radical density value with an accuracy of $\pm 5-10\%$.

The width and shape of the EPR spectrum contain information about the environment of the free radical. Isolated electrons localized on a single structural unit display a well resolved EPR spectrum consisting of a number of absorption lines which are due to spin orbital interactions.³⁹ The complex nature of coal results in an EPR spectra displaying a single symmetrical resonance near $g=2$. Spectral fine structure is never seen in the EPR spectrum of coal.⁴⁰ Spectral line widths (ΔH_{pp}), measured from peak to peak on the derivative of the EPR absorption curve can vary from a few tenths of a gauss to nearly 100 gauss depending on the rank of the coal.^{2,41,42} A typical EPR absorption is displayed in Figure 2. Normally, the EPR spectral line width is approximately 7 gauss.⁴³

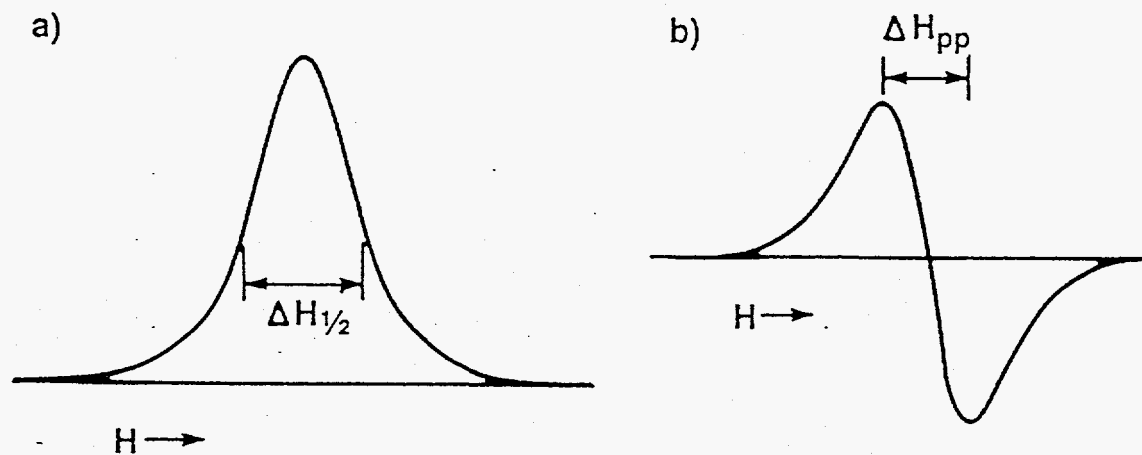


Figure 2. A schematic reproduction of the EPR absorption (a) and its derivative (b) with a definition of the quantity ΔH_{pp} .

Source: Silbernagel, B.G.; Gebhard, L.A.; Dyrkacz, G.R.; Bloomquist, C.A.A. In "Chemistry and Characterization of Coal Macerals," ACS Symp. Ser., 1984, 252, 121.

Interactions including spin orbital coupling or dipolar interactions between magnetic spins of electrons, can contribute to the linewidth increase. Electron motion or strong exchange coupling between electrons can narrow the EPR linewidth.

The g value is a unitless EPR spectral parameter that is obtained from the relationship

$$h\nu_0 = g\beta H_0 \quad (1)$$

In equation (1), h is Planck's constant, ν is the resonance frequency, β is the Bohr magneton and H is the external magnetic field. Typically g values of organic free radicals differ only slightly from the value of the free electron $g_e = 2.00232$. Careful experimental work can measure g values to ± 0.000005 .⁴⁴ Small variations in g values can give great insight into the molecular environment of an unpaired electron.

Yen and Sprang discovered that the g values of coals displayed a systematic trend with heteroatom content.⁴⁵ The relationship between the g value of coals and coal rank is reasonably well understood. The high g values observed for peats and lignites can be interpreted in terms of the presence of aromatic radicals, with some localization of the unpaired spins on heteroatoms, generally oxygen.

Coalification decreases g values suggesting the

radicals become more hydrocarbon-like. The g values of many vitrains from bituminous and young anthracite coals compare favorably with those exhibited by aromatic hydrocarbon radicals.³⁰

Anthracites and Meta anthracites display large g values. This is due to the large condensed graphite-like aromatic structures present in the high rank coals. Retcofsky³¹ noted that there is a small but reproducible anisotropy in the g values of some anthracites with respect to the bedding plane of the coal. This observation suggests that ordering of the polynuclear condensed aromatic rings is occurring.

Support for the relationship between heteroatoms and g values is depicted in figure 3. The plots for g values vs. oxygen content of coals implies that the radicals in low rank coals interact with oxygen in the sample. Statistical treatment of the data revealed that the g values of two coals fall outside of the dashed lines in the first plot in figure 2. These coals are unique in the fact that they contain a high content of aromatic sulfur.^{33,46} The second plot in figure 3 has the sulfur content factored in weighted by its spin orbital coupling constant. This displays the fact that radicals in coal interact with sulfur as well as oxygen. Silbernagel et al. have shown that the g value of liptinite radicals vary

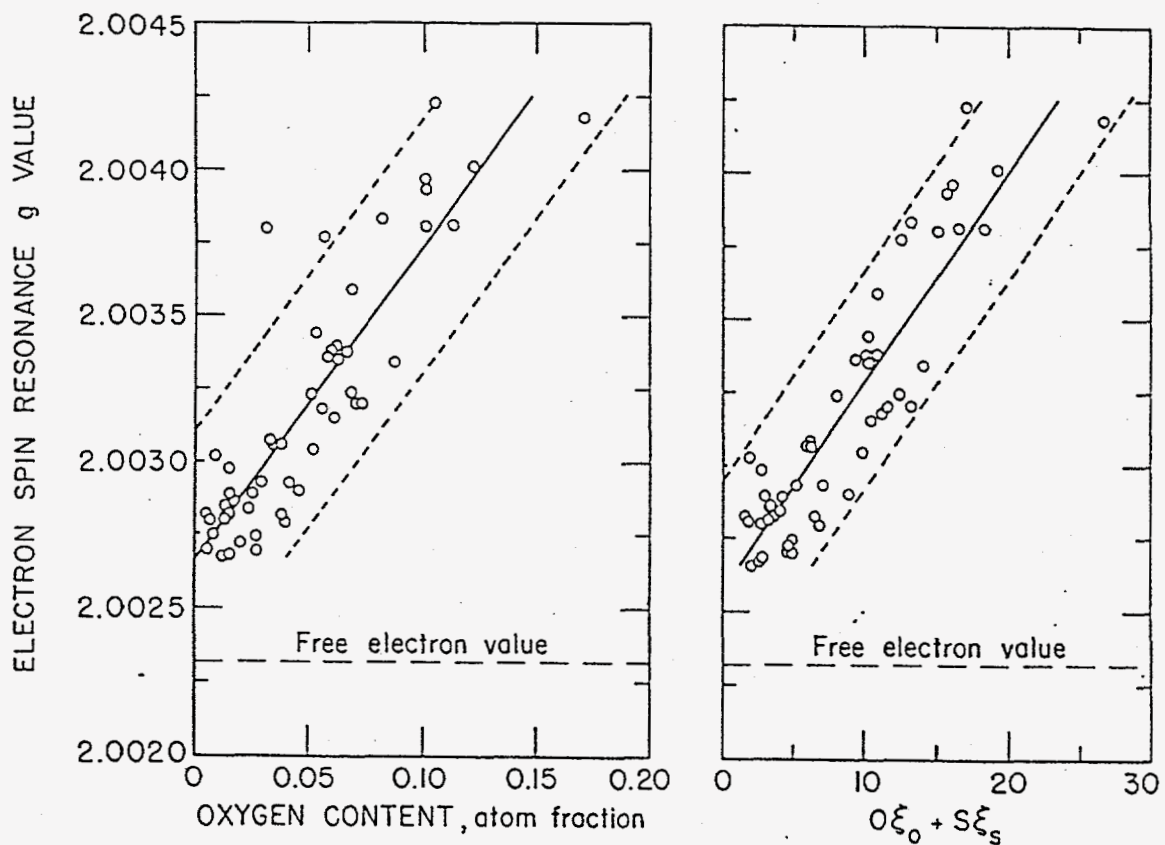


Figure 3. Functional dependencies of the EPR g values of vitrains from selected coals

Source: Retcofsky, H.L. in "Coal Science, vol. 1" (eds. Gorbaty, M.L.; Larsen, J.W.; Wender, I.) Academic Press, New York, 1983, p. 50.

with nitrogen content implying that nitrogen also interacts with the unpaired spins in coal.⁴³

The chemical heterogeneity of coal hampers the determination of g values and electron densities for the various macerals in coal. With the evolution of maceral separation techniques,⁴⁷ EPR observations were made on the different maceral groups contained within coal.⁴³

Vitrinite radicals in subbituminous and high volatile bituminous coals are associated with oxygen while higher rank vitrinites have g values associated with aromatic radicals.⁴⁸ Vitrinite radical densities increase with coal rank. The vitrinites tend to follow trends in g values and radical densities that correspond to the extent of coalification. For this reason, vitrinites are the most thoroughly studied and understood of the maceral groups.

Unlike vitrinites, inertinites are not well understood. Inertinites are believed to have undergone rapid metamorphism with little or no changes occurring after the peat or lignite stages of coalification.⁴⁹ Retcofsky, however, suggests that inertinite metamorphism may continue into the bituminous stages of coalification.³¹ Work done by Terres et al.⁵⁰ suggest that inertinites were formed in forest fires or some other thermal process.

Inertinite radicals have uniform g values that suggest aromatic structure. Inertinites also have the highest radical concentrations of all of the macerals. The linewidth of inertinites is narrow (1-2 Gauss). The narrow linewidth is probably due to the delocalization of the unpaired spins on the fused aromatic ring system.

Free radicals are assumed to play an important role in the conversion of coal, oil shale and heavy crude oils to lighter products. For this reason, EPR and recently ENDOR spectroscopies have been used to study the reactivity of unpaired spins in fuel conversion processes. In 1959 Smidt and van Krevelen¹⁷ reported the first study of heat treated vitrains. They found that the number of free radicals remains constant till about 300 °C. Beyond 400 °C a sharp increase in the spin density occurs, followed by a decrease of the spin density between 500 to 600 °C. The increase in spin density at 400 °C is due to bond breaking. The coal probably softens enough above 500 °C to allow recombination or polymerization of the radicals formed by the thermal process.

Petrakis and Grandy repeated Smidt and van Krevelen's study with the exception that they used ground coals instead of vitrains. They also used a specially designed EPR vessel⁵¹ which allowed EPR studies under liquefaction conditions. Their spin density measurements agreed well

with van Krevelen's work but provided more detail concerning g values and linewidth measurements. The g values of Pocahontas #3 and Illinois #6 coal were found to decrease slightly from 2.0029 to 2.0027 indicating a minor change in radical structure. Wyodak subbituminous coal displayed a decrease from 2.0037 to 2.0027 in the g value. This is due to the loss of heteroatoms from the coal during heat treatment. The linewidth of the coals studied displayed a decrease beginning at 400 °C, followed by an increase in linewidth at higher temperatures. The minimum linewidth obtained upon heat treatment was found to be rank dependent.

Petrakis and Grandy systematically studied the dependence of free radical concentration and other EPR spectral parameters of radicals upon coal rank, maceral content, treatment temperature, heating rates and various solvents in order to understand the role of free radicals in coal pyrolysis and liquefaction.⁵² Maceral content is of concern here. It was found that the initial concentrations of free radicals from the various macerals vary by 5 orders of magnitude. Inertinites have the highest radical concentration and are the least reactive. The radical density of vitrinites increases above 400°C, approaching the spin concentration of inertinites. Liptinites show little dependence with temperature but the

g value changes upon heating suggesting chemical reaction.

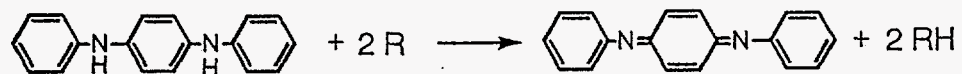
The fundamental question of the reactivity of native free radicals remained unanswered until recently. The question was addressed in a study by Stock et al.⁵³ These experiments were directed toward the development of a convenient method to decrease the free radical concentration in coal thereby enhancing the %C observed in ^{13}C NMR. Stock found that Samarium(II) Iodide was a favorable reducing agent. The reagent can easily be prepared in THF and diffuses into swollen coal. The untreated coals in this study contained about 1 spin/8750 carbon atoms. The reduced coal contained approximately 1 spin/35000 carbon atoms. It should be noted that there was no change in the %C or the hydrogen to carbon ratio of the coal. There is one possible problem with this study. Samarium (II)Iodide is converted to Samarium (III) in a reduction reaction. Samarium (III) contains an unpaired spin. Work in this group in collaboration with Exxon has shown that metals with unpaired spins can interact with carbon spins in coal making them unobservable in the EPR spectrum.⁵⁴

Our approach is fundamentally different from Stock's in that we use the radicals in coal to initiate a chemical reaction. A styrene analog, 4-vinylpyridine was chosen to determine whether the coal radicals initiate polymer-

ization. 4-vinylpyridine swells coals readily and does not undergo cationic polymerization. Typical recipes for bulk and emulsion polymerizations are available.⁵⁵ Free radical polymerization is typically complete in four hours. Conversion from monomer to polymer in coals would be controlled by diffusion into the network which would take a larger amount of time.⁵⁶ Diffuse reflectance infrared spectroscopy (DRIFT) was employed to detect the presence of poly(4-vinylpyridine) in the coals examined. EPR was used to characterize the types and numbers of radicals in the coals before and after 4-vinylpyridine treatment.

Polymerizations of styrene monomer have been carried out on the surface of carbon blacks. Carbon Blacks exhibit an EPR signal.^{57,58} and are capable of initiating or inhibiting free radical polymerization.^{59,60,61,62} An enormous amount of work was performed in this area to learn the mechanism by which polymer molecules become attached to the surface of carbon blacks. The polymerization of styrene in the presence of carbon blacks had no effect on the concentration of their radicals.

Another reaction carbon radicals undergo is hydrogen abstraction. The molecule N,N'-diphenyl-p-phenylenediamine (DPPD) reacts with carbon radicals to give hydrocarbons and the imine product shown on the next page.



DPPD and the polyaniline derived from it are antioxidants and their oxidation behavior has been well characterized.^{63,64,65,66} Typically, reactions of DPPD have been detected by ultraviolet absorption of the imine product. Coals are insoluble and coal dispersions scatter light making uv spectroscopy an ineffective tool for studying this system. We used EPR spectroscopy to characterize the radicals sufficiently reactive to abstract hydrogen from DPPD.

Chapter III

Experimental Procedures

Vapor swelling of Argonne Premium Coal Samples with 4-Vinylpyridine

The 4-Vinylpyridine used was distilled under vacuum (b.p. 54°C at 5mm Hg) from the purest grade monomer available from Aldrich (Milwaukee, WI). The 4-vinylpyridine collected by this method was stored under N₂ in a freezer at 0 °C. The coal samples were obtained from the Argonne National Laboratory Premium Coal Sample Bank and were stored under nitrogen. Table I contains the dry mineral matter free (dmmf) elemental analyses of the coals used.

Approximately 10g of each coal used was dried at 110 °C in a vacuum oven to constant weight. Each coal was individually placed in a dried and weighed thimble. The thimbles with coal were placed in a Soxhlet and extracted with 250 ml of pyridine until the pyridine in the Soxhlet remained clear for two days. The coal residue was dried to constant weight in a vacuum oven at 110 °C.

Each extracted coal was ground for three minutes in a Wig-L-Bug and approximately 500mg of each coal was weighed into a tared bottle and cap. The weighing bottles were placed into a vacuum dessicator with 10ml of 4-Vinylpyridine evacuated and backflushed with with dry

Table I

Weight Percent Elemental Analyses of (dmmf) Argonne
Premium Coal Samples

Coal	%C	%H	%N	%S	%O
Pocahontas #3	91.8	4.48	1.34	0.51	1.66
Upper Freeport	88.1	4.84	1.60	0.76	4.72
Lewiston-Stockton	85.5	5.44	1.61	0.67	6.68
Pittsburgh #8	85.0	5.43	1.68	0.91	6.90
Blind Canyon	81.3	5.81	1.59	0.37	10.9
Illinois #6	80.7	5.20	1.43	2.47	10.1
Wyodak-Anderson	76.0	5.42	1.13	0.48	16.9
Beulah-Zap	74.1	4.90	1.17	0.71	19.1

Source: Users Handbook For the Argonne Premium Coal
Samples

nitrogen three times. After 48 hours at room temperature the coals were removed from the dessicator. The coals were then dried to constant weight in a vacuum oven at room temperature. When the samples reached constant weight at room temperature the temperature was increased to 100 °C over one week. Most of the 4-vinylpyridine that evaporated from the coals was removed at room temperature. The coal samples were stored in a Vacuum Atmosphere drybox.

Deposition of N,N'-diphenyl-p-phenylenediamine (DPPD)
in Argonne Premium Coals

DPPD was used as received from Aldrich (Milwaukee, WI). Reagent grade Chlorobenzene obtained from Aldrich (Milwaukee, WI) was purged with dry nitrogen via a gas dispersion tube and sealed with a septum. 2.71 grams of DPPD was weighed into a volumetric flask and dissolved with 500 ml of Chlorobenzene. The solution was again purged under dry nitrogen employing a gas dispersion tube and sealed.

Pyridine residues obtained via soxhlet extraction of Argonne Premium coal samples were ground in a Wig-L-Bug for three minutes inside a Vacuum atmosphere drybox. Approximately 500 mg of each ground coal was weighed into a tared bottle and cap. The bottles containing the coal

were transferred to a vacuum desiccator under a dry nitrogen flow. Two ml of the 0.021 M DPPD solution in chlorobenzene was pipetted into each bottle. The desiccator was sealed under static nitrogen and the coals were allowed to swell for two week's time. The swollen coal samples were then transferred to a vacuum oven and dried to constant weight over one week's time by gradually increasing the temperature to 100 °C. After drying, the coals were weighed and stored in a Vacuum atmosphere drybox.

DRIFT determinations of 4-vinylpyridine swollen and dried coals

Diffuse reflectance infrared (DRIFT) spectra were obtained on a Mattson Sirius 100 Fourier transform infrared spectrometer equipped with Harrick optics and a sampling stage for diffuse reflectance. Spectra were recorded from the co-addition of 1000 scans of 9000 data points at 4 cm⁻¹ resolution against a background of KCl. A typical sample preparation involved seperately grinding 200 mg of coal and KCl in a Wig-L-Bug for three minutes, followed by co-grinding a 5% mixture of coal and KCl for an additional three minutes.⁶⁷

EPR determinations of 4-vinylpyridine, and DPPD, treated
coals

EPR measurements were obtained by Layce Gebhard and Bernie Silbernagel on a Bruker ER 300 Spectrometer operating at 9.8 GHz. Microwave frequencies were determined with an EIP Model 548 microwave frequency counter. The data were accumulated on a Bruker computer data system using the ESP 350 Data Acquisition Program. The carbon radicals were studied using a central field value of 3500 G, a field scan range of 50 G swept in a one minute scan time, and a microwave power of one μW . All spin density measurements were made relative to a Varian standard consisting of pitch in KCl. The pitch, a secondary standard, when compared with an NBS ruby standard, was found to represent a level of 3.67×10^{15} radicals in the spin cavity. A typical sample preparation involved weighing approximately 20 mg of coal into a 4mm o.d. spectroscopic quality quartz tube to a height of approximately 1 cm. The tube was then evacuated to 10^{-1} torr, backfilled with nitrogen, and sealed.

Chapter IV

Results and Discussion

The first part of this thesis is concerned with the reactivity of native free radicals in coal. The first section deals with the ability of radicals in coal to initiate the polymerization of a styrene analog, 4-vinylpyridine. 4-vinylpyridine swells coals readily and does not undergo cationic polymerization. The coals were swollen with 4-vinylpyridine vapor and dried. Diffuse reflectance FTIR was used to determine whether the retained 4-vinylpyridine had polymerized or if it was trapped in the coal network. EPR was used to determine what role coal radicals played in the polymerization process.

The second section contains a description of the use of N,N'-diphenyl-p-phenylenediamine (DPPD) to study the reactivity of radicals in coal. DPPD is an antioxidant that reacts with carbon radicals to convert them to hydrocarbons. If coal radicals are sufficiently reactive to abstract hydrogen from DPPD, the radical density of the coal will decrease. EPR was used to measure any decrease in radical density.

A. Determination of the Reactivity of Native Free Radicals in Argonne Premium Coals with 4-vinylpyridine

Gravimetric Vapor Swelling measurements

Vapor phase gravimetric swelling of Argonne Premium coal samples with 4-vinylpyridine were carried out on coals that had been exhaustively Soxhlet extracted with pyridine and biobeads (SX-4). The extraction data for the coals are contained in Table II. Biobeads were used as a control. The coals or biobeads were exposed to 4-vinylpyridine vapor in a vacuum dessicator until they reached constant weight. Constant weight was attained after 48 hours. Pre-extraction of the coals with pyridine was necessary for two reasons: 1) Extractable material present in the coals during swelling prevents equilibrium swelling from being reached in a finite amount of time⁶⁸; and, 2) The residue from an extracted coal gives a cleaner IR spectrum which is needed to determine whether polymerization of 4-vinylpyridine occurred. The swelling data are contained in Table III. The gravimetric swelling ratio (W_s) was determined on a dry coal basis by the equation shown below.

$$W_s = \frac{\text{weight swollen coal}}{\text{weight of dry coal}}$$

After the gravimetric swelling determinations, the

coals and biobead samples were dried in a vacuum oven for 48 hrs. The temperature was gradually increased to 100°C over one week. Essentially all of the 4-vinylpyridine that evaporated from the coals was removed at room temperature. The temperature was increased to 100 °C to try to remove all of the 4-vinylpyridine which may not have evaporated under vacuum at room temperature. The purpose of this drying was to determine how much 4-vinylpyridine was retained in the coals. If any polymerization had occurred, the polymer held in the coal network would remain while the volatile monomer would evaporate. If polymerization of the 4-vinylpyridine occurred by a mechanism other than coal radical initiation, a significant amount of 4-vinylpyridine would be left in the biobeads after drying. It is probable that not all of the 4-vinylpyridine would evaporate because it would be trapped in the coal network in a manner similar to pyridine.⁶⁹ Table IV displays the weight retention of 4-vinylpyridine in the coals and biobead samples. These data show that a significant amount of 4-vinylpyridine was retained in the coals while almost all of the 4-vinylpyridine was removed from the biobeads. DRIFT spectroscopy was used to distinguish between retention and polymerization of 4-vinylpyridine in the coal samples.

Table II
Pyridine Extraction Data for Argonne Premium Coals

<u>Coal</u>	<u>% Extractability</u> ^a
Wyodak Subbituminous	38.0
Illinois #6	31.8
Pittsburgh #8	43.6
Upper Freeport	36.8
Pocahontas #3	1.49

a) Based on weight of recovered residue.

$$\% \text{ extractability} = \frac{W_c - W_r}{W_c} \times 100.$$

Wc

Table III

Gravimetric Swelling Factors of the Argonne Premium
 Coals and biobeads with 4-vinylpyridine

<u>Coal</u>	<u>Swelling Factor</u> ^a
Wyodak Subbituminous	1.96
Illinois #6	1.89
Pittsburgh #8	1.55
Upper Freeport	1.72
Pocahontas #3	1.77
biobeads (#1)	2.71
biobeads (#2)	2.65

a) Gravimetric swelling factor = $\frac{\text{weight swollen coal}}{\text{weight of dry coal}}$

Table IV

Retention of 4-vinylpyridine by Coals and biobeads
Heated to 100°C Under Vacuum

<u>Coal</u>	Retention of 4-vinylpyridine (% of starting coal extraction <u>residue weight</u>)
Wyodak subbituminous	16.3
Illinois #6	19.4
Pittsburgh #8	9.6
Upper Freeport	13.2
Pocahontas #3	13.8
biobeads (#1)	0.27
biobeads (#2)	0.29

Diffuse Reflectance Infrared (DRIFT) Spectra

Diffuse reflectance infrared (DRIFT) spectroscopy is a relatively new type of infrared spectroscopy designed to obtain spectra from powdered samples or surfaces. DRIFT spectroscopy offers a number of advantages for IR coal studies compared to absorbance or transmittance IR spectroscopy. First, loose powders can be sampled without the need for pressing them into pellets. Second, a scattering sample is mandatory, therefore, spectra do not show an energy loss at high wavenumbers which is characteristic of transmittance spectra of samples that scatter light. Third, bulk samples mixed with a non-absorbing powder like KBr or KCl display a greater percentage absorption in diffuse reflectance spectra than if the same amount of sample was pressed in a disc. At low concentrations of finely ground (average particle diameter 10 μ m) sample in KBr or KCl, the true absorption spectrum of the sample is approached. Under these conditions most of the coal is sampled by the IR radiation and the resulting spectrum is that of the bulk coal, not the surface. ^{67,70}

DRIFT spectroscopy has a number of disadvantages. Diffuse reflectance may be low if a sample absorbs in certain spectral regions. In these regions bands may not be displayed. There is also a lack of reproducibility of

band intensities in DRIFT spectroscopy because of the variation of the scattering coefficient each time a sample is loaded into the cell. Complete subtraction of bands in the sample becomes very difficult. Recently Griffiths et al.⁷¹ designed a procedure for obtaining reproducible DRIFT spectra. This procedure appeared too late to be used in this study.

Early published coal IR absorbance spectra generally contained a low signal to noise ratio (SNR) because coal particles tend to scatter and absorb infrared light. DRIFT spectroscopy employing Harrick Praying Mantis optics allows high quality coal spectra to be obtained with good SNR. Figure 4 contains the Harrick Praying Mantis optics employed in our studies. The main advantage of this unit is that the input and output beams are not in the same plane, so the specularly reflected component of the light is discriminated against. The design in Figure 4 incorporates ellipsoidal focusing and collecting mirrors avoiding the need for a sphere with a diffusely reflecting surface.

Sample concentration in KCl and radiation intensity from scattered light are related by the Kubelka-Munk^{72,73} function shown below.

$$f(R) = (1 - R)^2 / 2R = k/s$$

R is the absolute reflectance of the sample, s is a

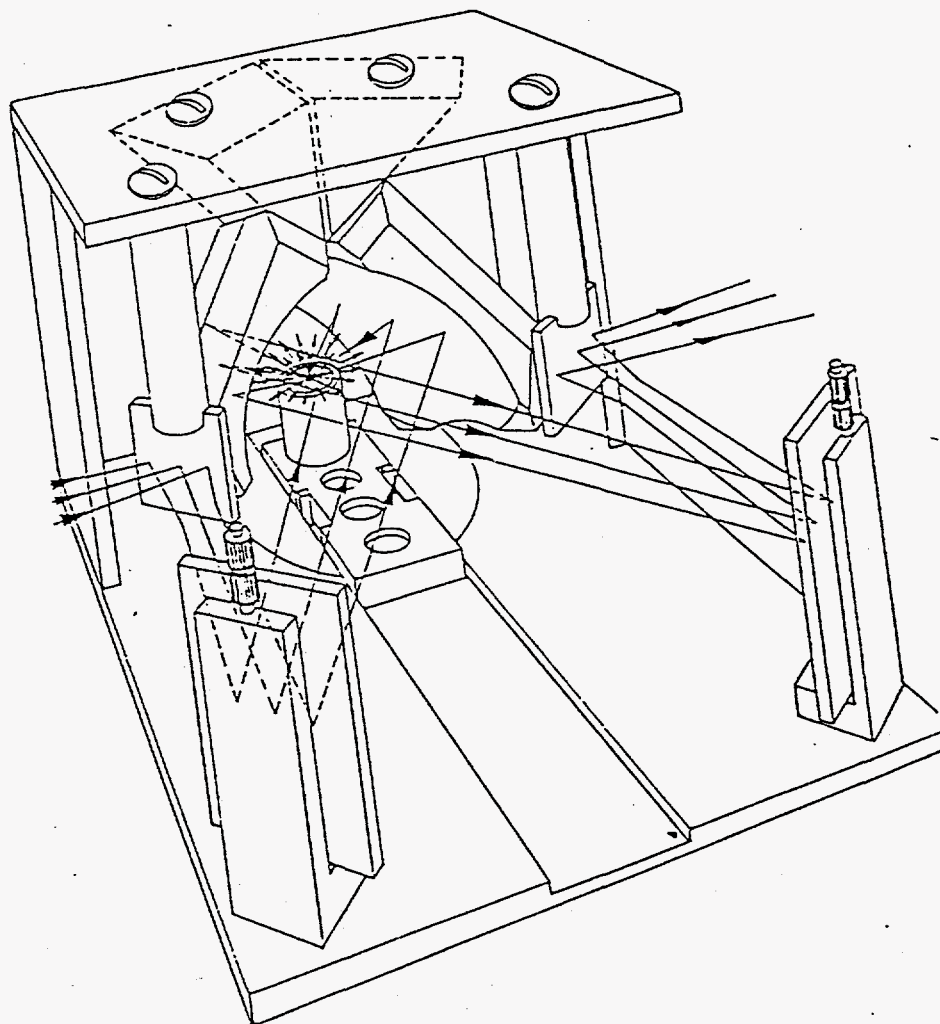


Figure 4. Harrick Praying Mantis accessory for diffuse reflectance infrared spectroscopy.

scattering coefficient and k is the molar absorption coefficient. This function allows a smooth baseline and a relatively narrow bandwidth to be obtained as long as the concentration of substrate in KCl or another highly reflecting powder is small.⁶⁷ All DRIFT spectra are plotted using the Kubelka-Munk function as the ordinate. Figure 5 contains the DRIFT spectrum of 4-vinylpyridine. Figure 6 contains the spectrum of poly(4-vinylpyridine). The fingerprint regions of 4-vinylpyridine and poly(4-vinylpyridine) are very similar. The differences occur in the CH stretching frequencies. 4-Vinylpyridine has one band at 3000 cm^{-1} . Poly(4-vinylpyridine) displays two bands at 2900 and 3050 cm^{-1} .

Figure 7 displays the difference spectra obtained by subtracting the spectrum of Illinois #6 coal from the same coal containing 4-vinylpyridine. Figure 8 displays the difference spectrum obtained by subtracting the spectrum of Wyodak subbituminous coal from the same coal containing 4-vinylpyridine. The difference spectra of Illinois #6 and Wyodak display the presence of poly(4-vinylpyridine) in the coals. This can be observed most readily by examining the CH stretching frequencies which clearly correspond to the CH stretching frequencies of poly(4-vinylpyridine). Particularly convincing is the peak at 3050 cm^{-1} , which is absent in the starting coals.

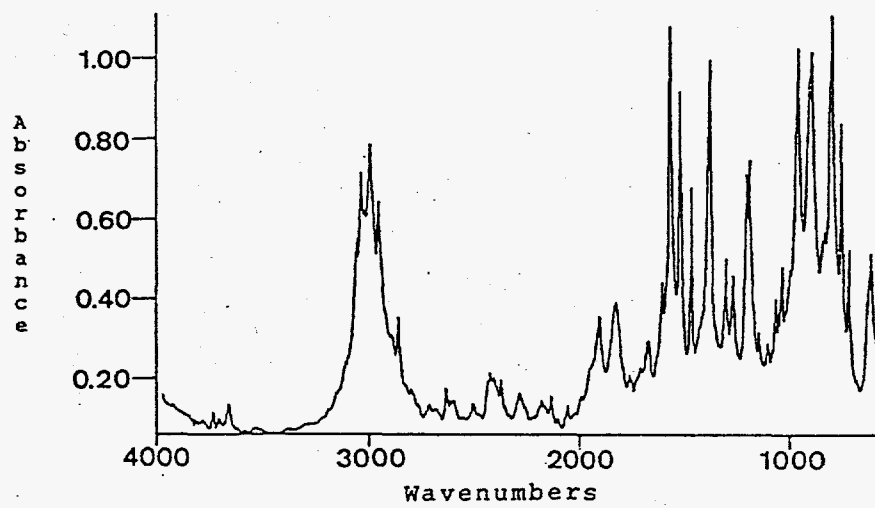


Figure 5. Absorbance Spectrum of 4-vinylpyridine

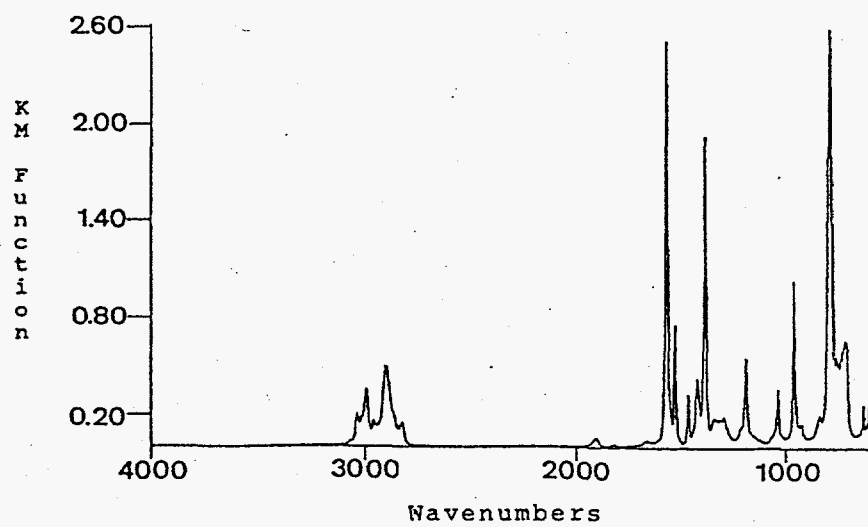


Figure 6. DRIFT Spectrum of Poly(4-vinylpyridine).

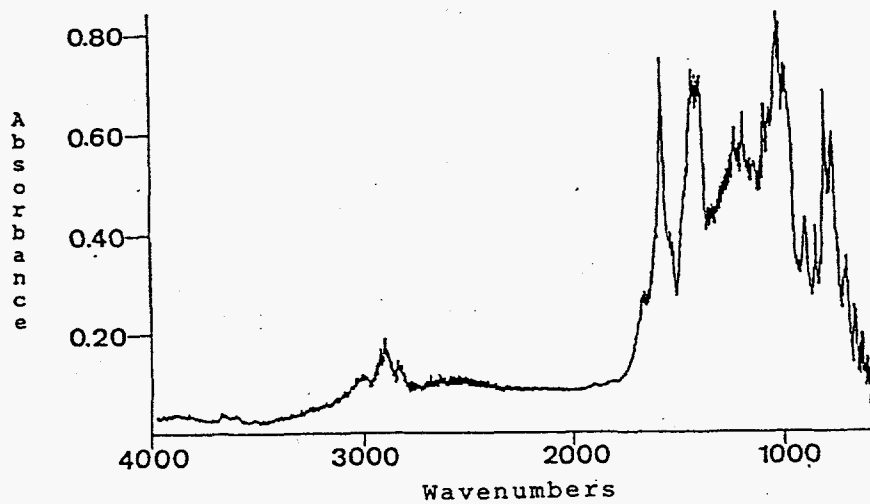


Figure 7. Difference spectrum of Illinois #6 containing 4-vinylpyridine - Illinois #6.

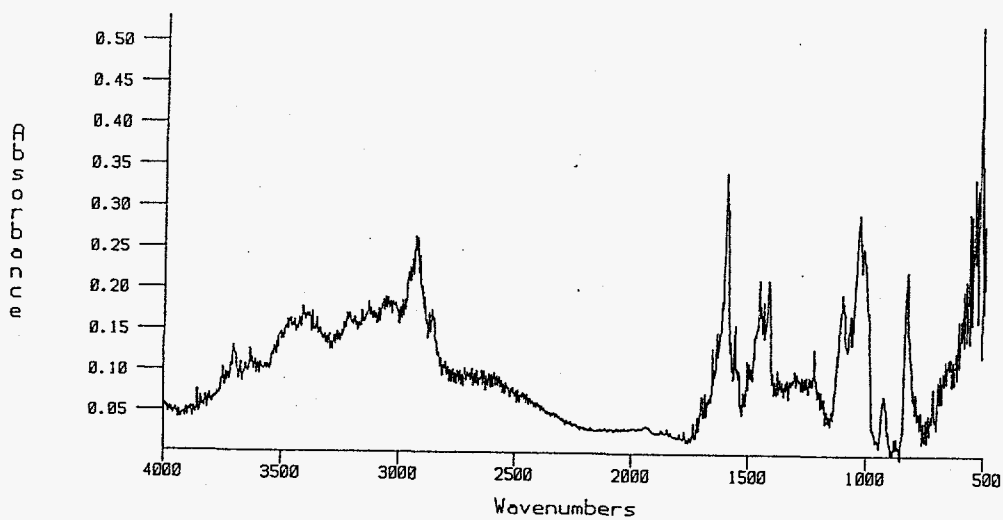


Figure 8. Difference Spectrum of Wyodak containing 4-vinylpyridine - Wyodak.

Difference spectra could only be obtained on the Illinois #6 and Wyodak coal samples. Subtraction experiments were performed on co-ground mixtures of coal and polystyrene. We found that it was difficult to obtain a subtraction spectrum of polystyrene on coal samples containing less than 15% by weight polystyrene.

Electron Paramagnetic (EPR) Spectroscopy

It is important to establish the role of coal radicals in the polymerization of 4-vinylpyridine. 4-Vinylpyridine does not undergo cationic polymerization due to the basic character of the pyridine ring, so the polymerization must be radical initiated. The pyridine residues of the Argonne Premium coal samples and the same samples swollen with 4-vinylpyridine were thoroughly studied with Electron Paramagnetic Resonance (EPR) spectroscopy. EPR spectroscopy is the best tool to employ when looking at the types and numbers of coal radicals involved in a chemical reaction.

Figure 9 contains the EPR spectrum of the pyridine extracted Illinois #6 coal and the spectrum of that coal containing poly(4-vinylpyridine). These spectra are similar to those of Illinois #6 and Wyodak pyridine residues. For the extracted coal, two components are

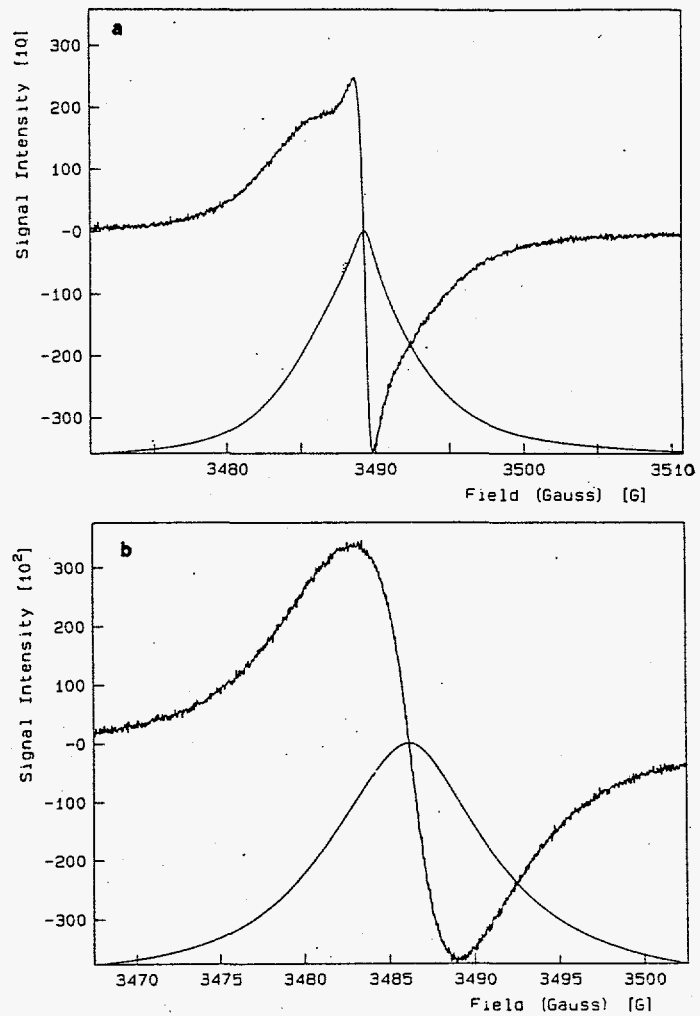


Figure 9. (a) EPR spectrum of Illinois #6 pyridine residue; (b) EPR spectrum of Illinois #6 containing 4-vinylpyridine.

observed: a broad component associated with a vitrinite and a narrow component associated with an inertinite maceral phase.⁴⁸ The narrow inertinite EPR absorption is absent in the polymer-containing coal. There is little change in the vitrinite radical density or environment. Based on line-width variations there has been little change in the mean electron density.

The EPR spectrum of the pyridine extracted Pittsburgh #8 displays no inertinite signal. The same coal containing 4-vinylpyridine displayed no changes in the EPR spectrum or radical density. It is also interesting that the Pittsburgh #8 retained the least amount of 4-vinylpyridine after being dried to constant weight.

The EPR spectrum of pyridine extracted Pocahontas #3 displays a prominent inertinite signal. Compared to the spectrum of the same coal swollen with 4-vinylpyridine, pyridine extracted Pocahontas #3 displays small changes in the EPR spectrum and radical density. Pocahontas #3 is a low volatile bituminous coal (91 %C) and does not swell appreciably. It is likely that there is no mechanism for transport of the 4-vinylpyridine monomer into the coal.

The radical densities of the five pyridine residues compared to the residues containing 4-vinylpyridine are displayed in Table V. Table V also contains the radical

Table V

The Radical densities (spins/gram) for the Pyridine Residues and the Residues containing 4-vinylpyridine

<u>Coal</u>	<u>spins/gram pyridine residue</u>	<u>spins/gram residue + 4-vp</u>	<u>Normalized Spins/Gram of Coal</u>
Wyodak	9.5×10^{18}	5.8×10^{18}	6.7×10^{18}
Illinois #6	3.4×10^{18}	2.4×10^{18}	2.9×10^{18}
Pittsburgh #8	7.1×10^{18}	6.0×10^{18}	6.8×10^{18}
Upper Freeport	8.9×10^{18}	6.4×10^{18}	7.0×10^{18}
Pocahontas #3	1.4×10^{19}	9.5×10^{18}	1.0×10^{19}

densities for the coal containing 4-vinylpyridine which were normalized to give spins/gram of coal. The radical density changes are small with the Wyodak residue displaying the most noticeable difference. The Pittsburgh #8 radical density displays almost no change.

The fact that the narrow inertinite signal disappears (except for Pocahontas) may occur because; (a) The inertinite radicals have reacted, or (b) the inertinite EPR signal is broadened and becomes indistinguishable from the vitrinite EPR signal. The total integrated intensity of the narrow inertinite component of the EPR spectrum is significantly smaller than the broad vitrinite component. It is possible that the inertinite signal is broadened due to protons on 4-vinylpyridine which are spatially close to the inertinite radicals. Our understanding of the chemistry of 4-vinylpyridine and previous work performed on carbon blacks suggest that the inertinite radicals serve as initiators.

The data presented do not unequivocally demonstrate that the polymerization of 4-vinylpyridine, which must be radically initiated, is initiated by coal inertinite radicals. The fact that the coal inertinite radical concentration decreases occur coincidentally with polymerization is best explained if they are responsible for polymerization.

B. Determination of the Reactivity of Native Free Radicals in Argonne Premium Coals with N,N'-Diphenyl-p-phenylene diamine (DPPD)

Swelling of Argonne Premium Coals With 0.02 M DPPD in Chlorobenzene.

Five coals from the Argonne Premium coal sample bank (Wyodak subbituminous, Illinois #6, Pittsburgh #8, Upper Freeport and Pocahontas #3) were Soxhlet extracted with pyridine under dry nitrogen and dried in a vacuum oven at 100 °C to constant weight. The pyridine residues were ground in a Wig-L-Bug for 3 minutes and approximately 500 mg of each residue was weighed into a tared bottle and cap. Two ml of 0.02 M DPPD in chlorobenzene was placed in each sample. These samples were allowed to swell for two week's time under dry nitrogen. The samples were then dried in a vacuum oven gradually increasing the temperature to 100 °C over one week's time. The samples were then reweighed to calculate the amount of retained chlorobenzene. Table VI displays the amount of chlorobenzene retained for each coal sample.

DPPD is soluble in chlorobenzene. Good coal solvents such as pyridine or THF do not dissolve DPPD. Although chlorobenzene is not considered a good coal solvent it

Table VI

The amount of chlorobenzene retained in Argonne coal samples which were swollen with 0.02 M DPPD in chlorobenzene

<u>coal</u>	<u>amount (mg) of chlorobenzene retained</u>
Wyodak Subbituminous	33
Illinois #6	49
Pittsburgh #8	28
Upper Freeport	29
Pocahontas #3	50

should swell the coal sufficiently over a two week period to allow transport of the DPPD to the coal radicals.

Attempts were made to obtain IR spectra of the coal-DPPD samples. The C=N stretch obtained after hydrogen abstraction from DPPD is located between 1630-1670 cm^{-1} . The C=N stretch could not be located. Coals contain a broad peak in the 1600 cm^{-1} region which may overlap the C=N stretch. Also, there may not be enough DPPD in the coal to detect using IR techniques.

Electron Paramagnetic (EPR) Spectroscopy

Because DRIFT spectroscopy was not useful in determining whether any reaction between coal radicals and DPPD had occurred, EPR spectroscopy was employed. Table VII displays a small but real decrease in the radical spin densities of four pyridine residues as compared to the residues containing DPPD. Wyodak displays the greatest decrease in radical density. Pittsburgh #8, Upper Freeport and Pocahontas #3 samples containing DPPD also display small decreases in radical density as compared to the starting samples. The Illinois #6 pyridine residue containing DPPD displays a small increase in the radical density when compared to the starting residue. This result does not fit with the rest of the data and no

Table VII

Comparison of the radical spin densities of pyridine residues before and after treatment with DPPD.

<u>Residue</u>	<u>Spins/g x 10⁻¹⁸</u>	<u>Residue-DPPD</u>	<u>Spins/g x 10⁻¹⁸</u>
Wyodak	9.5	Wyodak	5.8
Illinois #6	3.4	Illinois #6	4.2
Pittsburgh #8	7.1	Pittsburgh #8	4.0
U. Freeport	8.9	U. Freeport	6.9
Pocahontas #3	14.6	Pocahontas #3	12.3

mechanism can be rationalized to explain this result.

Figure 10 displays the EPR spectrum of a Wyodak subbituminous pyridine residue and the same residue containing DPPD. The spectrum of the coal containing DPPD displays a loss of the inertinite band. The EPR spectra for Upper Freeport and Pocahontas #3 coals display analagous results.

The Wyodak, Upper Freeport and Pocahontas #3 samples containing DPPD display a decrease in spin density as compared to the starting coals. Coincident with this decrease is a loss or decrease of the narrow inertinite signal in the EPR spectrum of these coals. It is possible that the inertinite radicals may abstract hydrogen from DPPD, however, no other experimental technique was able to substantiate this.

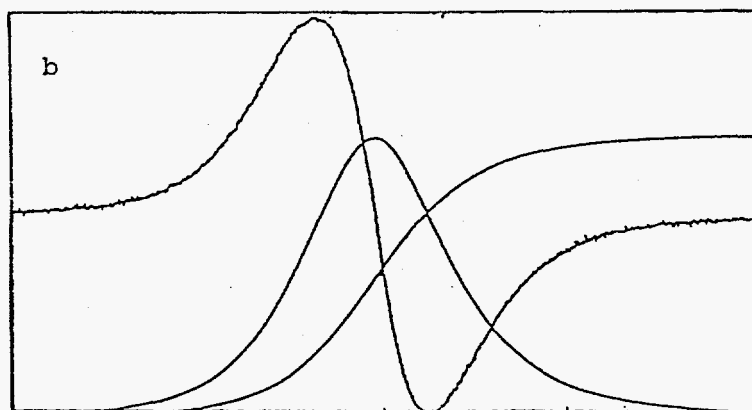
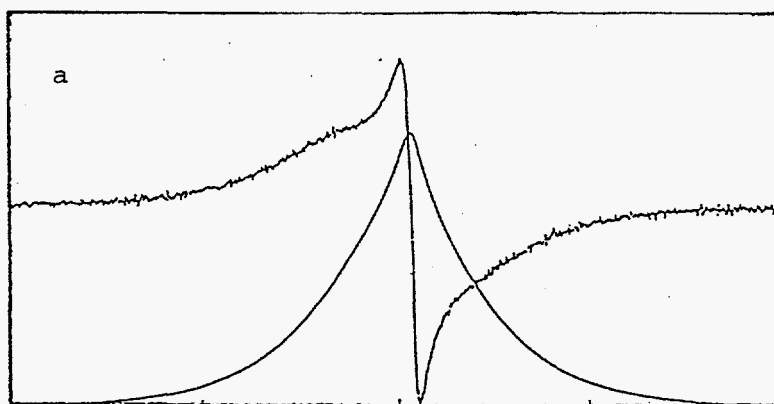


Figure 10. (a) EPR spectrum of Wyodak Subbituminous pyridine residue. (b) EPR spectrum of the same coal containing DPPD.

Part II

The Single Electron Donating Ability of Coal and Its
Relation to the Solid Structure Of Coal

Chapter V

Background

A small aromatic molecule such as benzene can act as a weak donor or a very weak acceptor in a charge transfer complex.⁷⁴ Donor ability increases with decreasing ionization potential I ; and acceptor ability increases with increasing electron affinity E . I decreases and E increases as an aromatic molecule becomes larger. $I=E$ in graphite and therefore it is as good as an electron donor as it is an electron acceptor. Aside from increasing or decreasing aromatic ring size, a molecule can become a good single electron acceptor or donor by adding electron withdrawing or releasing groups to it.

The principle organic constituent of coal is aromatic structures. A variety of polynuclear aromatic (PNA) systems are contained in coals, including heterocyclic systems. Low and medium rank coals contain many heteroatoms, mainly oxygen and sulfur.¹⁴ As coals increase in rank, the heteroatom content decreases and the size of the PNA systems remains constant up to about 89% carbon.⁷⁵ With rank increase, the major change is an increase in the concentration of PNA systems. Coals of all ranks have the potential to participate in charge transfer interactions. Eloffson and Schulz,³³ and Scwager and Yen³⁴ have previously proposed that charge transfer

interactions may be significant in coals.

7,7,8,8-Tetracyanoquinodimethane (TCNQ) and Tetracyanoethylene (TCNE) are two single electron acceptors of comparable electron affinities that belong to a class of compounds used in the area of electrically conducting salts. The field of electrically conducting organic salts is well reviewed.⁷⁶ TCNQ and TCNE may form stacks with donors such as tetrathiafulvalene which are one dimensional conductors. In these one dimensional conductors, extended stacks of donors and acceptors are formed. The overlapping orbitals give rise to conduction band electronic structure.

Stable anion radical salts are accessible from polycyano acceptors such as TCNQ and TCNE because of the high degree of resonance stabilization resulting from the many conjugated cyano groups. The derivatives of TCNQ constitute a unique series of compounds. This compound will form Π complexes with a variety of donors ranging from benzenoid hydrocarbons to planar metal chelates.

Several approaches have been used to describe the interaction of donors and acceptors in charge transfer interactions^{74,77} and more recently in one dimensional conductors.⁷⁸ Dewar⁷⁷ used a simple MO approach to describe inter-molecular transitions in charge-transfer complexes. In most complexes, the interaction energies of

the ground state are small compared to the transition energies from the ground state to the excited state. If the interaction between the donor and the acceptor is indeed small, the transition energy E_0 for the first charge transfer band should be given by:

$$E_0 = I_a - A_b + \text{constant}$$

I_a is the ionization potential of the donor (equal to the energy of its HOMO) and A_b is the electron affinity of the acceptor (equal to the energy of its LUMO). This equation may be replaced by the more general relation:

$$E_{ij} = A_i + B_j + \text{constant}$$

where E_{ij} is the transition energy for the charge transfer band involving the filled orbital i of the donor (A) and the empty orbital j of the acceptor B. If the acceptor in a charge transfer interaction is kept constant, E_{ij} should vary linearly with the ionization potential of the donor. This relationship has been observed in a number of cases.⁷⁹ A simple molecular orbital picture describing the transitions in a charge transfer complex is shown in figure 11.

Free electron models have also been used to describe

the interaction between a donor and an acceptor in a charge transfer complex.^{80,81} A one-dimensional free electron treatment considers that the transfer of charge is delocalized over the entire binary unit of Π electrons originating from the donor. Electrons fed into such a system occupy a set of energy levels defined by the geometry of the potential box. Transitions between these levels lead to the appearance of the characteristic charge-transfer bands displayed in the uv spectrum. The dimensions of the compartments within the box depend on the degree to which delocalization can occur in the donor and acceptor molecules. Figure 12 displays possible shapes for potential wells for a one dimensional treatment. These models are very useful in describing the charge transfer behavior of many Π complexes when they occur as discrete dimers. In the solid state these salts form extended stacks. The importance of the stability of the dimer is diminished in the solid state.⁷⁶ A number of models are available that describe the interactions of organic metals and other free radical crystals.^{82,83,84,85} Band theory⁸⁶ affords a simple, qualitative picture of the interaction between extended stacks of electron donors and acceptors. Efforts will be made to discuss this theory.

If one begins with a chain of equally spaced hydrogen

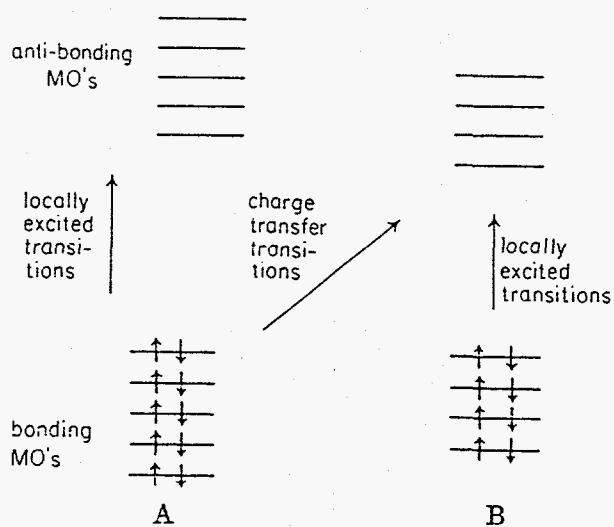


Figure 11. Orbital energies and transitions in a charge transfer complex formed by donor A and acceptor B.

Dewar, J.S.; Lepley, A.R. *J. Am. Chem. Soc.*, 1961, 83, 4560.

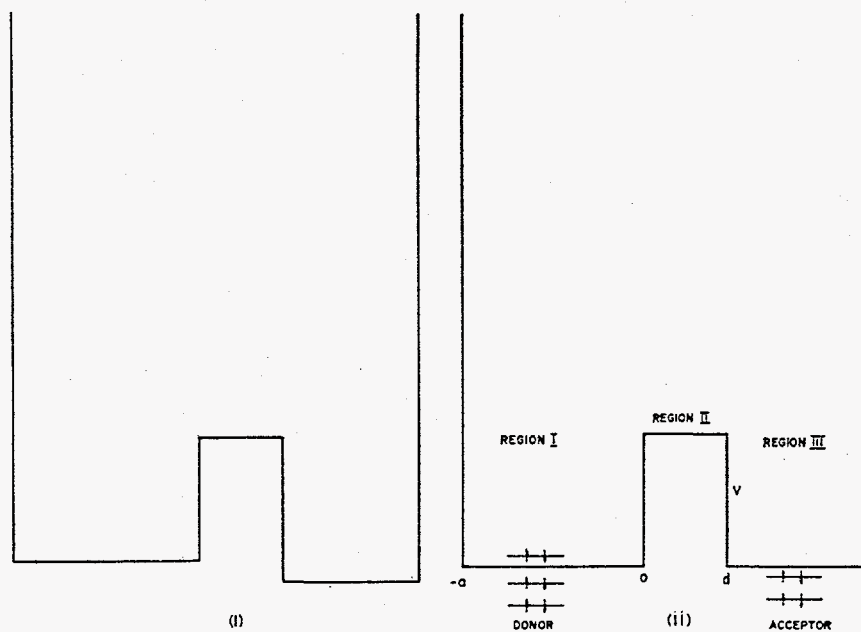


Figure 12. Possible shapes of potential wells for a one-dimensional treatment of donor acceptor compounds.

Boeyens, J.C.A. J. Phys. Chem., 1967, 71, 2969.

Picture two electrons, one on each of two nearest neighbor sites in a donor acceptor stack. If their spins are parallel (in a triplet state), the Pauli Principle precludes electron hops that places both electrons on one site. This material will be a Mott insulator.⁸⁷ If the neighboring electrons are in the singlet state, the material may be a conductor. The bands in figure 13 are nothing more than the interaction between the HOMO's of the donors and the LUMO's of the acceptors in a stack.

Infrared and Raman spectroscopy are powerful tools used to investigate the structure of organic conductors.^{88,89} The technique which is important in this discussion is the change of the $C\equiv N$ stretching frequency when the molecule it is in serves as an acceptor in a charge transfer interaction. Devlin, Van Duyne and Pecile and their groups have performed a significant amount of work on the vibrational bands of TCNQ and its radical anion.^{90,91,92,93,94} The most interesting work for our purposes was performed by Chappel⁹⁵ and coworkers. They found that there was a linear relationship between the change in the $C\equiv N$ stretching frequency and the amount of electron density donated to TCNQ. This behavior is displayed in Figure 14. The electron transferred to TCNQ goes into the lowest unoccupied molecular orbital (LUMO) which is an

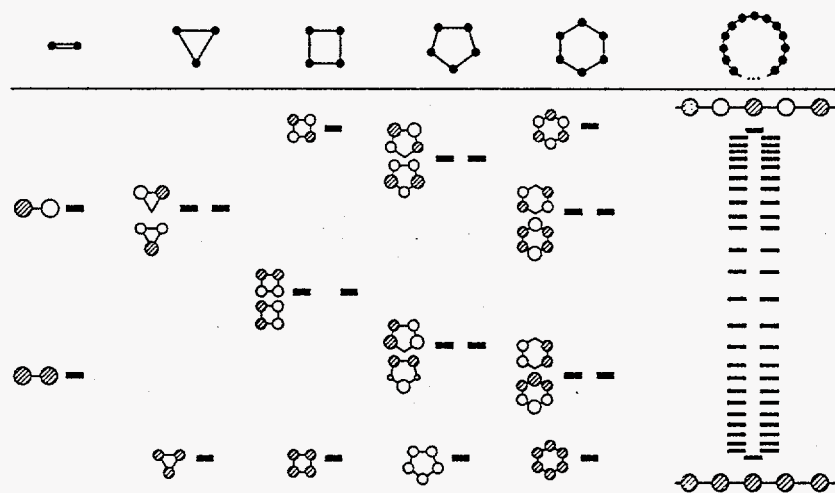


Figure 13. Orbital (band) diagram for some small cyclic compounds and a large ring.

* Hoffmann, R. *Angew. Chem.* (1987), 26, 846.

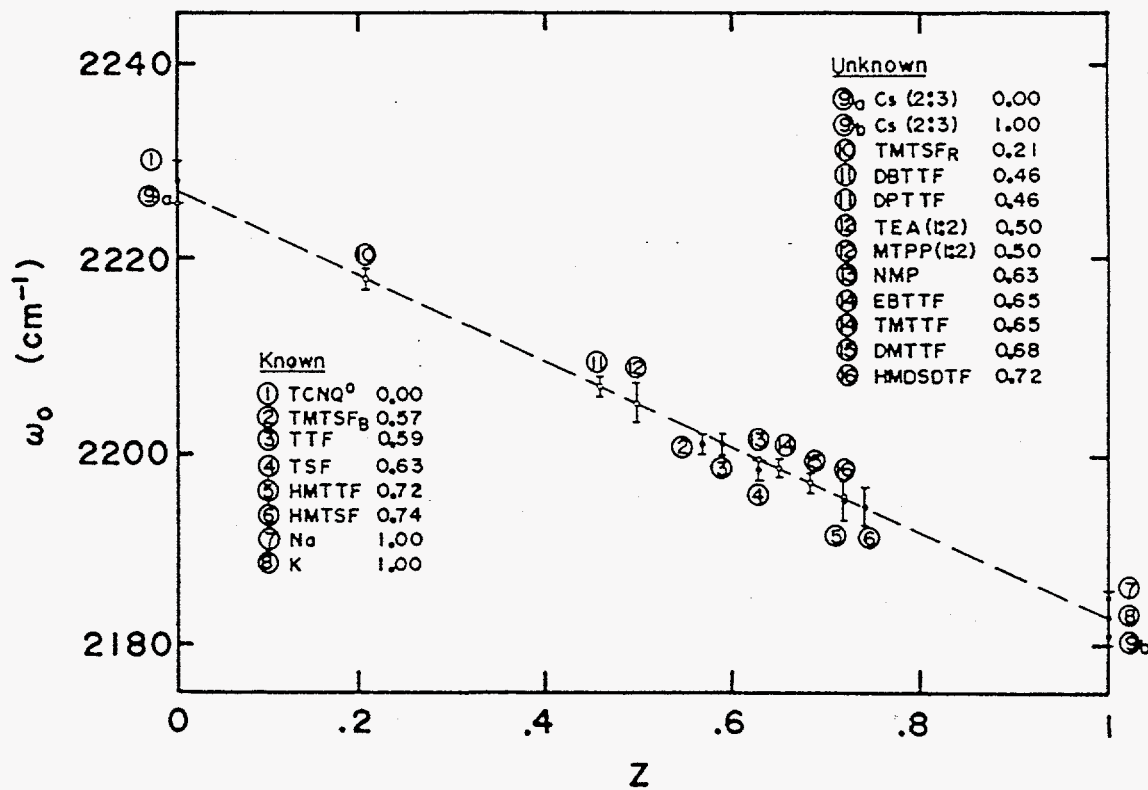


Figure 14. Nitrile stretching frequency of TCNQ for 19 salts.

Chappel, J.S.; Bloch, A.N.; Bryden, W.A.; Maxfield, M.; Poehler, T.O.; Cowan, D.O. J. Am. Chem. Soc., 1981, 103, 2442.

anti bonding orbital. Population of the LUMO weakens the conjugated system and there is a decrease in the $\text{C}\equiv\text{N}$ stretching frequency. Occupation of the LUMO of TCNQ by one electron gives rise to a 44 cm^{-1} shift in the $\text{C}\equiv\text{N}$ stretching frequency.

A number of groups have studied the infrared and Raman spectra of TCNE and its radical anion.^{96,97} Significant differences are found in the infrared spectra of TCNE and its radical anion. The nitrile stretching frequency of TCNE is located at 2236 cm^{-1} . The $\text{C}\equiv\text{N}$ stretch of the TCNE radical anion is located at 2187 cm^{-1} . The most striking difference occurs with the double bond of TCNE. The $\text{C}=\text{C}$ IR band of TCNE is forbidden by the point group D_{2h} selection rules. Upon transfer of an electron to TCNE, a band appears in the infrared spectrum at 1358 cm^{-1} . The appearance of this band is attributed to a back transfer of charge from the $\text{C}=\text{C}$ bonding molecular orbital to the d orbitals of the metal in the complex.^{98,99} Table VIII displays bond stretching frequencies for TCNE and its radical anion.

A number of studies have been performed on the complexes of aromatic systems with TCNE and TCNQ^{96,100} and only illustrative references are cited here. Typically the interaction of TCNQ and TCNE with aromatic systems in

Table VIII

Bond Stretching Frequencies (cm^{-1}) for TCNE and its Radical Anion.

<u>Assignment</u>	<u>TCNE</u>	<u>TCNE radical anion(a)</u>
$\text{C}\equiv\text{N}$	2236	2187(b)
$\text{C}=\text{C}$	1570(c)	1358
$\text{C}-\text{C}$	1155	1190

(a) Frequencies taken from the Cs(TCNE) infrared absorption spectrum.

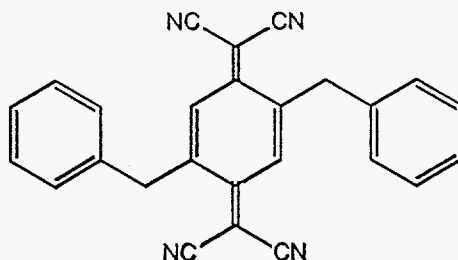
(b) Average value for infrared doublet.

(c) Derived from Raman studies by Rosenberg, A.; Devlin, J.P. Spectrochim. Acta, 1965, 21, 1613.

* Data obtained from, Moore, J.C.; Smith, D., Youhne, Y.; Devlin, J.P. J. Phys. Chem., 1971, 75, 325.

the solid state display very little charge transfer.

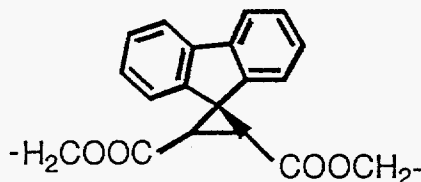
In 1983 Becker et al.¹⁰¹ designed a TCNQ molecule with benzyl groups in the 2,5 positions. The compound is displayed below.



This molecule forms segregated stacks in the solid state. IR studies found that 30% electron density was donated to the TCNQ from its own benzyl group. This is quite surprising because of the high ionization potential of benzene. One would suspect little or no charge transfer from benzene to TCNQ.

A number of groups have studied the interaction of various single electron acceptors with polymers having pendant aromatic groups. Typically the polymer shows small differences in its interactions with electron acceptors as observed by uv spectroscopy and Benesi-Hildebrand analysis of binding constants.^{102,103} The most important factor in these studies is that the spatial distribution of donor groups in polymers determines the strength of the interaction with electron acceptors. In 1972, Rolf Schulz¹⁰⁴ reported the

interaction of TCNQ with the oligomers and polymer of the fluorene monomer shown below.



The spiro group on the 9 position of the fluorene stacks the aromatic groups face to face. As the degree of polymerization increased, the binding constant between the polymer and TCNQ increased. The fluorene monomer had a binding constant of 2900. The polymer had a binding constant of over 20,000.

Grishna^{105,106} studied the interaction of TCNQ with activated carbons prepared from sugar coke at 900 °C. Grishna studied the interaction of TCNQ with the carbons using EPR spectroscopy. He suggests that the PNA's in the carbon have a sufficiently low ionization potential to donate an electron to TCNQ. One problem with this study is the fact that he does not see an increase in the radical density which corresponds to the loading of TCNQ in the sample. No explanation is given for this behavior in the EPR spectrum.

We used TCNQ and TCNE as probes to determine the ability of coals to donate an electron in some type of

charge transfer interaction. We followed the $C\equiv N$ stretch of TCNQ and TCNE in the infrared spectrum to estimate the amount of electron transfer to these materials from coals. EPR spectroscopy was employed to study the numbers and types of paramagnetic centers formed in these interactions.

Chapter VI

Experimental Procedures

Deposition of TCNQ and TCNE on Argonne Premium Coals

TCNQ and TCNE from Aldrich (Milwaukee, WI) were dried in a vacuum oven at room temperature for one week. All solvents, chlorobenzene, pyridine, and tetrahydrofuran were obtained from Aldrich (Milwaukee, WI). Reagent grade pyridine was dried over potassium hydroxide. Pyridine and chlorobenzene were purged with dry nitrogen via a gas dispersion tube and sealed with a septum. Anhydrous tetrahydrofuran in a Sure Seal bottle was used as received.

The TCNQ or TCNE were transferred to a Vacuum Atmosphere drybox. A typical sample preparation involved weighing 20 mg of TCNQ or TCNE into a previously weighed 100 ml roundbottom flask. Next, approximately one gram of an Argonne Premium coal was weighed into the flask. A magnetic stirrer was placed into the flask and it was sealed with a septum. The flask was then removed from the drybox and 50 ml of solvent added via a syringe. The mixture was stirred for one week. The solvent was removed using a rotary evaporator with a water bath in the range of 30 - 40 °C. The sample was dried in a vacuum oven at room temperature until it reached constant weight. This procedure was used for TCNQ or TCNE loadings up to 100 mg

of the electron acceptor per 1 gram of coal sample.

100% TCNQ or TCNE loadings (one electron acceptor per one polynuclear aromatic)⁷⁵ were prepared by adding a stock solution of the electron acceptor dissolved in pyridine to the coal sample as described in the preceding paragraph. A 0.03 M solution of TCNQ in pyridine was prepared by weighing 6.316 grams of TCNQ into a tared one liter volumetric flask and dissolving it in pyridine. The solution was purged with dry nitrogen and sealed with a septum. 100 ml of this solution would correspond to a 100 % loading of TCNQ on 1 gram of Illinois #6 coal. The mixture of stock solution and coal were stirred for one week under dry N₂. The solution was then rotovapped to remove the solvent. The coal doped with TCNQ was then dried in a vacuum oven at room temperature until it reached constant weight. It could not be determined whether the TCNQ was contained in the bulk of the coal or on the surface.

The volume of solution placed into coal to correspond to a 100% loading based on PNA's could be varied for the different Argonne premium coal samples depending on average aromatic cluster size and percent aromaticity.

Demineralization procedure

Approximately 6 g of coal were weighed into a Nalgene beaker. 40 ml of 49% aqueous HF solution was added to the

coal and the mixture was heated to 55-60 °C and magnetically stirred under dry nitrogen for one hour. The coal/HF solution was diluted with water to 600 ml, cooled and filtered through a medium porosity sintered glass funnel and washed with 150 ml of warm distilled water. The coal was transferred to a glass beaker and 50 ml of 5N HCl was added to the beaker. The suspension of coal in aqueous HCl was heated to 55-60 °C and magnetically stirred under dry nitrogen for one hour. The coal/HCl suspension was diluted to 250 ml, filtered through a medium porosity sintered glass funnel and washed with 600 ml of warm distilled water in 25 ml portions. Litmus paper was used to check for acidity in the wash water. When the wash water was neutral the coal was transferred to a tared bottle and placed in a vacuum oven at 110 °C and dried to constant weight.

Preparation of Aromatic-TCNQ and TCNE complexes

The aromatic compounds and single electron acceptors used were obtained from Aldrich (Milwaukee, WI). Gold Label aromatic compounds were used when available. Typical sample preparation involved dissolving equimolar amounts of the aromatic compound and TCNQ (or TCNE) in separate vials each containing five ml of chloroform and mixing the solutions. Usually, the solution would change

color. The solution was then stirred magnetically for 1 hr. under a dry N_2 atmosphere.

DRIFT determinations of Argonne Premium coals containing TCNQ and TCNE

DRIFT spectra were obtained on a Mattson Series 100 Fourier transform infrared spectrometer and on a Mattson Polaris Fourier transform infrared spectrometer. Both spectrometers were equipped with Harrick optics and a sampling stage for diffuse reflectance. Spectra were recorded from the co-addition of 1000 scans of 18000 data points at 2 cm^{-1} resolution against a background of KCl. A typical sample preparation involved separately grinding 200 mg of coal-TCNQ and KCl in a Wig-L-Bug for three minutes, followed by co-grinding a 5% mixture of coal-TCNQ and KCl for an additional three minutes. DRIFT spectra of TCNQ and TCNE displayed no shifts in the nitrile stretching frequency upon grinding in a Wig-L-Bug.

FTIR measurements of aromatic-TCNQ or TCNE complexes in Solution

FTIR spectra were obtained on a Mattson Polaris Fourier transform infrared spectrometer. Spectra were recorded from the co-addition of 1000 scans of 54000 data points at 0.5 cm^{-1} resolution against a background of

chloroform in a KCl infrared solution cell. The path length of the cell was 0.25 mm. A typical sample preparation involved transferring a solution of the aromatic-single electron acceptor complex into a solution cell and placing the cell in the spectrometer. The cell was tilted 5 degrees from perpendicular to the incident light beam to avoid any secondary or tertiary interferograms.

FTIR measurements of aromatic-TCNQ or TCNE complexes in the solid state

FTIR spectra were obtained on the Mattson Polaris Fourier transform infrared spectrometer. Spectra were recorded from the co-addition of 400 scans of 18000 data points at 2 cm^{-1} resolution against a background of KCl. A typical sample preparation involved mixing the complex with KCl in a vial (5% by weight) and placing this mixture in a pellet press. The sample was pressed into a transparent pellet, placed in an absorbance/transmittance sample holder and scanned.

EPR determinations of TCNQ and TCNE treated coals

EPR measurements were obtained by Layce Gebhard and Bernie Silbernagel on a Bruker ER 300 Spectrometer operating at 9.8 GHz. Microwave frequencies were determined with an EIP Model 548 microwave frequency

counter. The data were accumulated on a Bruker computer data system using the ESP 350 Data Acquisition Program. The carbon radicals were studied using a central field value of 3500 G, a field scan range of 50 G swept in a one minute scan time, and a microwave power of one μW . All spin density measurements were made relative to a Varian standard consisting of pitch in KCl. The pitch, a secondary standard, when compared with an NBS ruby standard, was found to represent a level of 3.67×10^{15} radicals in the spin cavity. A typical sample preparation involved weighing approximately 20 mg of coal into a 4mm o.d. spectroscopic quality quartz tube to a height of approximately 1 cm. The tube was then evacuated to 10^{-1} torr, backfilled with nitrogen, and sealed.

Chapter VII

2. Characterization of the Single Electron Donor Capability of Coal.

The second part of this thesis discusses the use of TCNQ and TCNE as probes to determine the ability of coals to donate an electron in some type of charge transfer interaction. The nitrile stretch of TCNQ and TCNE is a sensitive indicator of electron transfer from a donor to these acceptors. We used diffuse reflectance FTIR to study shifts of the nitrile band of TCNQ and TCNE in order to estimate the amount of electron transfer to these acceptors. EPR spectroscopy was employed to study the numbers and types of paramagnetic centers formed in these interactions.

The initial focus of this work was to determine the numbers and types of single electron donors in coal. We discovered that there were cooperative interactions between TCNQ or TCNE and the aromatic species in coal. This interaction leads to the formation of an extended valence band structure involving the LUMO of TCNQ or TCNE. This behavior was found to be a bulk property of the coal dependent on its solid structure. This behavior can not be modelled using individual molecules.

A. Diffuse Reflectance Infrared (DRIFT) Spectra of Whole Coals with TCNQ and TCNE

The usefulness of DRIFT spectroscopy for obtaining coal spectra was described in an earlier section and no further discussion is needed here.

Infrared spectroscopy may be very useful for studying the electron donor or acceptor characteristics of charge-transfer complexes. When there is only weak interaction between molecules in a complex, the infrared spectrum appears to be only a superposition of the two molecules. Any lack of change in the infrared spectrum upon complex formation is used to distinguish between weak complexes and the products of single electron transfer.^{107,108,109}

The sensitivity of the nitrile stretching frequencies of TCNQ and TCNE to electron transfer are very useful.⁹⁵ The nitrile stretching frequency of these molecules lies in a region of the IR spectrum where no coal IR peaks are found. The frequency shifts are large and easily monitored. Changes in intensity are difficult to quantify using DRIFT spectroscopy.

Figure 15 contains the DRIFT spectra of TCNQ and TCNE. The nitrile band of TCNQ is located at 2227 cm^{-1} . The nitrile band of TCNE is located at 2236 cm^{-1} . It should be noted that these bands are narrow and sharp. Upon transfer of electron density from a donor to these

acceptors, the bands shift and become broad.

TCNQ and TCNE can readily be deposited in coals from pyridine solution. Initially 20 mg of TCNQ and TCNE were deposited on 1 gram of Illinois #6 coal. It is not certain whether all of the TCNQ is deposited in the coal or on the surface. Figure 16 contains the DRIFT spectrum of Illinois #6 and the same coal containing 20 mg of TCNQ. The $C\equiv N$ stretching frequency of TCNQ in the Illinois #6 displays a 44 cm^{-1} shift which is indicative of complete electron transfer.⁹⁵ It is also clear that there is peak at 2121 cm^{-1} . This band indicates the presence of an isocyanate group. The TCNQ radical anion is known to undergo reactions with oxygen to form isocyanates. It was obvious that care must be taken during sample preparation to exclude oxygen. Changes in the OH stretching region between 3500 and 3000 cm^{-1} occur upon the addition of TCNQ to the coal. Rough subtraction spectra show a loss of hydrogen bonding in the 3500 to 3000 cm^{-1} region. This indicates that the TCNQ is preferentially transferred to PNA's containing hydrogen bonding functionalities. It is surprising that these changes are visible at such low loadings of TCNQ.

Figures 17 through 22 display The spectra of a 20 mg TCNQ loading per gram of coal with Beulah-Zap lignite,

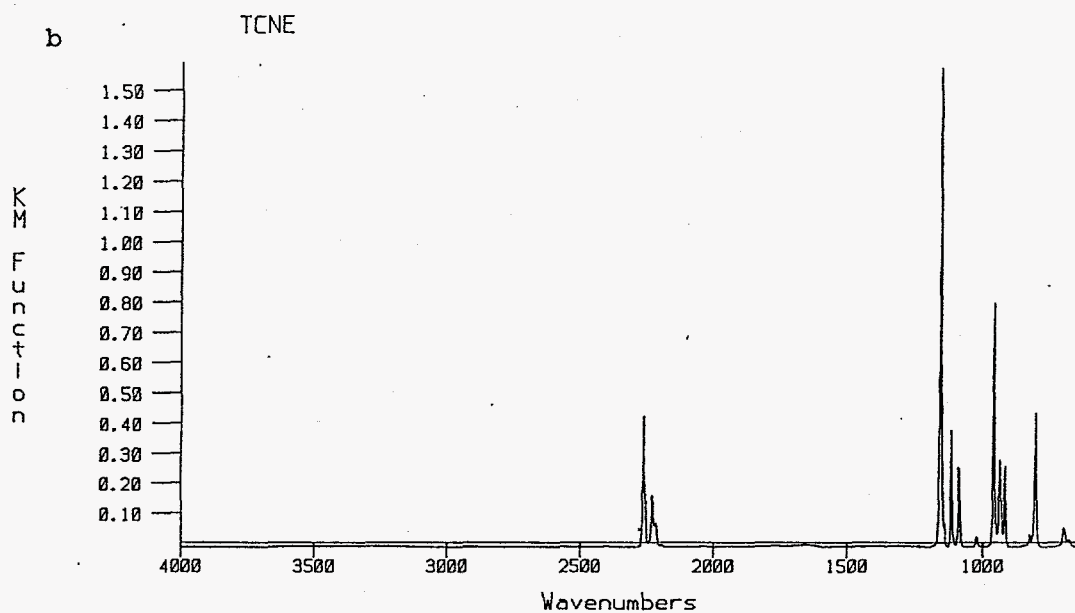
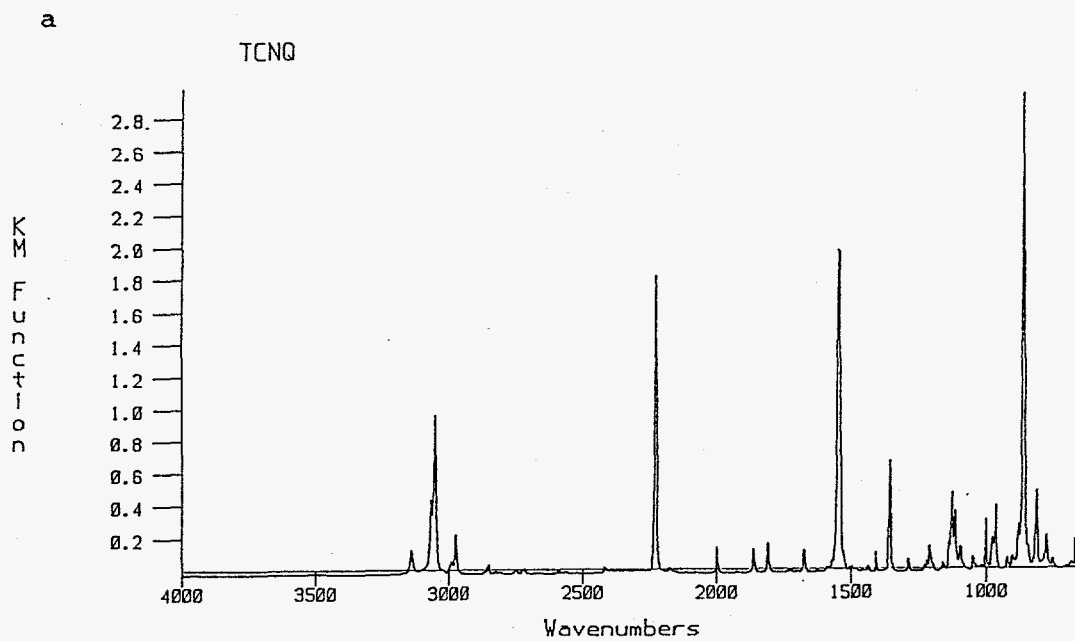


Figure 15. (a) DRIFT spectrum of TCNQ. (b) DRIFT spectrum of TCNE.

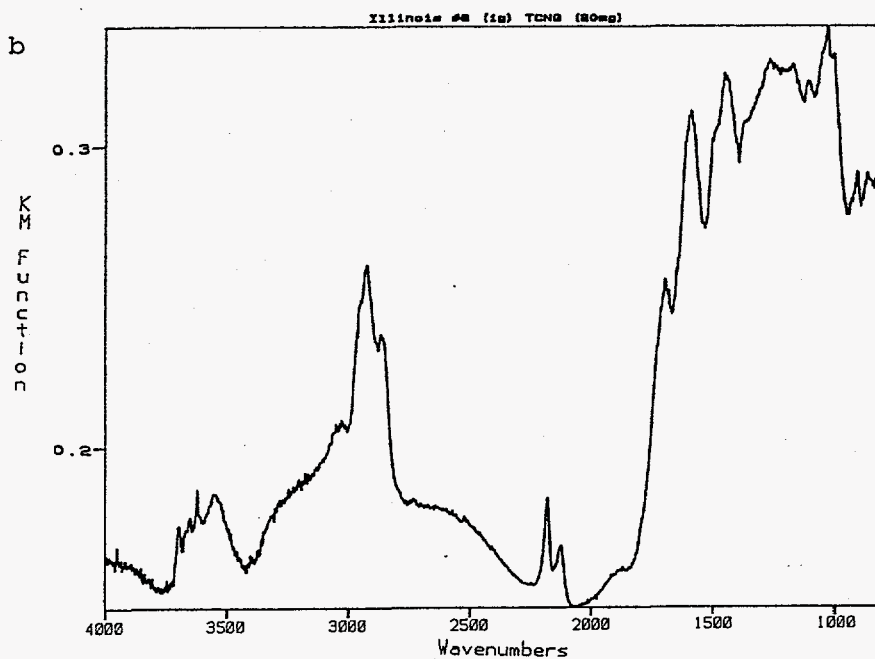
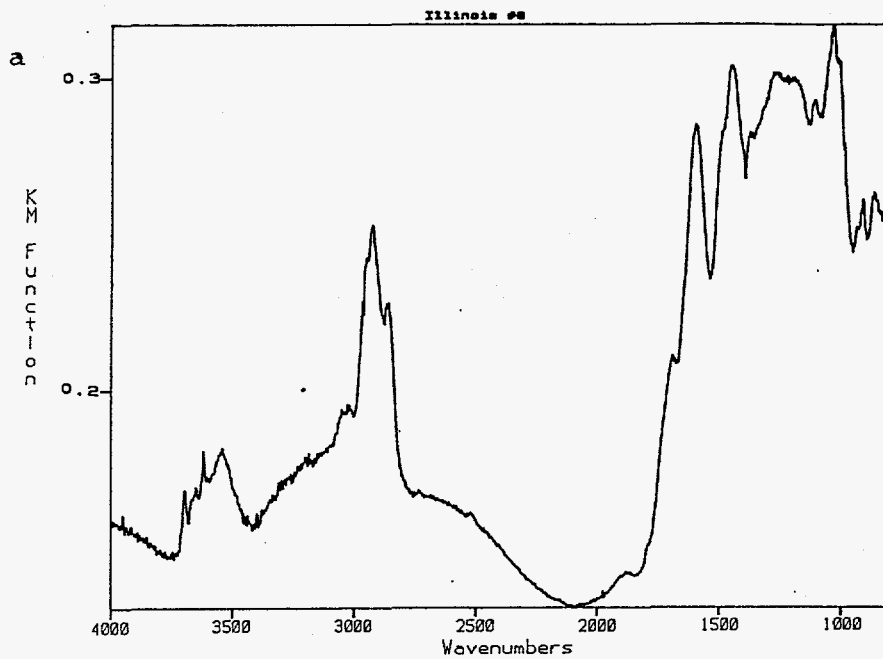


Figure 16. a) DRIFT spectrum of Illinois #6 coal; b) DRIFT spectrum of Illinois #6 coal containing 20 mg TCNQ/gram of coal.

Wyodak, Blind Canyon, Pittsburgh #8, Lewiston Stockton and Upper Freeport displayed with their parent coals respectively. All of these spectra display the same $C\equiv N$ stretch for the nitrile band of TCNQ. The results are consistent with those described above for the Illinois #6 TCNQ coal sample.

The immediate concern was whether it was the organic or inorganic portion of the coal which was responsible for the shift of the TCNQ nitrile band. 20 mg of TCNQ was deposited into 1 gram of a demineralized Pittsburgh #8 coal sample. Figure 23 displays the DRIFT spectrum of a demineralized Pittsburgh #8 coal containing TCNQ. The nitrile band is shifted 44 cm^{-1} for this sample.

The nitrile stretch of TCNE in the Illinois #6 coal in Figure 24 displays a 36 cm^{-1} shift. The nitrile stretch of the TCNE radical anion is located at 2189 cm^{-1} .⁹⁶ If there is a linear relationship between the amount of electron transfer and the stretching frequency of the nitrile in TCNE, this shift would correspond to 67% electron transfer.

The initial focus of this work was to determine the amount and types of single electron donors in coal. As the amount of TCNQ in the coal was increased, it was expected that the concentration of good electron donors in

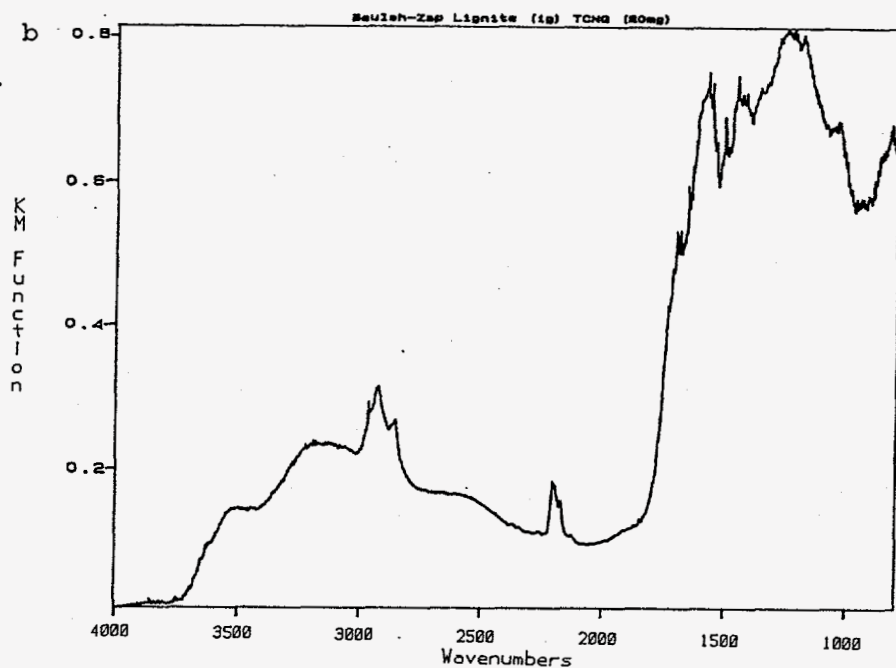
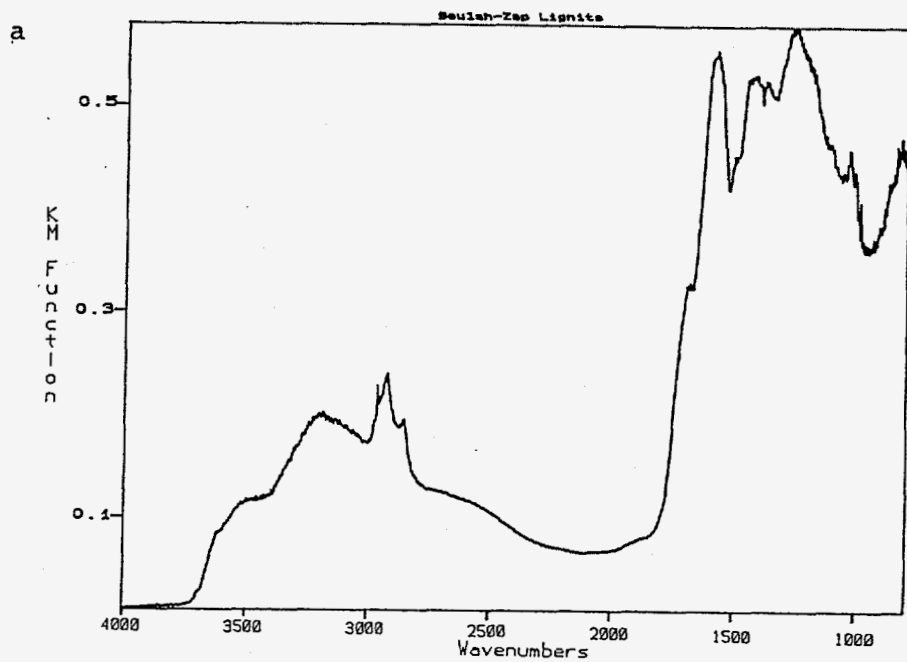


Figure 17. a) DRIFT Spectrum of Beulah-Zap Lignite;
 b) DRIFT Spectrum of Beulah-Zap Lignite Containing 20 mg
 TCNQ/gram of Coal.

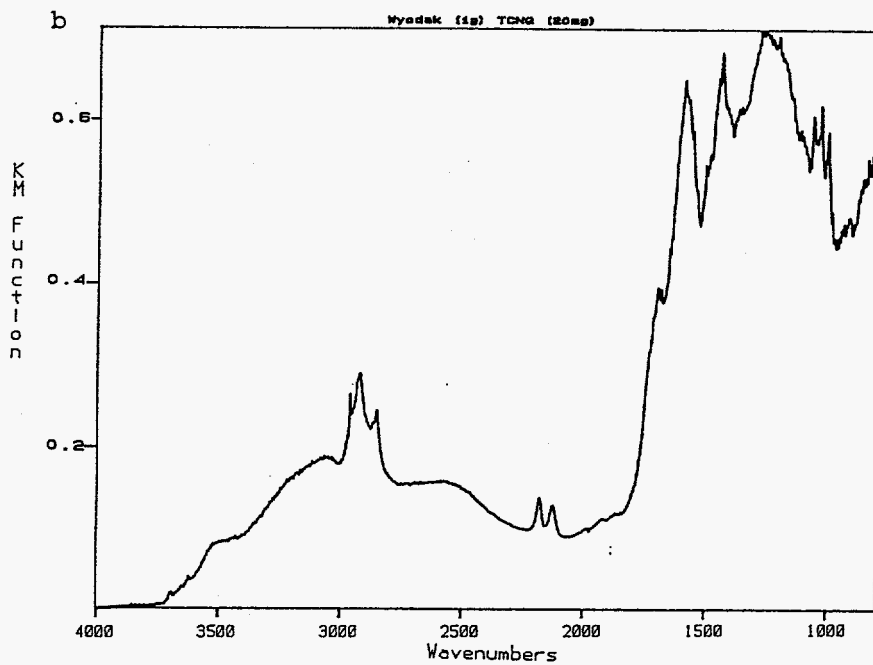
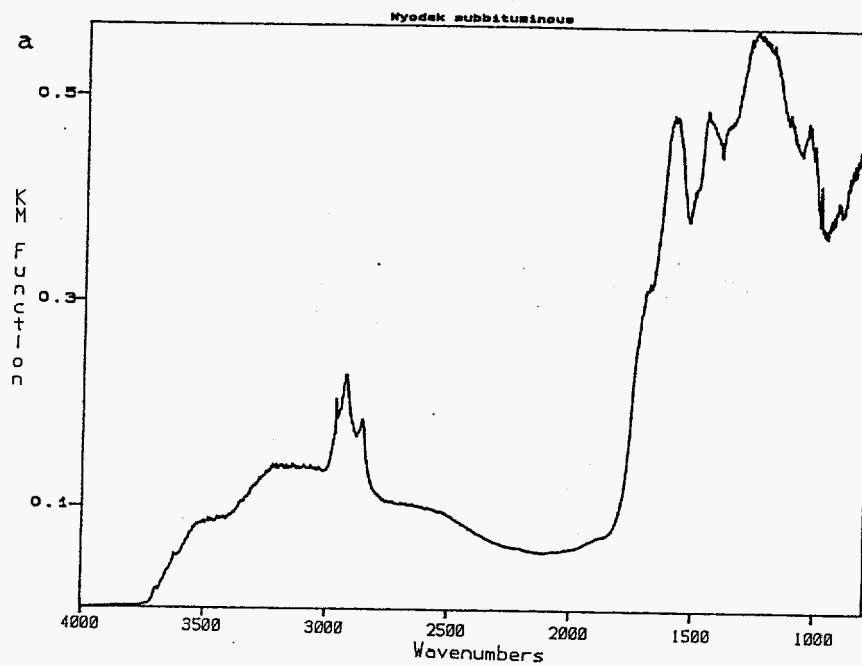


Figure 18. a) DRIFT Spectrum of Wyodak coal; b) DRIFT Spectrum of Wyodak Coal Containing 20 mg TCNQ/gram of coal.

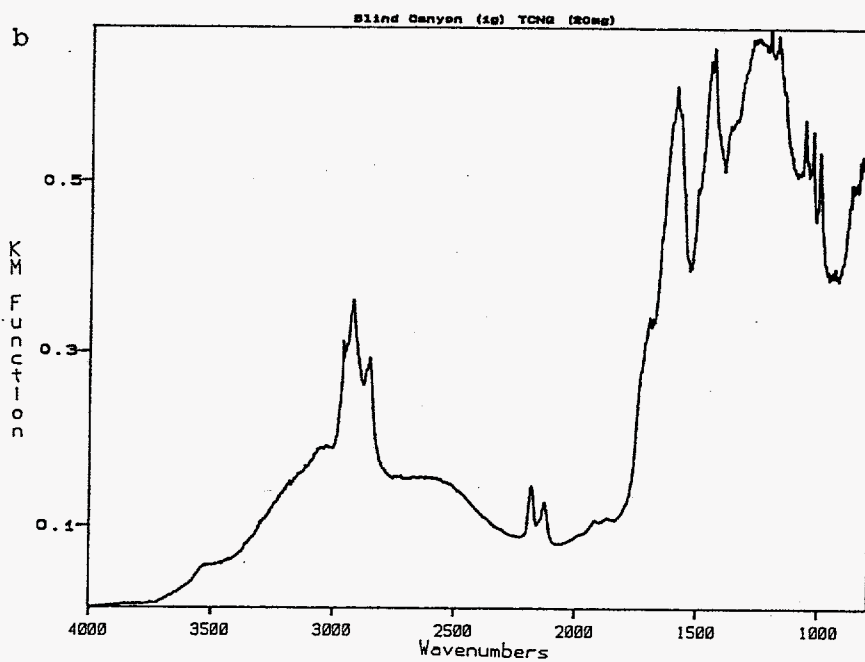
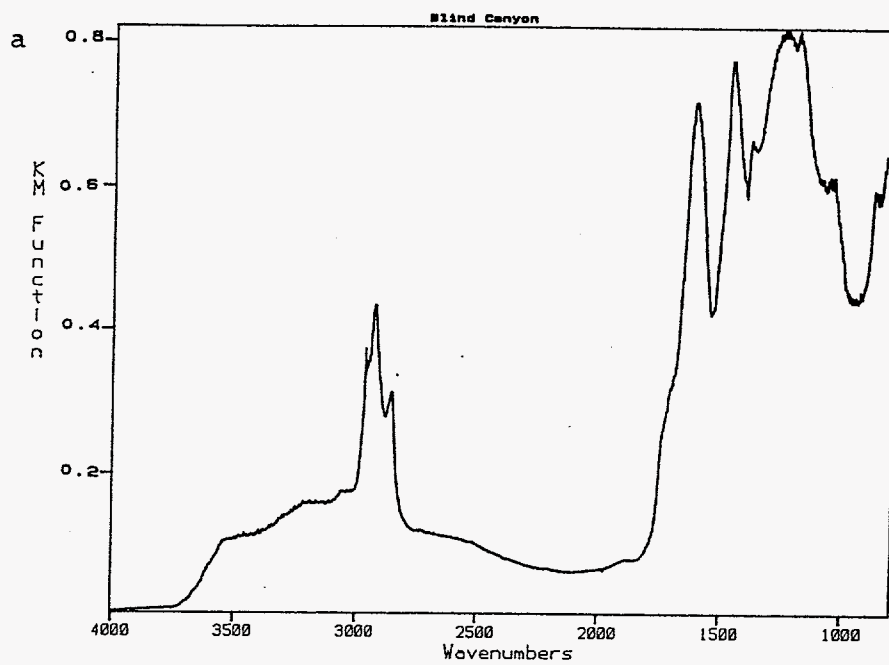


Figure 19. a) DRIFT Spectrum of Blind Canyon Coal; b) DRIFT Spectrum of Blind Canyon Coal Containing 20 mg TCNQ/gram of Coal.

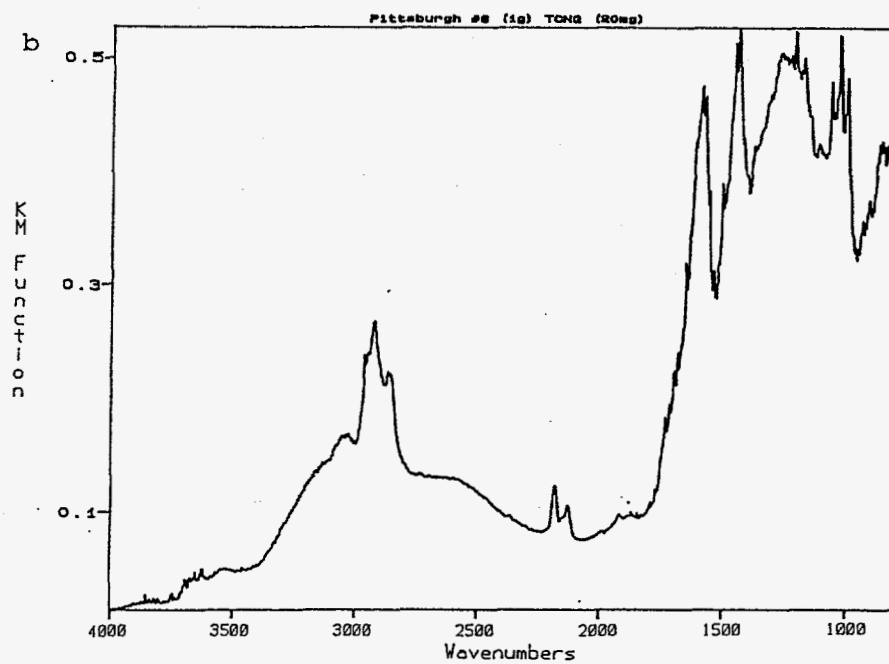
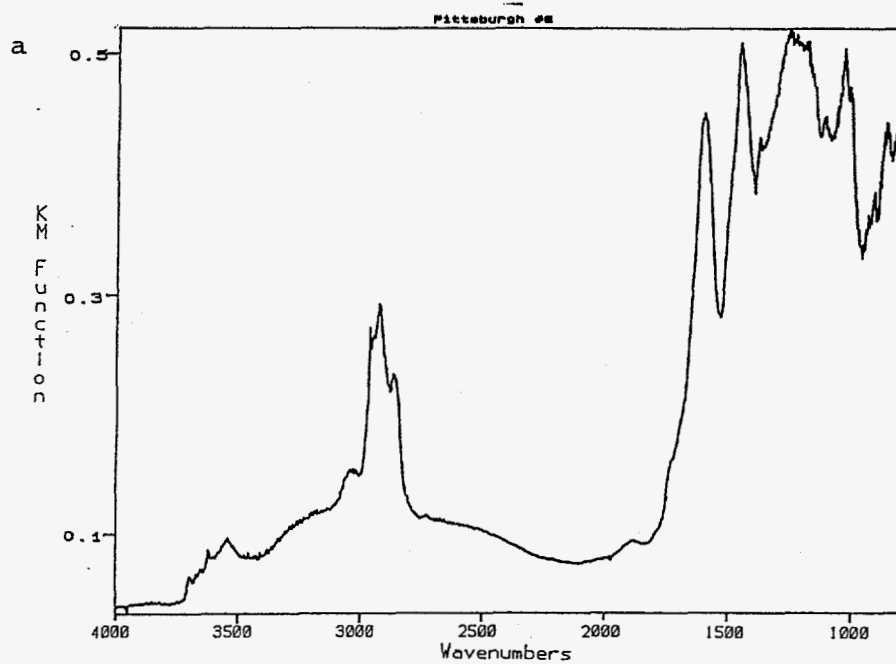


Figure 20. a) DRIFT Spectrum of Pittsburgh #8 Coal; b) DRIFT Spectrum of Pittsburgh #8 Coal Containing 20 mg TCNQ/gram of Coal.

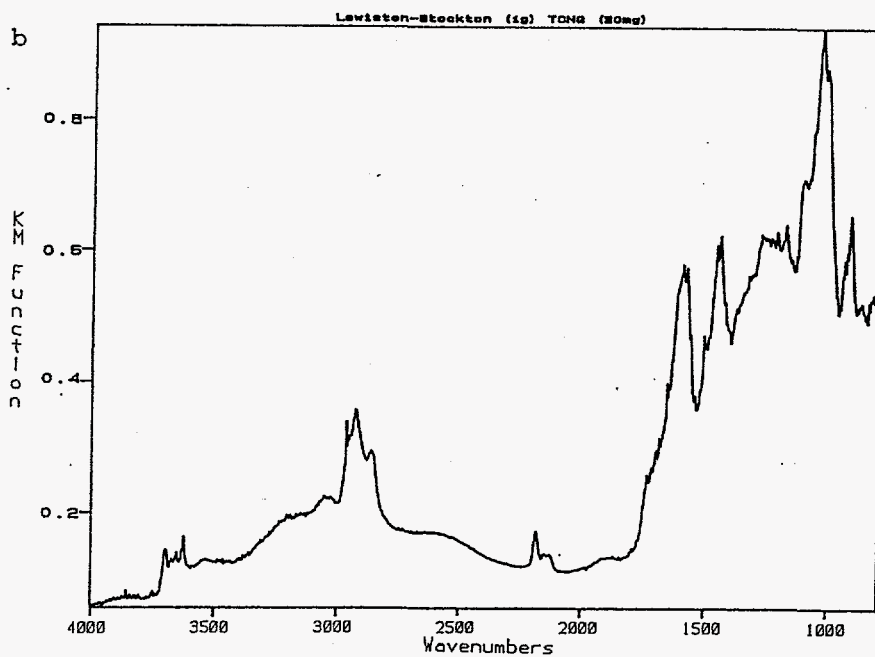
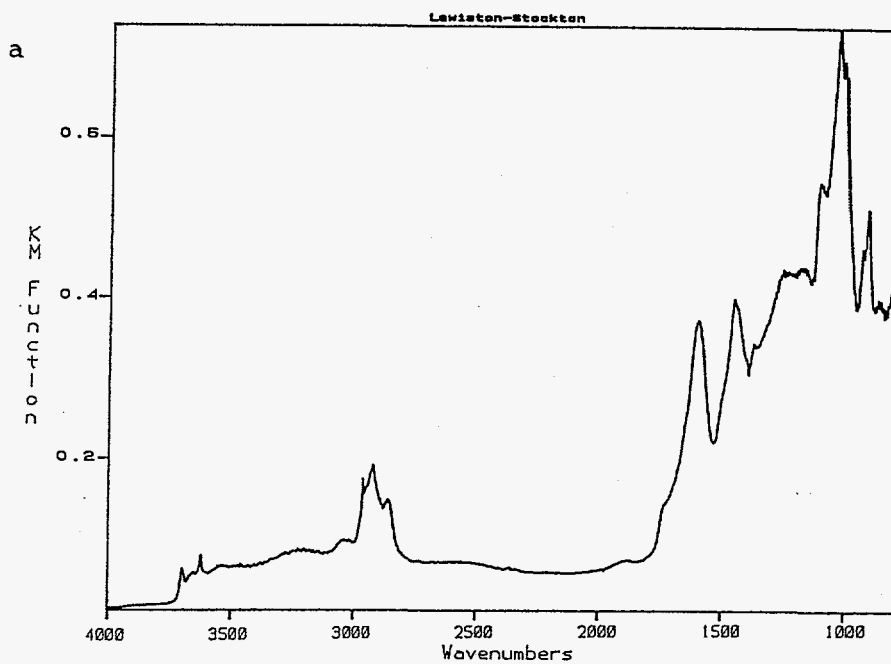


Figure 21. a) DRIFT Spectrum of Lewiston-Stockton Coal;
 b) DRIFT Spectrum of Lewiston-Stockton Coal Containing 20 mg TCNQ/gram of Coal.

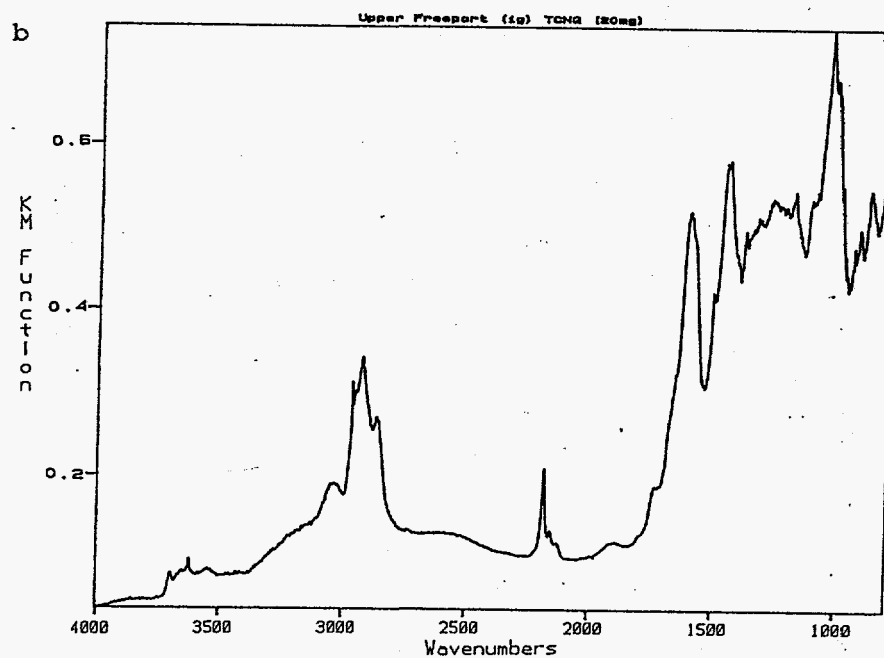
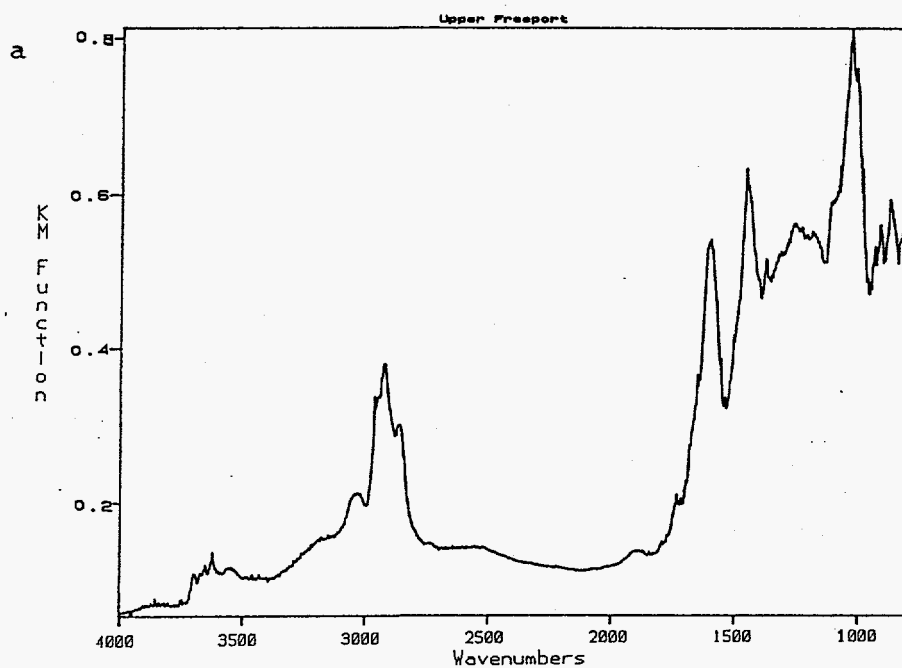


Figure 22. a) DRIFT Spectrum of Upper Freeport Coal; b) DRIFT Spectrum of Upper Freeport Coal Containing 20 mg TCNQ/gram of Coal.

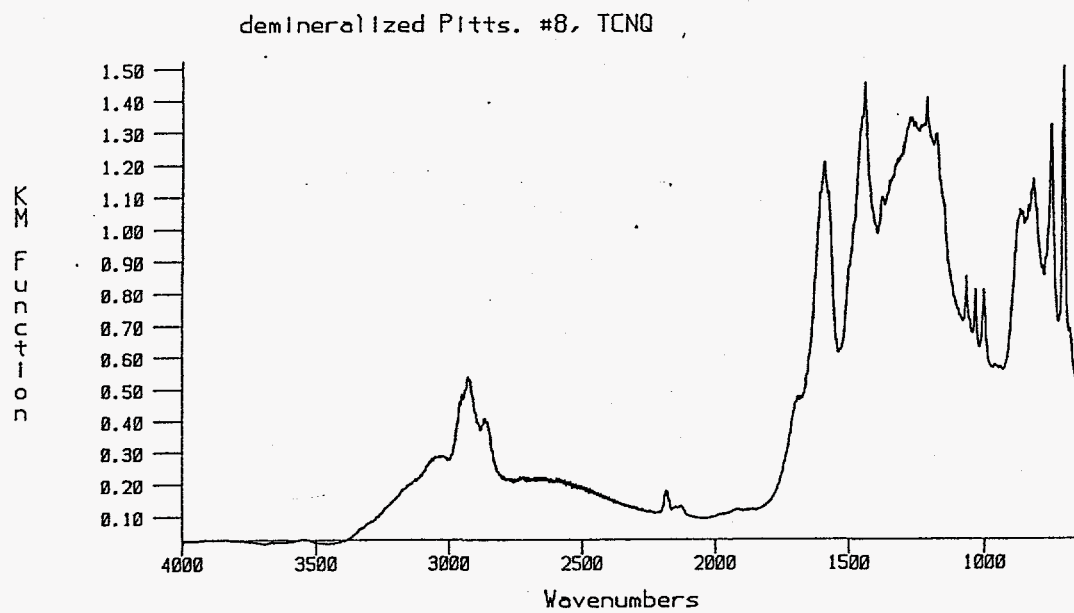


Figure 23. DRIFT Spectrum of a Demineralized Pittsburgh #8 Coal Containing 20 mg TCNQ/gram of Coal.

Illinois #6, TCNE (chlorobenzene)

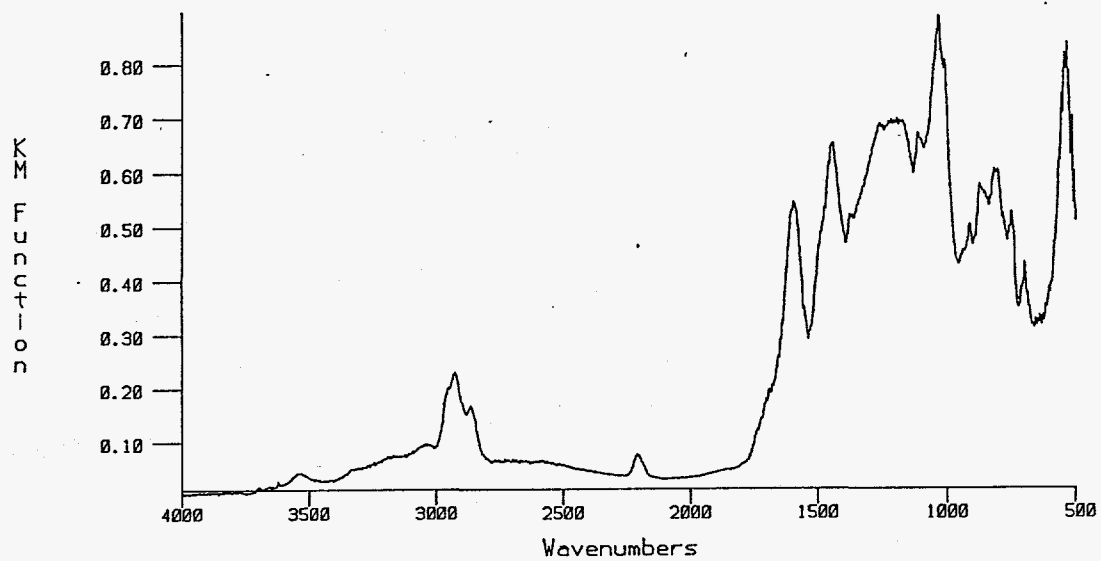


Figure 24. DRIFT Spectrum of Illinois #6 Coal Containing 20 mg TCNE/gram of Coal.

coal would be exceeded resulting in smaller shifts in the $C\equiv N$ stretching frequencies of TCNQ and TCNE. A plot of $C\equiv N$ stretching frequency versus concentration of TCNQ or TCNE in the coal would be a titration curve characterizing both the number and strength of electron donors in coal. Beulah Zap lignite was chosen as a model coal. Because it is a lignite, and has a low aromatic content which is highly oxygenated, it was expected that its donor sites would be quenched rapidly. The coal was loaded with 20, 50 and 100 mg of TCNQ/gram of coal. The resulting IR spectra contained a $C\equiv N$ stretch indicative of complete electron transfer in each case. Figure 25 displays Beulah-Zap with a 100mg loading of TCNQ per gram of the coal.

In 1989, Pugmire et al.⁷⁵ investigated the eight Argonne Premium coal samples using a ^{13}C CP/MAS NMR technique. The data collected from these experiments along with integrations over selected chemical shift ranges were used to derive structural parameters such as percent aromaticity and average PNA size. Table IX displays the %C (dmmf) and the percent aromaticity and average ring sizes as determined by Pugmire and coworkers. Using these data, it was possible to calculate the number of aromatic donors in coal and in turn calculate the

Table IX

Percent aromatic carbon and aromatic carbons per cluster obtained by Pugmire⁷⁵ and coworkers.

<u>Coal</u>	<u>%C(dmmf)</u>	<u>% Aromatic C</u>	<u>Aromatic Carbons per Cluster</u>
Beulah Zap	74.1	54	9
Wyodak	76.0	55	14
Blind Canyon	81.3	63	16
Illinois #6	80.7	70	15
Pittsburgh #8	85.0	70	15
Stockton	85.5	75	14
U. Freeport	88.1	80	18
Pocahontas #3	91.8	85	20

dmmf- dry mineral matter free

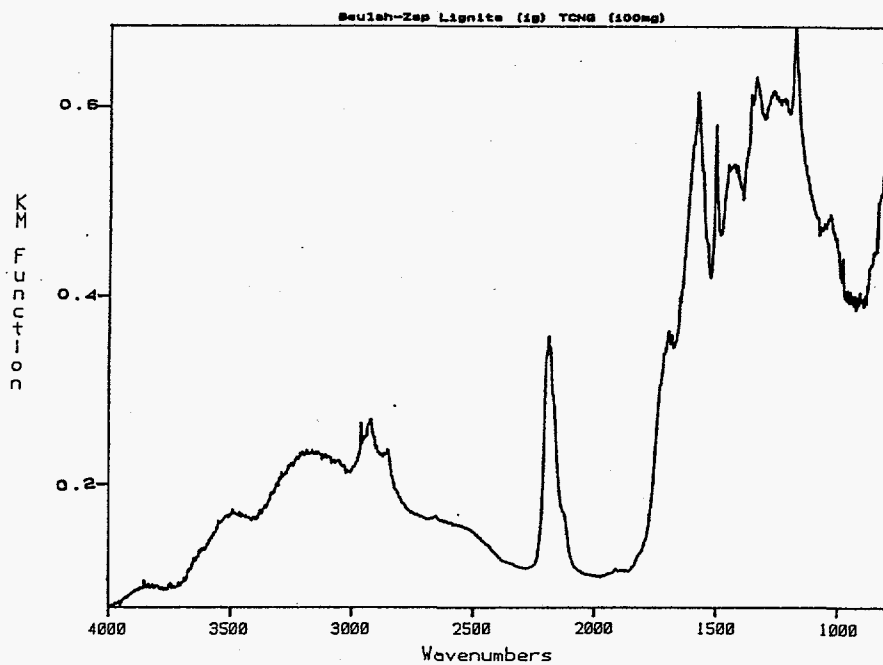


Figure 25. DRIFT Spectrum of Beulah-Zap Lignite Containing 100 mg TCNQ/gram of Coal.

amount of TCNQ or TCNE needed in each coal to make a 1-1 complex with the aromatic donors in coal. The number of aromatic donors for a one gram coal sample was calculated by multiplying the percent carbon of the coal by the percent aromatic carbon⁷⁵ and dividing by 12.011 g/mole. This number was multiplied by Avagadro's number which gave the number of aromatic carbons in the sample. The number of aromatic carbons was then divided by the average number of aromatic carbons per cluster⁷⁵ which gave a rough estimate of the number of PNA's per gram of coal.

Figure 26 shows DRIFT spectra of Illinois #6 coal with 100% loading of TCNQ and TCNE based on the PNA's in the coal. In the case of TCNQ, the nitrile shift corresponds to complete electron electron transfer from the coal to TCNQ. The TCNE Illinois #6 spectrum shows a 36 cm^{-1} shift. Figures 27 through 29 contain spectra of the 1-1 complexes of TCNQ and TCNE (based on PNA's) for Beulah Zap, Pittsburgh #8 and Lewiston Stockton. The nitrile stretch in these spectra also show the same behavior discussed for Illinois #6 coal.

One major feature of all of the spectra containing a 100% loading of TCNQ is the presence of a structureless absorption between $3700\text{ to }2300\text{ cm}^{-1}$. This band may be due to an electronic transition that lies in the infrared

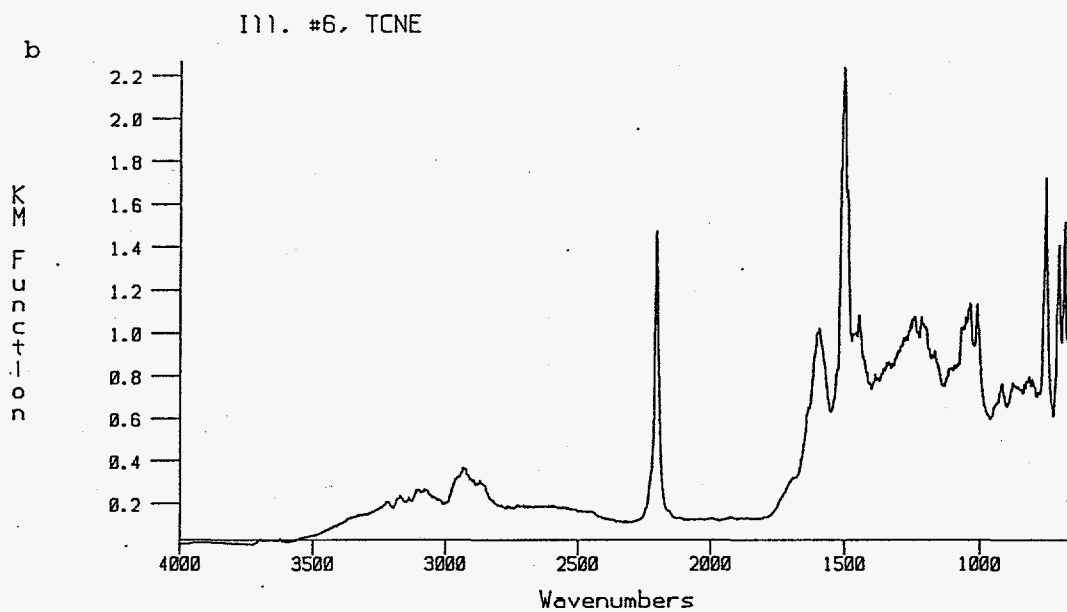
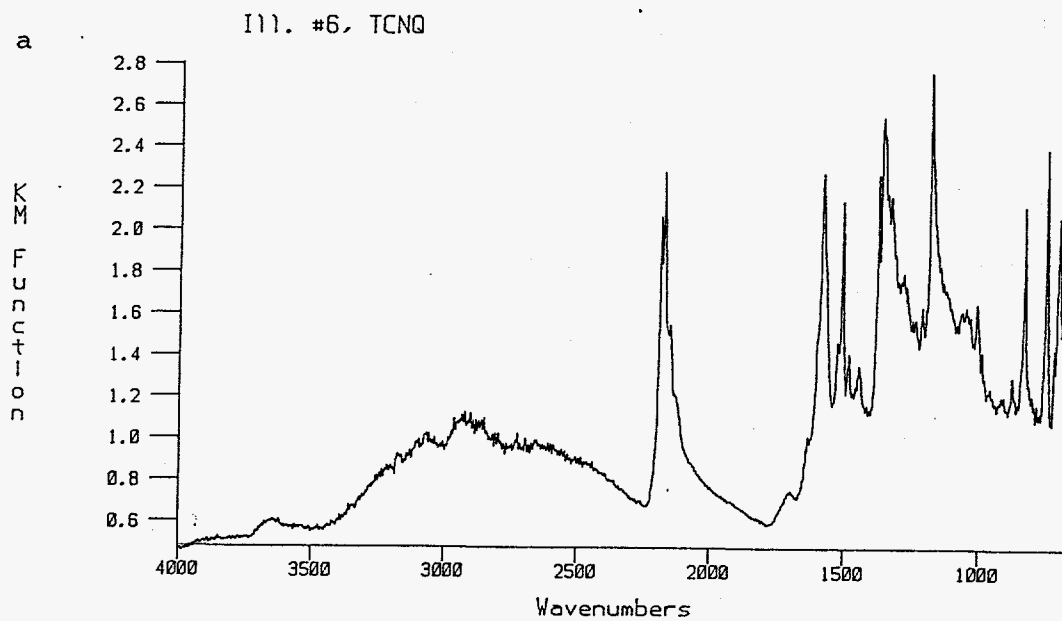


Figure 26. (a) DRIFT Spectrum of Illinois #6 Coal With a 100% Loading of TCNQ. (based on PNA's) (b) DRIFT Spectrum of Illinois #6 Coal With a 100% Loading of TCNE. (based on PNA's)

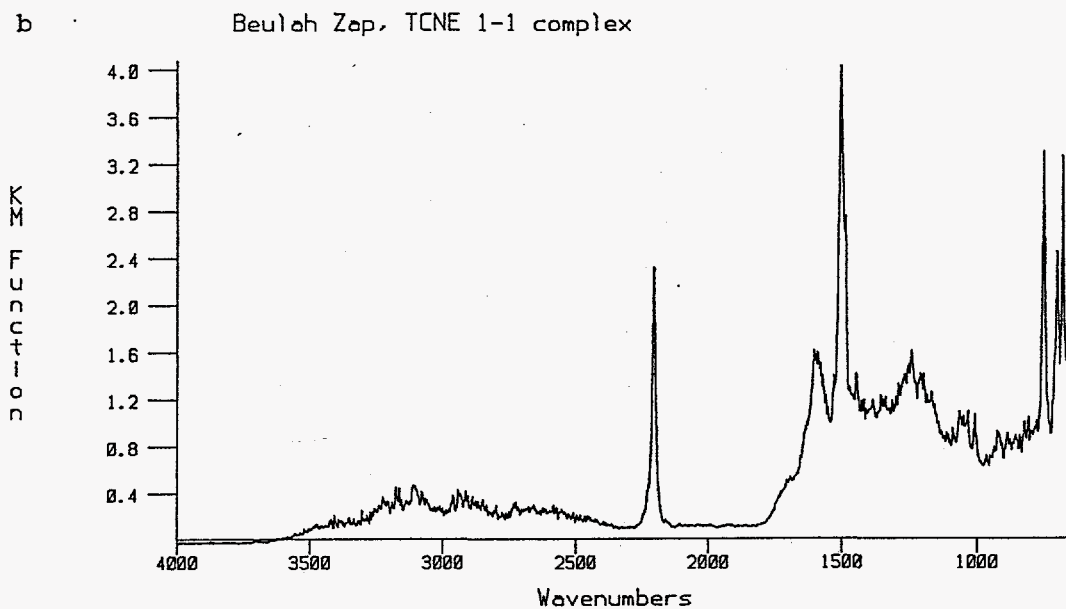
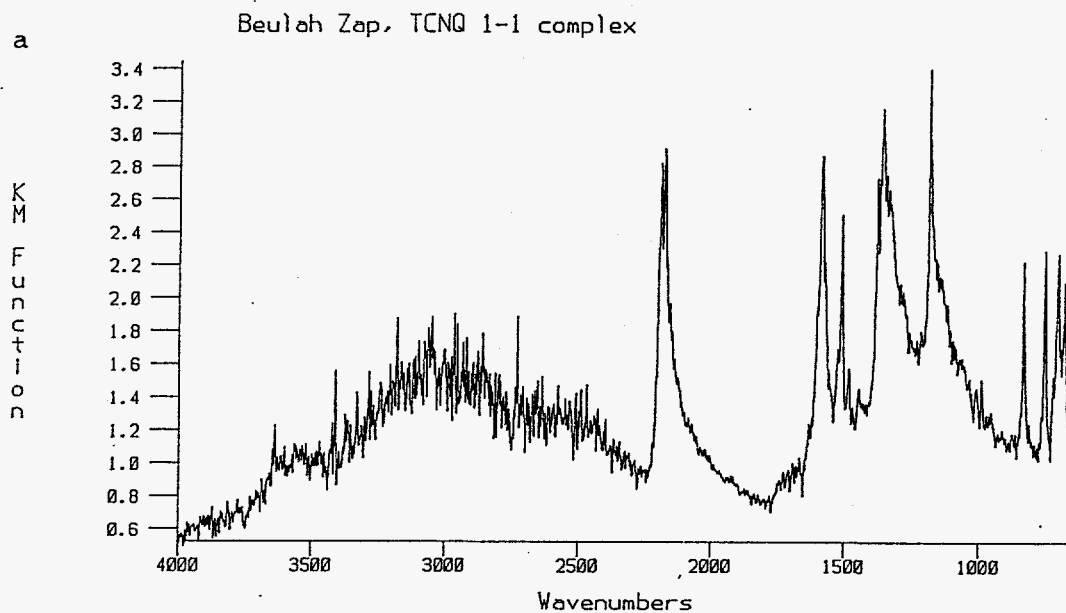


Figure 27. (a) DRIFT Spectrum of Beulah-Zap Lignite With a 100% Loading of TCNQ. (based on PNA's) (b) DRIFT Spectrum of Beulah-Zap Lignite With a 100% Loading of TCNE. (based on PNA's)

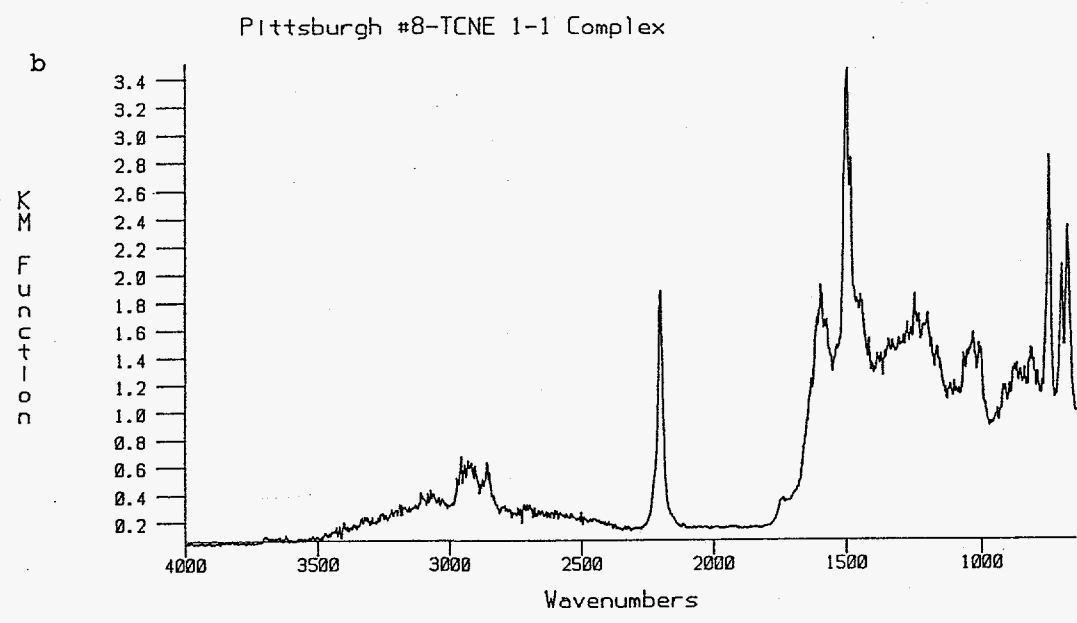
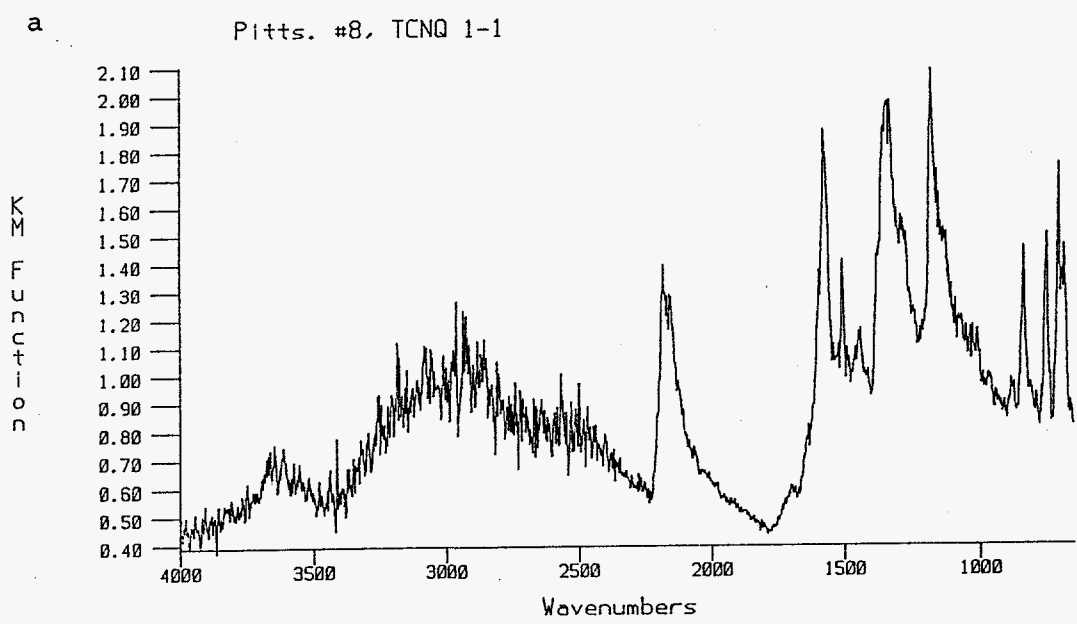


Figure 28. (a) DRIFT Spectrum of Pittsburgh #8 Coal With a 100% Loading of TCNQ. (based on PNA's) (b) DRIFT Spectrum of Pittsburgh #8 Coal With a 100% Loading of TCNE. (based on PNA's)

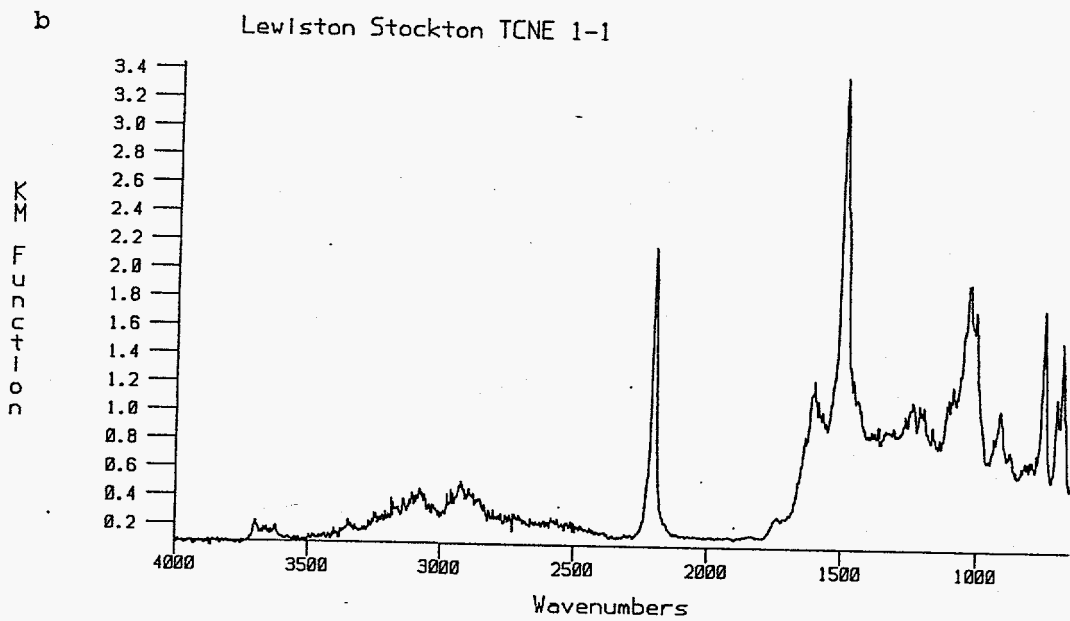
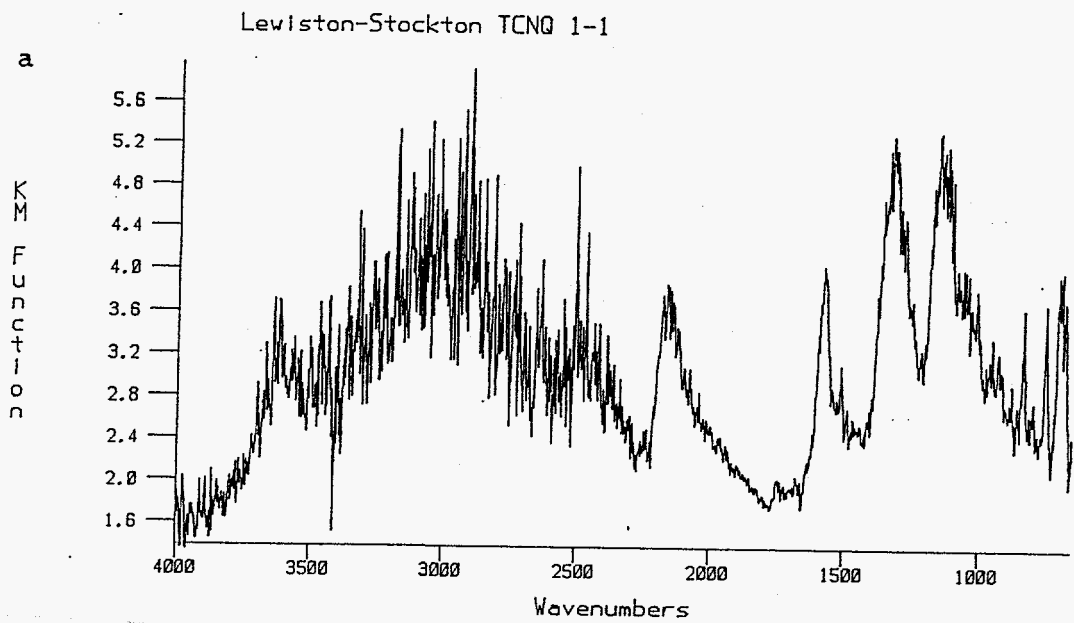


Figure 29. (a) DRIFT Spectrum of Lewiston-Stockton Coal With a 100% Loading of TCNQ. (based on PNA's) (b) DRIFT Spectrum of Lewiston-Stockton Coal With a 100% Loading of TCNE. (based on PNA's)

region. If some type of PNA-TCNQ stack is formed, the energy difference between the HOMO's and LUMO's in such a stack may be sufficiently small for electronic transitions to lie in the infrared region.¹¹⁰

Figures 30 and 31 display the spectra for Upper Freeport and Pocahontas #3 with a 100% loading of TCNQ and TCNE based on PNA's. It is apparent with TCNQ, only a small amount of the acceptor is interacting with the coal. The parent $\text{C}\equiv\text{N}$ stretch at 2227 cm^{-1} dominates the spectrum and only a small amount appears to be completely shifted. The TCNE however, displays a large shift in these coals consistent with the other coals discussed above. Coals above 87% C do not swell appreciably and it is possible that the TCNQ molecule may be too large to penetrate these coals. The TCNE is smaller and even a small amount of swelling may make possible diffusion of the TCNE into the coal network.

The simplest explanation for these shifts is that there exists in coal single electron donors which are capable of transferring an electron to TCNQ in the ground state. All of the TCNQ placed in the coal appears to be converted to the radical anion as displayed in the IR spectrum for all of the coals except for the 100% loading in the two high rank coals. The low loadings of TCNQ (20

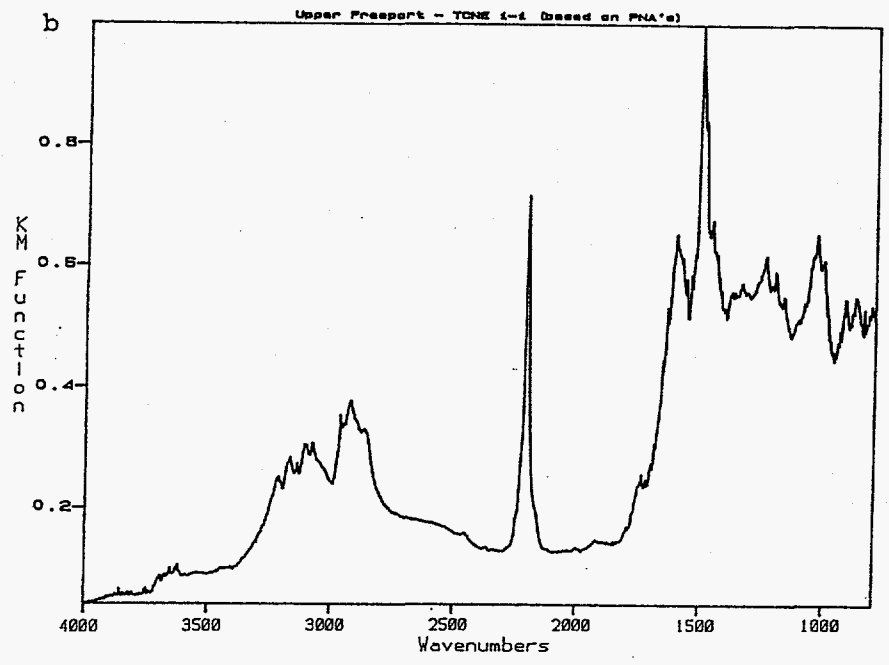
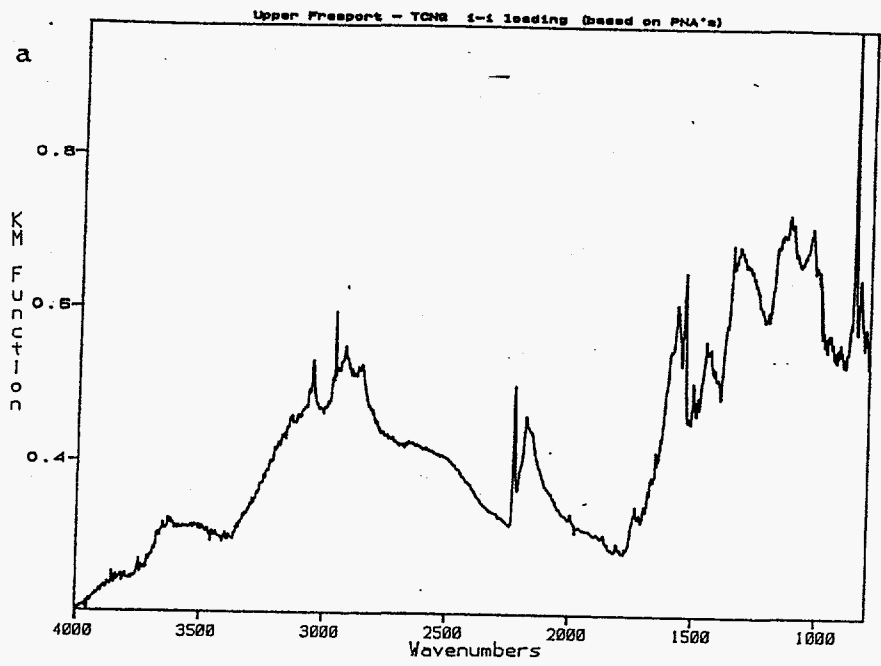


Figure 30. (a) DRIFT Spectrum of Upper Freeport Coal With a 100% Loading of TCNQ. (based on PNA's) (b) DRIFT Spectrum of Upper Freeport Coal With a 100% Loading of TCNE. (based on PNA's)

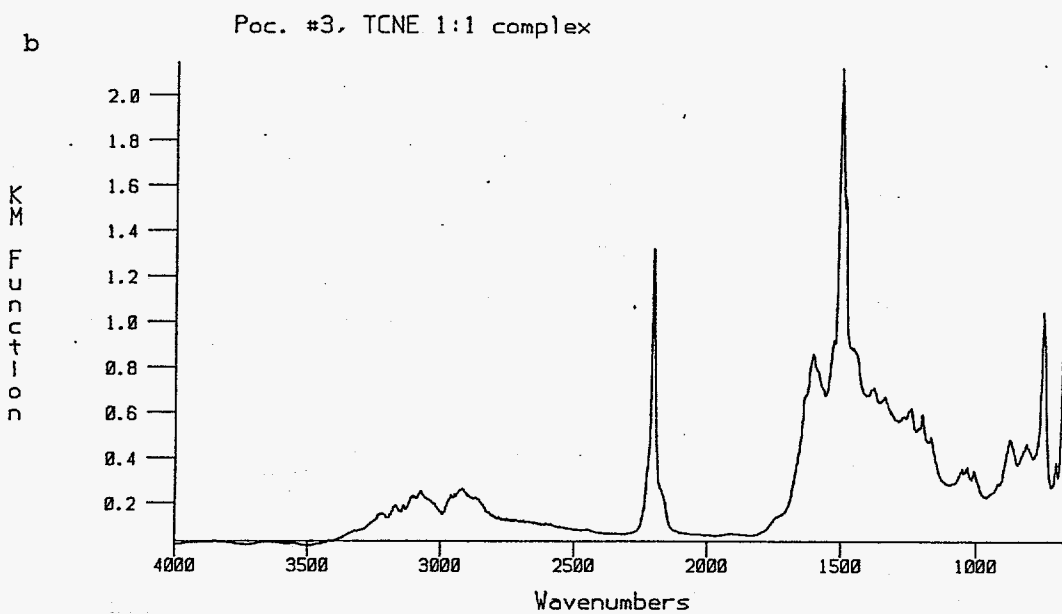
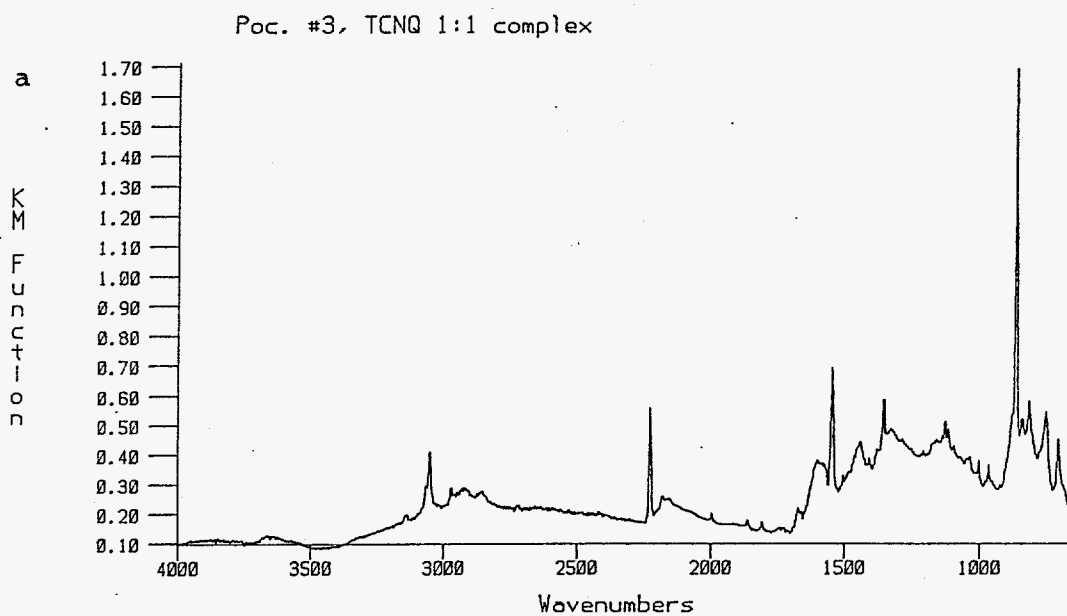


Figure 31. (a) DRIFT Spectrum of Pocahontas #3 Coal With a 100% Loading of TCNQ. (based on PNA's) (b) DRIFT Spectrum of Pocahontas #3 With a 100% Loading of TCNE. (based on PNA's)

mg acceptor/g of coal) contain enough TCNQ to form a complex with 3% of the PNA's in coal. It is very possible that 3% of the PNA's in coal have a sufficiently low ionization potential to transfer an electron to TCNQ. However, in a 100% loading, it is highly unlikely that all or most of the PNA's in coal have a sufficiently low ionization potential to donate an electron to TCNQ.

Another explanation for the shift is that there are cooperative interactions between the TCNQ or TCNE with the aromatic species in the coal. The TCNQ or TCNE form extensive stacks with the aromatic groups in coals. This interaction leads to the formation of an extended valence band structure with the TCNQ LUMO being half filled; occupied with one electron. In the case of TCNE, its LUMO is approximately 30% occupied.

It is known that when coals are swollen with pyridine that not all of the pyridine can be removed from coal.⁶⁹ If stacks are being formed between PNA's in the coal and TCNQ or TCNE, it is possible that pyridine may be participate in the formation of these stacks. Table X displays the amount of pyridine in five of the Argonne coals studied containing a 100% loading of TCNQ (based on PNA's) after drying. Table X also compares the moles of pyridine retained with the moles of TCNQ in each sample. These data show that pyridine may be important for the

Illinois #6 and Pittsburgh #8 samples containing a 100% loading of TCNQ (based on PNA's) but is much less important for the Beulah-Zap, Lewiston-Stockton and Pocahontas #3 samples. Work performed using acetonitrile instead of TCNQ (see figure 25) indicates that the presence of pyridine is not necessary to form these stacks.

Table X

Amount of Pyridine Contained (in grams and moles) in Argonne Premium Coals With a 100% Loading of TCNQ (based on PNA's) Compared to the Number of Moles of TCNQ.

<u>Coal</u>	<u>Grams Pyridine Retained</u>	<u>Moles Pyridine</u>	<u>Moles TCNQ</u>	<u>Moles pyridine/ Moles TCNQ</u>
Beulah-Zap	0.08	1.0×10^{-3}	1.8×10^{-2}	0.06
Illinois #6	0.06	7.6×10^{-4}	2.5×10^{-3}	0.30
Pittsburgh #8	0.06	7.6×10^{-4}	3.3×10^{-3}	0.23
Lewiston-Stockton	0.04	5.1×10^{-4}	1.9×10^{-2}	0.03
Pocahontas #3	0.08	1.0×10^{-3}	1.6×10^{-2}	0.06

B. Diffuse Reflectance Infrared (DRIFT) Spectra of Pyridine Coal Residues and Extracts with TCNO and TCNE

Coal pyridine extracts and residues are believed to be representative of the whole coal in the sense that they contain roughly the same aromatic and elemental ratios as the whole coals from which they were obtained. In 1989 Davis et al. published ^{13}C CP/MAS and ^1H liquid NMR studies of an Illinois #6 whole coal and its pyridine extract and residue.¹¹¹ Their results show that short and straight chain alkyl groups are transferred preferentially to the extract of the coal, but for the most part, the structural distribution in the extract and residue resembles that of the original coal.

The physical structure of whole coals compared to the pyridine residues are very different. Table XI displays the fractal dimensionalities of the pore surfaces of an Illinois #6 and Pittsburgh #8 whole coal compared with the pyridine extracted coals. The fractal dimensionalities were obtained from small angle X-ray scattering (SAXS).¹¹² The fractal dimensionality is a global measure of surface irregularity and always lies between two and three ($2 \leq D \leq 3$).

The pyridine residues of the Illinois #6 and the Pittsburgh #8 coals have a lower fractal dimensionality

Table XI

Fractal Dimensionalities of Argonne Illinois #6 and
Pittsburgh #8 Coals Compared to Their Pyridine Residues.

<u>Coal</u>	<u>D (SAXS)</u>
Illinois #6	2.85
Illinois #6 pyridine residue	2.57
Pittsburgh #8	2.68
Pittsburgh #8 pyridine residue	2.51

*Results obtained by Dr. Peter Hall and Patrick Wernett

than the whole coals from which they were derived. Essentially, the surface of the coal residues are less rough.

Figure 32 displays a differential scanning calorimetry (dsc) thermogram comparing a fresh Pittsburgh #8 coal with a pyridine extracted and dried Pittsburgh #8 coal. The dsc thermogram plots the heat capacity change of the samples vs. temperature. The fresh coal displays a higher heat capacity than the pyridine extracted coal. This implies that the fresh coal has more degrees of freedom than the extracted coal. After the pyridine extraction process, the movement of coal molecules in a Pittsburgh #8 sample is restricted.

The different interactions of the pyridine extracts and residues with TCNQ and TCNE as compared to coals may help elucidate whether it is the physical or chemical structure of coals which is responsible for the interactions with these acceptors in whole coals. If individual PNA's in coals are transferring an electron to TCNQ, the same behavior observed for the whole coals should be observed for residues and extracts. If the spatial distribution of groups in the coal or some other physical structural features are important, the interaction with TCNQ and TCNE will be different.

TCNQ and TCNE were deposited in Illinois #6 and

Effect of Pyridine Extraction and Drying on
Low Temperature DSC of Pittsburgh #8

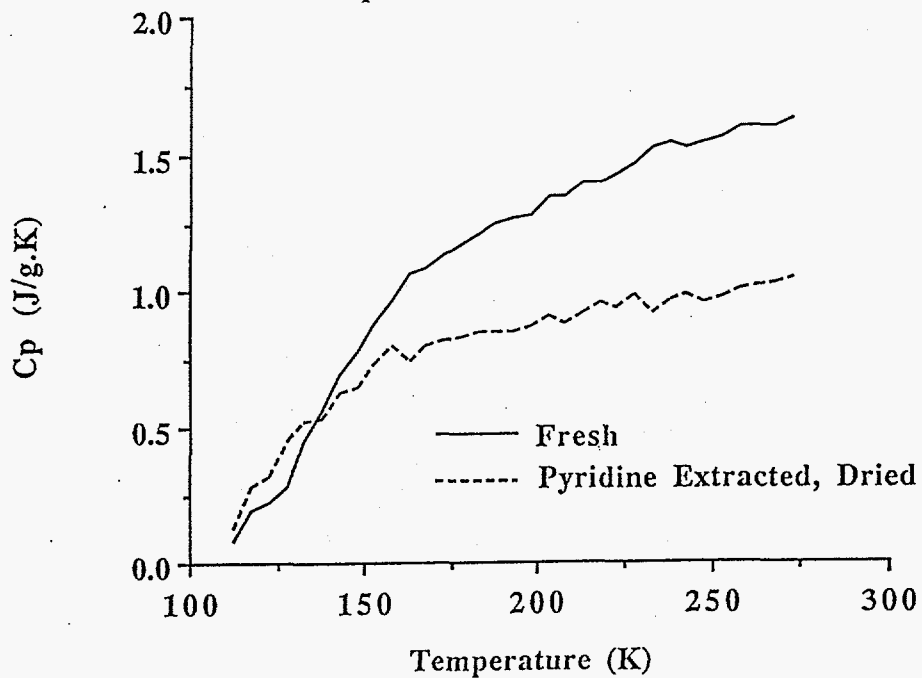


Figure 32. Diferential Scanning Calorimetry (dsc) Thermogram Comparing the Heat Capacity (Cp) of Pittsburgh #8 Coal and a Pittsburgh #8 Pyridine Residue.

Pittsburgh #8 pyridine extracts and residues in increments of 10, 50 and 100% loadings based on the PNA's in each sample.⁷⁵ Figures 33 through 35 contain DRIFT spectra of samples prepared with 10, 50 and 100% loadings of TCNQ on an Illinois #6 residue. The 10% loading of TCNQ on the residue in Figure 33 looks typical of the $C\equiv N$ shifts observed with the parent Illinois #6 coal. The only difference is that the spectra appear to be quite noisy. Figure 34 contains the DRIFT spectrum of the Illinois #6 residue with a 50% loading of TCNQ. Large changes compared to the parent coal are obvious. First, not all of the TCNQ $C\equiv N$ stretch is shifted the full 44 cm^{-1} . A significant amount of the TCNQ is not shifted. Similarly to the 10% loading, the 50% loading is very noisy. Figure 35 displays an Illinois #6 pyridine residue with a 100% loading of TCNQ based on PNA's. The spectrum is similar to the 50% loading of TCNQ.

Figures 36 and 37 display a 50 and 100% loading of TCNQ (based on PNA's) on an Illinois #6 pyridine extract. In both cases there is a large unshifted TCNQ $C\equiv N$ stretch, reminiscent of the spectra of TCNQ with an Illinois #6 pyridine residue. It is clear that the pyridine residues and extracts from an Illinois #6 coal react differently with TCNQ than does the whole coal.

Figures 38 through 40 display the DRIFT spectra of an

Ill. #6 pyridine residue, 10% TCNQ

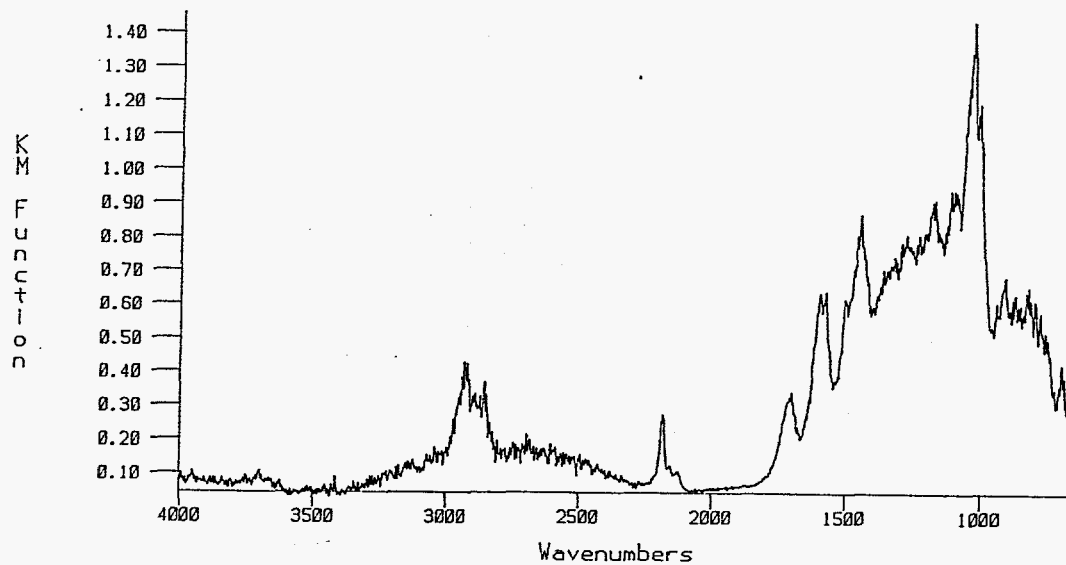


Figure 33. DRIFT Spectrum of an Illinois #6 Pyridine Residue with a 10% Loading of TCNQ. (based on PNA's)

Ill. #6 pyridine residue, 50% TCNQ

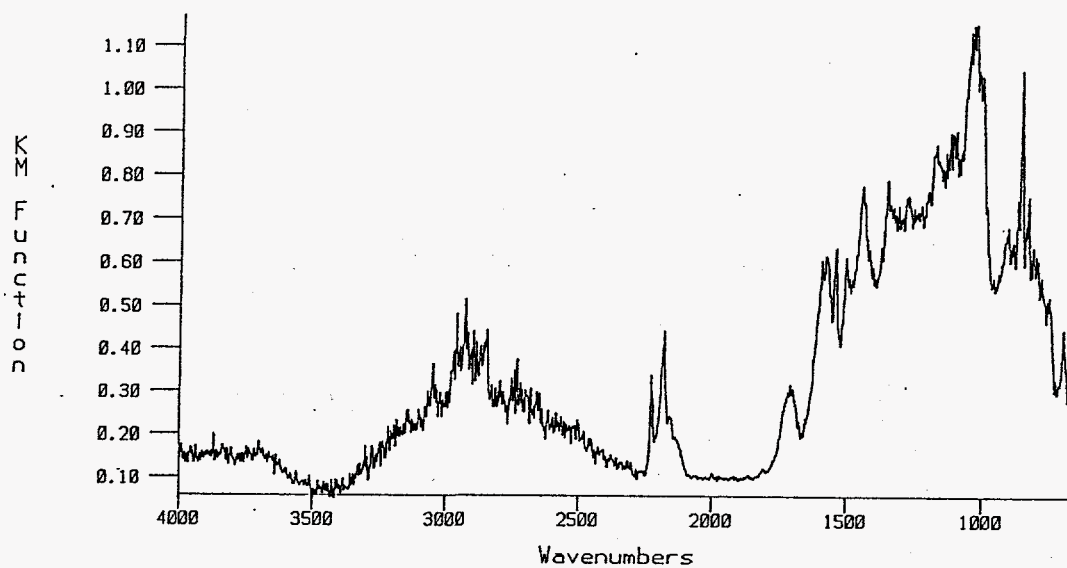


Figure 34. DRIFT Spectrum of an Illinois #6 Pyridine Residue with a 50% Loading of TCNQ. (based on PNA's)

Ill. #6 pyridine residue, 100% TCNQ

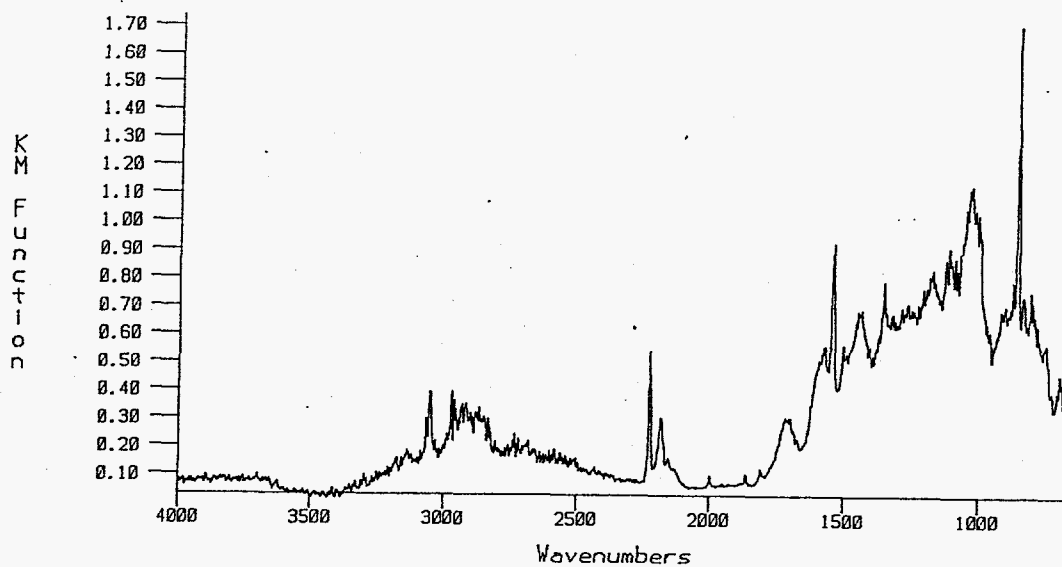


Figure 35. DRIFT Spectrum of an Illinois #6 Pyridine Residue with a 100% Loading of TCNQ. (based on PNA's)

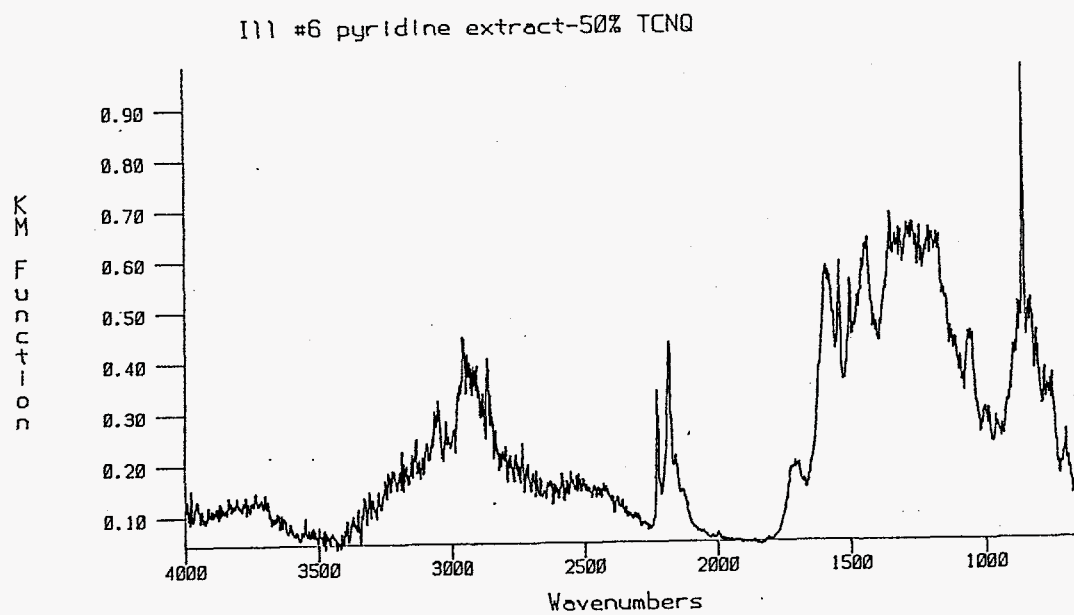


Figure 36. DRIFT Spectrum of an Illinois #6 Pyridine Extract with a 50% Loading of TCNQ. (based on PNA's)

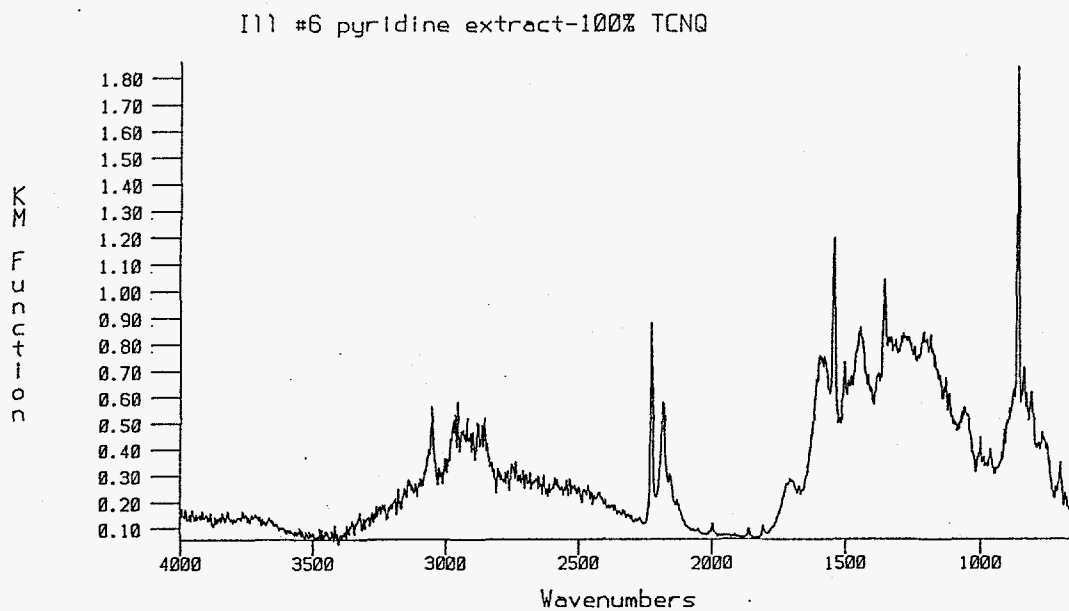


Figure 37. DRIFT Spectrum of an Illinois #6 Pyridine Extract with a 100% Loading of TCNQ. (based on PNA's)

Illinois #6 pyridine residue with 10, 50 and 100% loadings of TCNE. (based on PNA's) The 10 and 50% loadings display the 36 cm^{-1} shift that was observed with the whole coal. The 100% loading in Figure 40 begins to show a shoulder at 2254 cm^{-1} which is the asymmetric $\text{C}\equiv\text{N}$ stretch of TCNE. Again, these spectra are also very noisy. Figures 41 through 43 display 10, 50 and 100% loadings of TCNE on a Illinois #6 pyridine extract. The same behavior is observed for these samples that was observed for the same loadings on the corresponding Illinois #6 pyridine residues.

Pittsburgh #8 pyridine residues and extracts have the same behavior as the Illinois #6 pyridine residues. Figures 44 and 45 display a Pittsburgh #8 pyridine extract with a 50% loading of TCNQ and TCNE respectively. Again, even at 50% loadings there is uncomplexed TCNQ and TCNE present in the DRIFT spectrum. These data show that the pyridine residues and extracts interact differently with TCNQ and TCNE than do the whole coals.

Work performed with single electron acceptors and polymers (discussed in the introduction) have shown that the spatial distribution of aromatic donors is important in determining the strength of binding between single electron acceptors and polymers. It is certain that pyridine extractions of coal disrupts its network system.

Ill. #6 pyridine residue, 10% TCNE

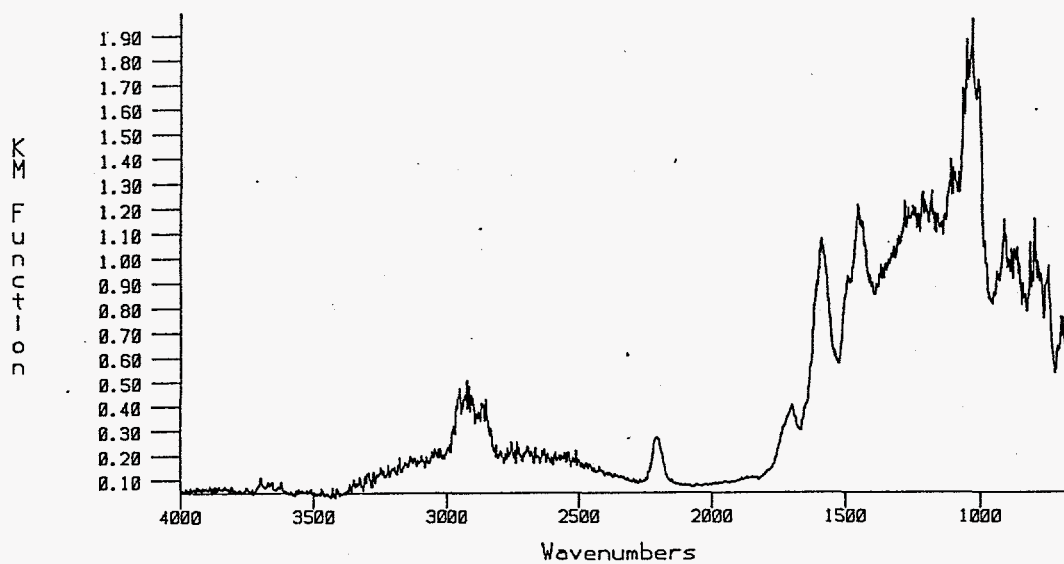


Figure 38. DRIFT Spectrum of an Illinois #6 Pyridine Residue With a 10% Loading of TCNE. (based on PNA's)

Ill. #6 pyridine residue, 50% TCNE

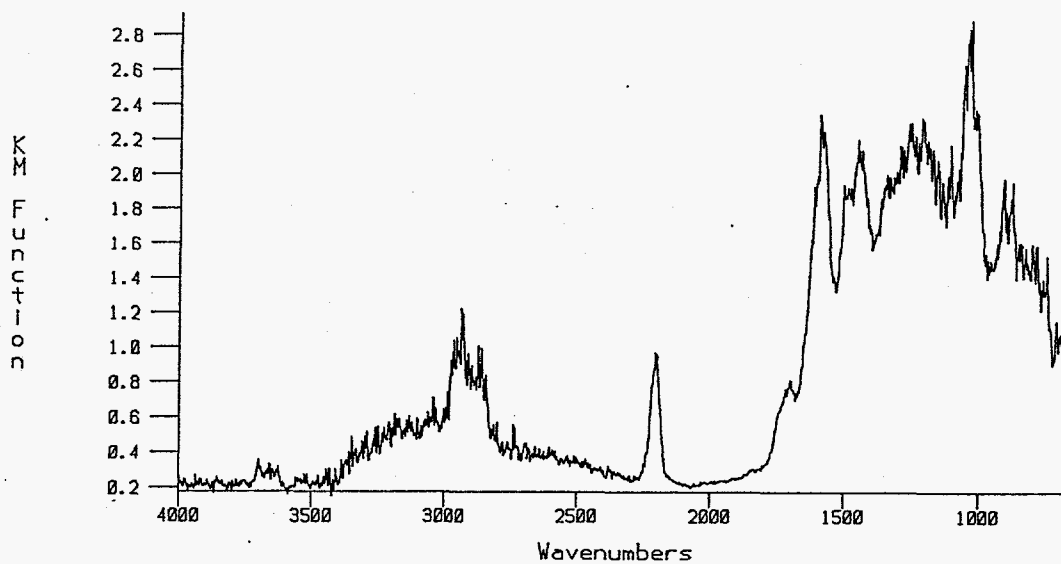


Figure 39. DRIFT Spectrum of an Illinois #6 Pyridine Residue With a 50% Loading of TCNE. (based on PNA's)

Ill. #6 pyridine residue, 100% TCNE

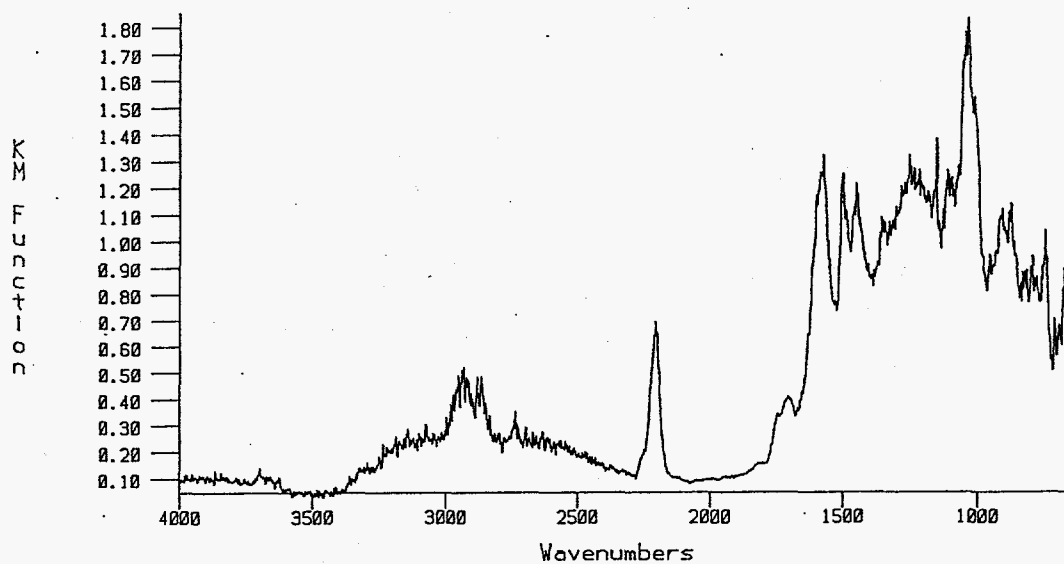


Figure 40. DRIFT Spectrum of an Illinois #6 Pyridine Residue With a 100% Loading of TCNE. (based on PNA's)

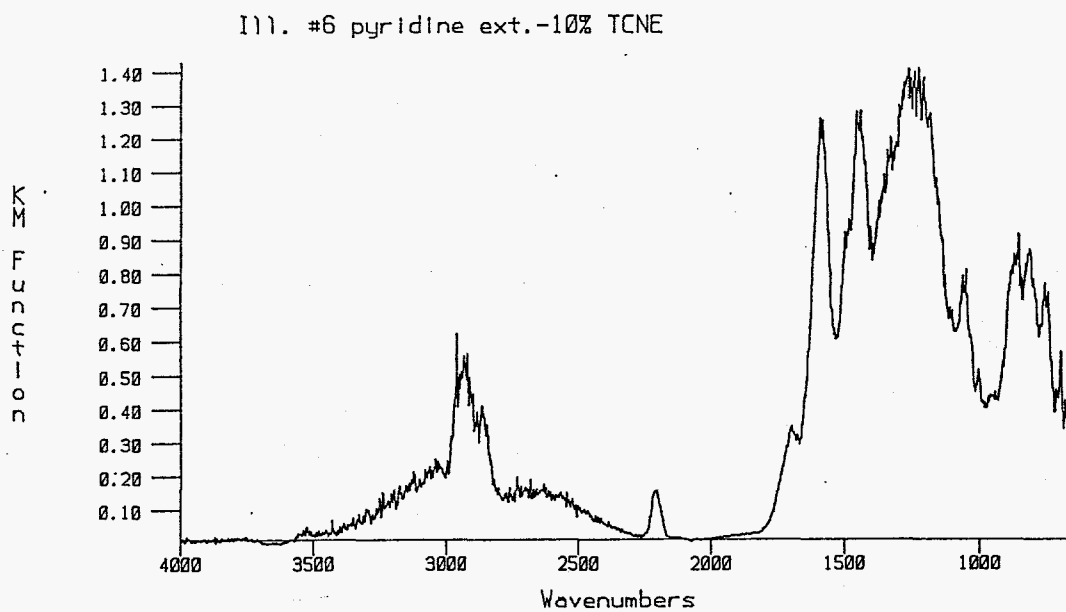


Figure 41. DRIFT Spectrum of an Illinois #6 Pyridine Extract With a 10% Loading of TCNE. (based on PNA's)

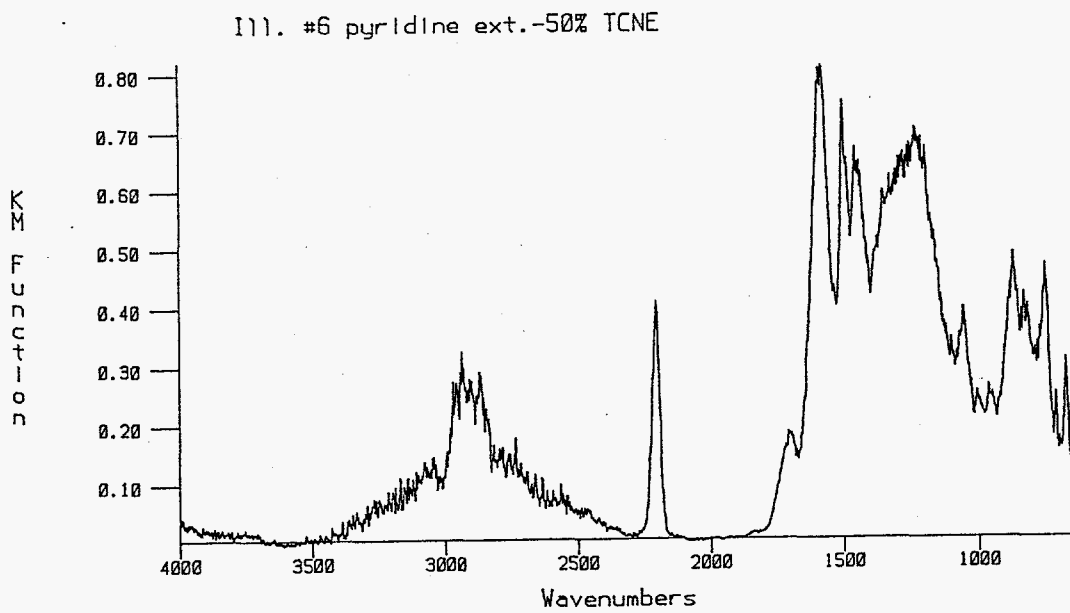


Figure 42. DRIFT Spectrum of an Illinois #6 Pyridine Extract With a 50% Loading of TCNE. (based on PNA's)

Ill. #6 pyridine ext.-100% TCNE.

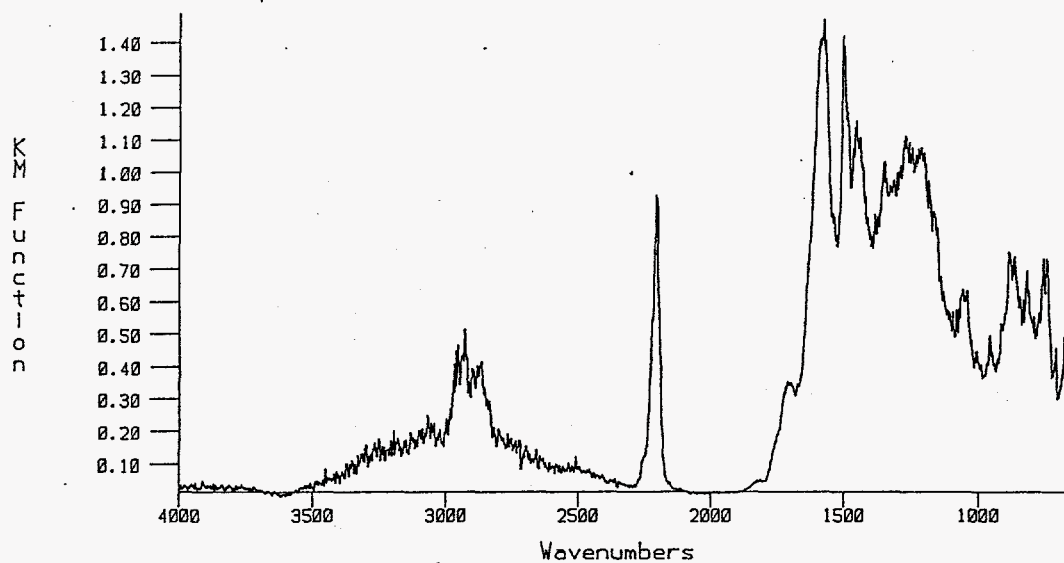


Figure 43. DRIFT Spectrum of an Illinois #6 Pyridine Extract with a 100% Loading of TCNE. (based on PNA's)

Pitts #8 pyridine extract-50% TCNQ

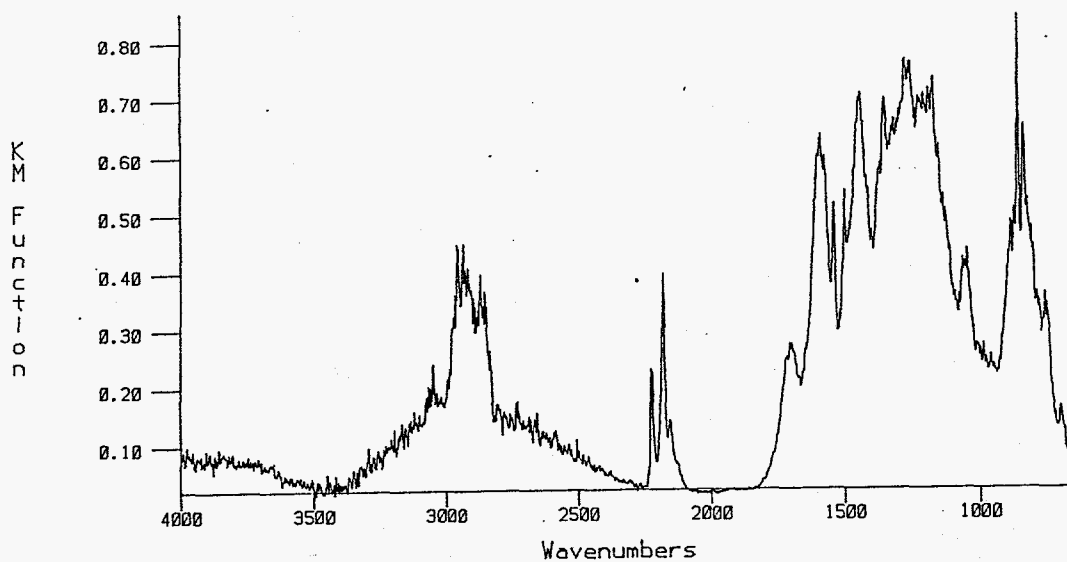


Figure 44. DRIFT Spectrum of a Pittsburgh #8 Pyridine Extract With a 50% Loading of TCNQ. (based on PNA's)

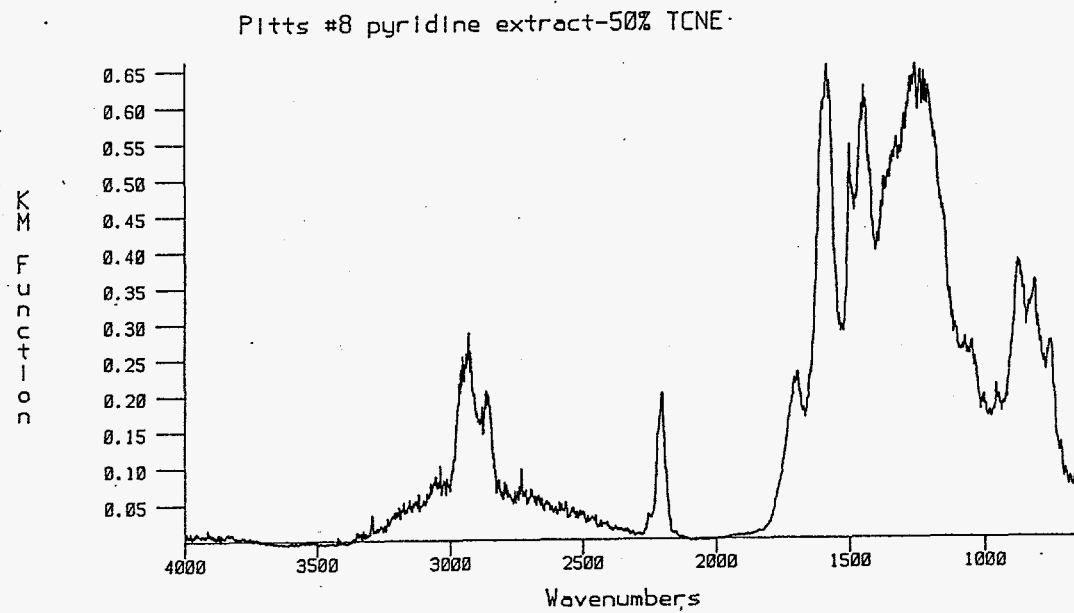


Figure 45. DRIFT Spectrum of Pittsburgh #8 Pyridine Extract With a 50% Loading of TCNE. (based on PNA's)

The decrease in surface area of residues and their lower heat capacities support this conclusion. It is quite possible the arrangement of aromatic systems in whole coals is conducive to forming stacks with TCNQ and TCNE. To understand the large $C\equiv N$ stretching frequency shift observed, it was necessary to study some complexes of TCNQ and TCNE with some PNA's which may be found in coals.

C. Absorbance Infrared Spectra of Aromatic Compounds with TCNQ and TCNE in Solution and in the Solid State.

The interaction between single electron acceptors and aromatic donors has been well studied. The molecules involved in these assemblies are referred to as charge transfer complexes. In 1949 Benesi and Hildebrand¹¹³ reported that solutions containing an aromatic hydrocarbon and molecular Iodine contained an electronic absorption band in the ultraviolet spectrum which could not be attributed to either compound alone. In 1952 Mulliken suggested that the characteristic absorption observed in the uv spectrum could arise through an inter-molecular charge-transfer transition.¹¹⁴ The resulting valence bond treatment proposed by Mulliken for complex formation between electron donors and acceptors provided an explanation for many previous observations and was the main stimulus for the extensive developments in this area since 1952.

Dewar has criticized the term "charge-transfer" because the term reflects a particular valence-bond description. In many of these charge transfer complexes single electron transfer does not provide the major contribution to binding in the ground state.^{115,116} Dewar provided a rational explanation that attributes the binding in these charge-transfer complexes to dispersion,

dipole-dipole and dipole-induced dipole forces.

Nonetheless, the term charge-transfer complex has a wide usage in the literature describing weak interactions between electron donors and acceptors.

Typically, charge transfer complexes are studied by employing uv spectroscopy. UV spectroscopy in tandem with the Benesi-Hildebrand equation, allows one to obtain a binding constant for these complexes. The literature in this area is well reviewed.^{22,117} Abundant data are available showing that the equilibrium constants for TCNE and aromatic donors are low.^{118,119} Equilibrium constants for TCNQ and aromatic donors are rare because of the limited solubility of TCNQ.

We decided to study the interactions of TCNQ and TCNE with aromatic donors in solution. In solution these charge transfer complexes form discrete 1-1 dimers.⁷⁶ Solid state complexes form extensive stacks whose properties are very complex and different than the discrete dimers formed in solution. If 1-1 complexes are being formed between the electron acceptors and PNA's in the coal network, solution studies will provide insight into the process.

We obtained the IR spectra of complexes formed between TCNQ, TCNE and a number of aromatic donors. Table XII contains a list of aromatic donors with TCNQ and

the observed change in the $C\equiv N$ stretching frequency. Table XIII displays a list of aromatic donors with TCNE and the observed change in the $C\equiv N$ stretching frequency. The nitrile shifts for some of the solid state complexes with TCNQ and TCNE are displayed in Tables XII and XIII respectively. The FTIR solution spectra of these complexes were obtained on a Mattson Polaris FTIR spectrometer. The solutions prepared for IR analysis were millimolar in complex concentration to avoid any solubility problems with the complex and TCNQ or TCNE.

It is immediately apparent that none of the molecules complexed with TCNQ is capable of donating a significant amount of electron density in solution. In the solid state coronene and phenothiazine donate a fair amount of electron density to TCNQ. Coronene (structure shown below) is a large aromatic ring system which probably has a low ionization potential compared to the other PNA's complexed with TCNQ. Phenothiazine (shown below) contains sulfur which is a good single electron donor.

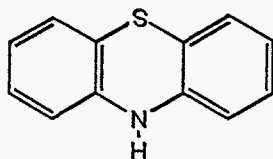
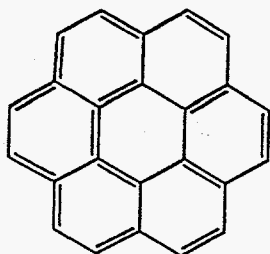


Table XII
 Model aromatic compounds complexed with TCNQ. The nitrile shift is displayed in chloroform solution and the solid state

Compound	$\Delta C\equiv N$ stretch (CHCl ₃)	$\Delta C\equiv N$ stretch (solid state)
Fluoranthene	3.2	8.0, 31
9-Methylanthracene	3.6	7.0
2-Methoxynaphthalene	3.7	
1-Methoxynaphthalene	3.2	6.0
Pyrene	4.4	7.0
Hexamethylbenzene	3.7	
Dibenzofuran	3.4	
1-Naphthol	3.5	
3,5-Dimethoxyphenol	3.6	
3-Methoxyphenol	3.9	
Phenanthrene	3.5	5.1
Dibenzothiophene	3.4	
1,2,3,4-Dibenzanthracene	3.7	
4-Phenylphenol	3.7	9.0
Phenothiazine	2.7	13.8
Pyrazole	3.6	
2-Ethylanthracene	3.4	4.0
Biphenyl	3.2	6.0
Toluene	2.4	

Table XII (continued)

Compound	$\Delta C\equiv N$ stretch ($CHCl_3$)	$\Delta C\equiv N$ stretch (solid State)
9-Hydroxy-4-methoxyacridine	3.9	
2,3,5-Trimethylpyrazine	3.4	
1,3,5-Trimethoxybenzene	3.2	4.0
Coronene		9.0
Pyridine	3.0	
9-Phenanthrol	3.9	

Table XIII
 Model Aromatic Compounds Complexed with TCNE. The Nitrile Shift is Displayed in Chloroform Solution and the Solid State

Compound	$\Delta C\equiv N$ stretch (CHCl ₃)	$\Delta C\equiv N$ stretch (solid state)
Phenanthrene	3.3	
Dibenzothiophene	3.5	14.0
Pyrene	3.3	
1,3,5-Trimethoxybenzene	3.0	
1-Methoxynaphthalene		
Dibenzofuran	3.0	19.0
Hexamethylbenzene	3.0	
DPPD	8.0	
Perylene	3.3	
Benzo[e]pyrene	2.8	
9-Methylantracene	(-)	
Thianaphthene	3.0	
Benzo[a]pyrene	2.8	
Carbazole	3.4	
2,6-Dimethylnaphthalene	3.0	
2,3-Dihydroxynaphthalene	(-)	16.0
9-Phenanthrol	5.5	11.0
Fluoranthene	3.1	
1,3-Dimethoxybenzene	3.0	

(-) denotes chemical reaction

The solid state absorbance IR spectra of fluoranthene and pyrene both have shoulders in the $C\equiv N$ stretch at 2200 cm^{-1} . The Fluoranthene-TCNQ complex was interesting because its color resembled metallic copper. Figure 46 shows the solid state absorbance spectrum of mixed fluoranthene and TCNQ. The $C\equiv N$ stretch shows an 8 cm^{-1} shift and a shoulder at 2200 cm^{-1} . Peter Hall obtained an X-ray spectrum of this complex. The spectrum displayed normal van der Waals distance between the TCNQ and Fluoranthene.¹²⁰ Charge transfer complexes with a high amount of electron transfer usually display molecular distances about 0.4 \AA less than normal van der Waals distances.¹¹⁷

The solution spectra of TCNE display similar nitrile shifts as the IR spectra of the TCNQ complexes. One difference is the 8 cm^{-1} nitrile shift for the DPPD-TCNE complex. Aromatic amines such as DPPD are known to be good donors in charge transfer complexes. Another major difference is the TCNE undergoes more reactions with the PNA's studied. 9-methylanthracene undergoes a Diels Alder type reaction with TCNE. Upon mixing TCNE and 9-methylanthracene, the solution immediately turns blue. Within a matter of a few seconds the solution becomes clear. The nitrile band in the IR spectrum is shifted

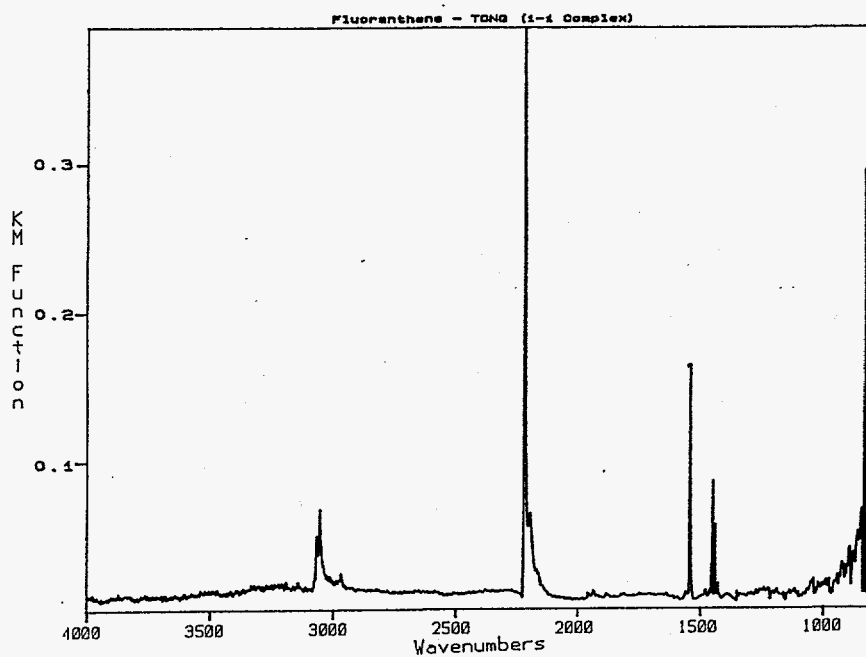
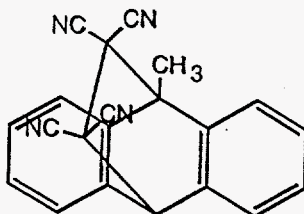


Figure 46. Solid State FTIR Absorbance Spectrum of a 1-1 Complex of Fluoranthene and TCNQ.

to 2254 cm^{-1} which is indicative of an aliphatic nitrile. Figure 47 displays the ^1H NMR spectrum of The TCNE 9-methylantracene reaction product. Integration gives 8 protons in the aromatic region, 3 methyl group protons at 2.45 ppm, and a proton at the 10 position of the anthracene at 5.05 ppm. The product is shown below



The molecule 2,3-dihydroxynaphthalene was initially thought to be oxidized by TCNE. Figure 48 displays the DRIFT spectra of 2,3-dihydroxynaphthalene and the TCNE-2,3-dihydroxynaphthalene complex. A band appears in the complex spectrum at 1700 cm^{-1} which suggests the presence of a carbonyl group. ^{13}C NMR spectra failed to show the presence of any carbonyl. The band may be due to an overtone.

The FTIR solution spectra of aromatic donors complexed with TCNQ and TCNE display no evidence for a significant amount of electron transfer. The association

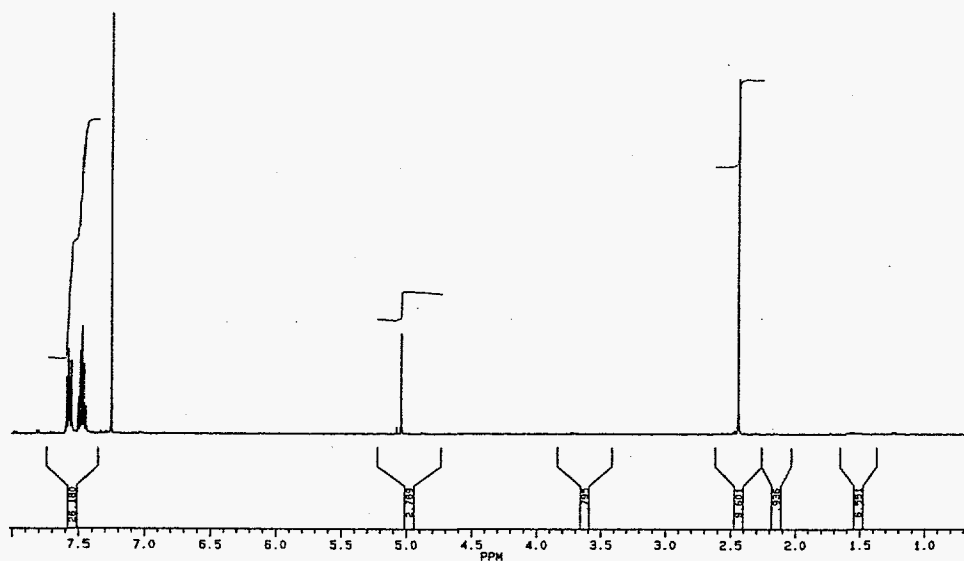


Figure 47. ^1H NMR Spectrum of Reaction Product of 9-Methylanthracene and TCNE.

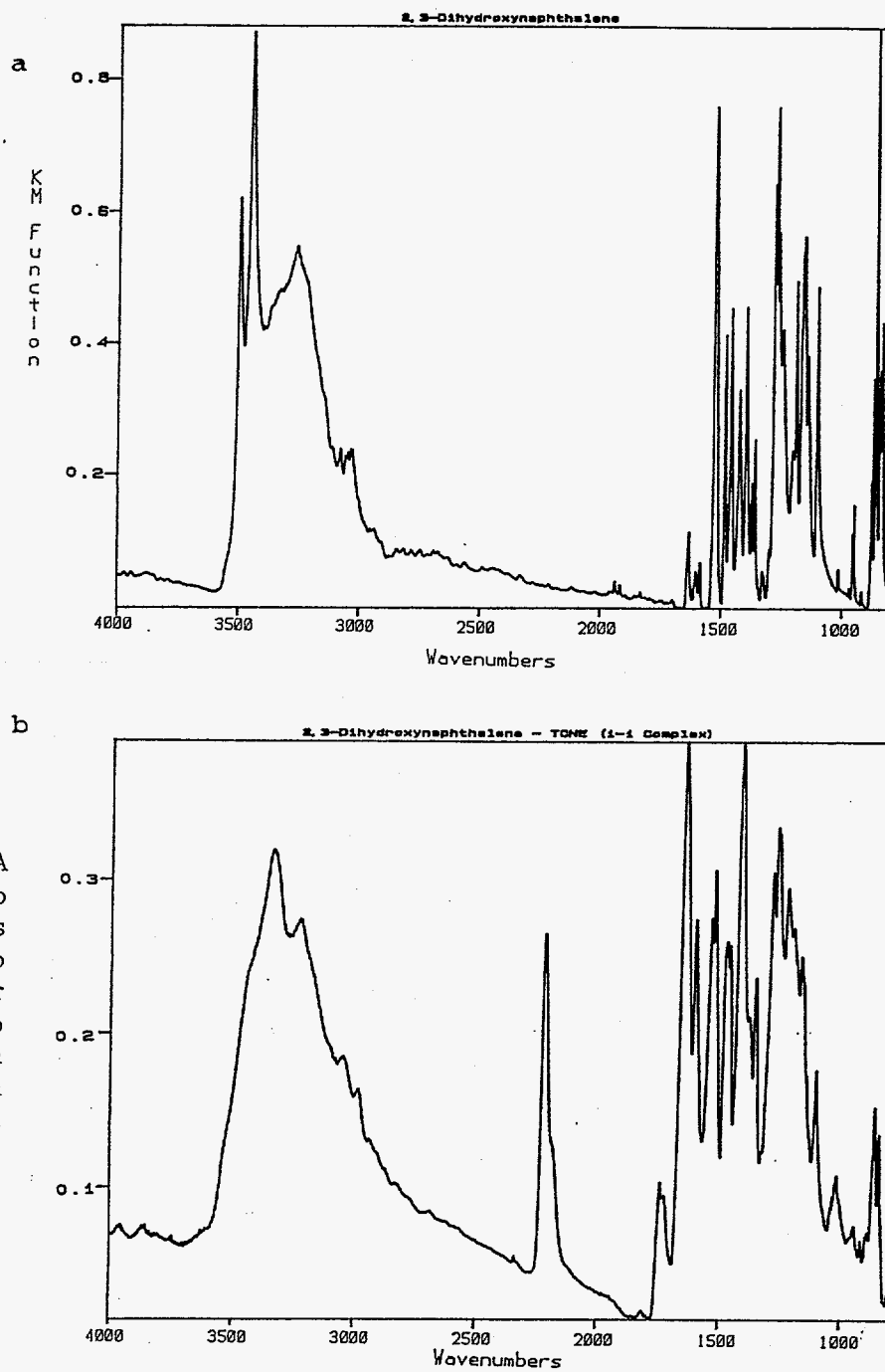


Figure 48. (a) DRIFT Spectrum of 2,3-Dihydroxynaphthalene. (b) DRIFT Spectrum of the 1-1 Complex of 2,3-Dihydroxynaphthalene and TCNE.

to form these complexes is due primarily to dipolar and van der Waals interactions, not stabilization caused by charge transfer. These data show that it is unlikely that the change in the $C\equiv N$ stretching frequency in coals is due to the formation of ground state charge transfer dimers between coal PNA's and TCNQ or TCNE.

D. Electron Paramagnetic Resonance (EPR) Spectra of Coals Containing TCNQ.

The DRIFT spectra of the whole coals with TCNQ display a $C\equiv N$ stretch that suggests the TCNQ radical was formed. If this is true, the coals containing TCNQ should display a greatly enhanced spin density.

Complete electron transfer from donor to acceptor in solution or the solid state implies the formation of radical cations and radical anions. Radical ion formation should be detectable employing EPR spectroscopy. If there is no exchange between radical ion pairs, the individual components would exist as a doublet. Therefore, the paramagnetic EPR signal intensity (I) for this complex would obey the Curie Law.¹²¹

$$I \propto 1/T$$

If there is exchange between pairs to produce a singlet ground state and a triplet excited state separated by the exchange energy J, then the intensity would follow:¹²¹

$$I \propto 1/T[\exp(J/kT) + 3]$$

At low temperatures the intensity would be small and would increase with temperature as the paramagnetic triplet

state becomes thermally populated. The intensity would reach a maximum at a temperature of approximately J/k . Above this temperature the intensity should obey Curie Law. A triplet ground state with an excited singlet state would display the greatest signal intensity at low temperatures and decrease with increasing temperature. The intensity then follows:¹²¹

$$I \propto 1/T[\exp(-J/kT) + 3]$$

The formation of solid, sometimes crystalline complexes by reaction of appropriate acceptors and donors is a common phenomenon. EPR examinations of such complexes was initially carried out by Bijl, et al. employing complexes derived from substituted quinones and p-phenylenediamines.¹²² In all the cases studied, the complexes follow Curie Law dependence, indicating that the ion radicals existed in a doublet electronic ground state. Singer et al. observed singlet-triplet behavior in the solid 1-1 perylene-Iodine complex.¹²³ Chestnut et al. studied the EPR behavior of the solid state 1-1 chloranil-diaminodurene complex. They found that the EPR behavior was best described by a singlet-triplet model, with the solid containing a small amount of doublet state

impurities.¹²⁴ Therefore the apparent Curie law behavior discovered by Bijl was ascribed to the presence of doublet state impurities.

Generally, only a small percentage of donor-acceptor molecules exist as paramagnetic species. Table XIV displays the spin concentrations for a few donors complexed with TCNQ. Table XIV demonstrates that there exists approximately 10^{20} unpaired spins per mole of donor acceptor pairs. Unfortunately, infrared spectra are not available for these complexes. It would be interesting to see if the $C\equiv N$ stretch of TCNQ displays complete electron transfer or if there is any neutral TCNQ in the infrared spectrum.

The interaction of TCNQ with coal is complicated by the fact that the numbers and types of aromatic donors can only be estimated by NMR experiments or various published coal structures. However, EPR will give insight into the nature of the interactions. Interactions between TCNQ and PNA's in coal that are dominated by van der Waals forces will not cause any changes in the coal EPR signal. Interactions dominated by electron transfer may cause an enhanced EPR signal.

Table XV displays the radical densities of Beulah-Zap lignite, Illinois #6 and Lewiston-Stockton coals with

Table XIV

Electron Spin Concentrations of Solid TCNQ Complexes.

<u>Acceptor</u>	<u>Donor</u>	<u>unpaired spins per mole</u>
TCNQ	p-Phenylenediamine	4×10^{20}
TCNQ	N,N'-Dimethyl-p-phenylenediamine	4×10^{21}
TCNQ	1,5-Diaminonphthalene	2×10^{19}

*Melby, R.L. in "The Chemistry of the Cyano Group" Z. Rappaport ed., Interscience, London, 1970, p.639.

various loadings of TCNQ. Also displayed in this table are the calculated radical densities which would be observed if all of the TCNQ deposited into each sample was converted to the radical anion. All of the EPR data were obtained by Dr. Bernard Silbernagel and Layce Gebhard. The TCNQ percentages in the table are based on the concentration of PNA's in the coal calculated from a ^{13}C CP/MAS study performed by Pugmire et al.⁷⁵ The radical densities in all cases are lower than would be expected if all of the TCNQ were converted to the radical anion. The data obtained with high loadings of TCNQ (100%) are particularly enlightening because the spin densities are a factor of 100 lower than the calculated values. These data indicate that the TCNQ radical anion is a minor component of the coal TCNQ system and are consistent with the model compound work which demonstrates that individual PNA's in coal cannot transfer an electron to TCNQ.

Figure 49 displays the EPR spectrum of Beulah Zap lignite. The spectrum is a typical coal spectrum. The EPR signal is broad and featureless with no fine structure. Figures 50 through 52 display the EPR spectra for Beulah Zap lignite with 3%, 20% and 100% loadings of TCNQ (based on PNA's) respectively. The EPR spectrum of the coal containing a 3% loading of TCNQ (Figure 50) displays a narrow line superimposed on the broad coal

Table XV

EPR Spin Densities (Measured and Calculated) of
Coals containing TCNQ

<u>Coal or Coal Derivative</u>	<u>Spin Density x 10⁻¹⁹ spins/gram</u>	<u>Calculated Spin Density for Complete Transfer</u>
Beulah-Zap Lignite	0.12	-
Beulah-Zap Lignite w/3% TCNQ	0.74	5.90
Beulah-Zap Lignite w/20% TCNQ	1.91	29.4
Beulah-Zap Lignite w/100% TCNQ	1.18	120
Illinois #6	0.34	-
Illinois #6 w/3% TCNQ		
Illinois #6 w/ 100% TCNQ	2.70	115
Lewiston-Stockton	0.91	-
Lewiston-Stockton w/3% TCNQ	0.80	5.90
Lewiston-Stockton w/100% TCNQ	7.03	130

* Spin Density EPR Measurements Were Obtained By Dr. Bernard Silbernagel and Layce Gebhard, Exxon Research & Engineering Company.

signal. The EPR spectrum of Beulah-Zap containing a 20% loading of TCNQ displays a narrow signal. Figure 52 shows the EPR spectrum of Beulah-Zap with a 100% loading of TCNQ. This spectrum is different than the other two in that it displays two narrow lines. The narrow lines in all of the EPR spectra are due to TCNQ species. The doublet displayed in Figure 52 is probably due to a TCNQ triplet species.

A triplet state contains two electrons with parallel spins. Biradicals also have this spin arrangement. In the triplet state interaction between electrons is strong and the EPR absorption is split to give two lines. Conversely, the interaction seen in biradical species are weak and behave independently as if the electrons are isolated on two different parts of the molecule.

Many ion-radical salts of TCNQ have been studied.^{125,126,127,128} Most of these salts display electron spin resonance spectra characteristic of a mobile, thermally excited triplet state which is thought to arise from an excited state of two or more electronically coupled TCNQ molecules.

Figures 53 and 54 display the EPR spectra of Lewiston-Stockton coal with 3% and 100% loadings of TCNQ respectively. Similarly to the EPR spectra of of the Beulah-Zap sample, the 3% loading of TCNQ on Lewiston-

Stockton shows a sharp signal superimposed on a broad signal. The 100% loading of TCNQ on Lewiston-Stockton again displays two narrow lines.

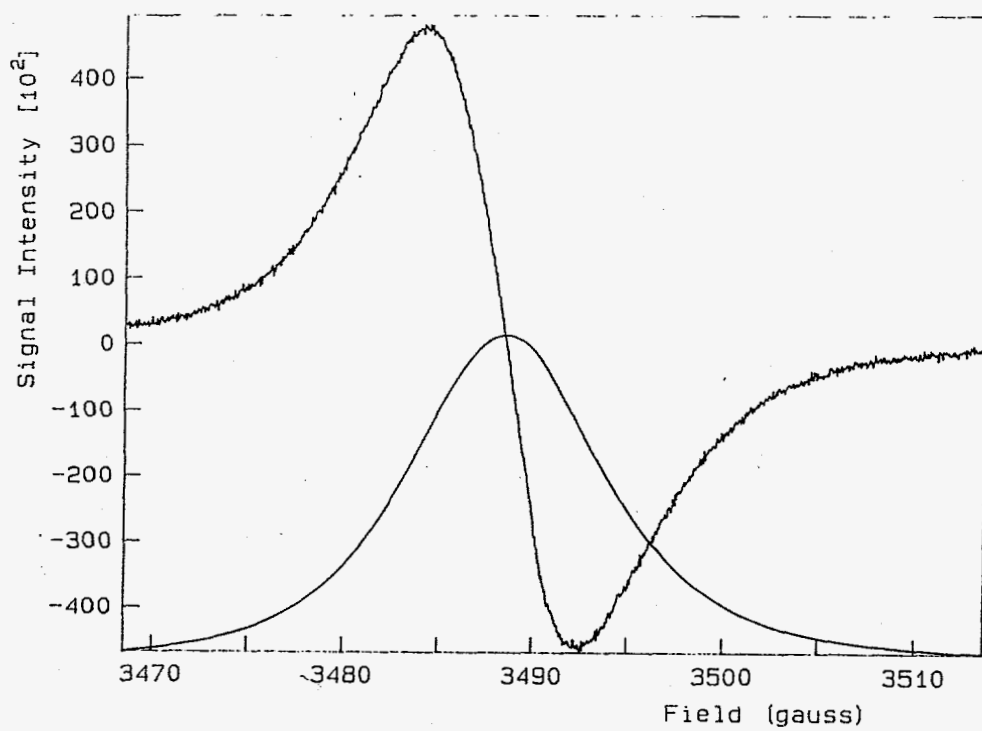


Figure 49. EPR Spectrum of Beulah-Zap Lignite.

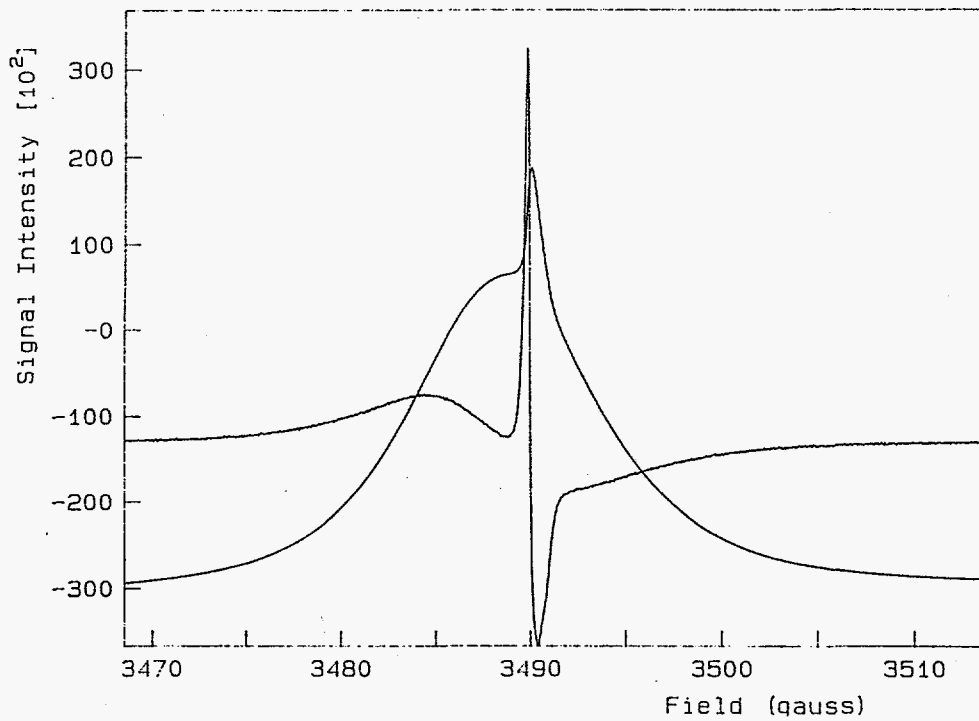


Figure 50. EPR Spectrum of Beulah-Zap Lignite Containing a 3% Loading of TCNQ. (based on PNA's)

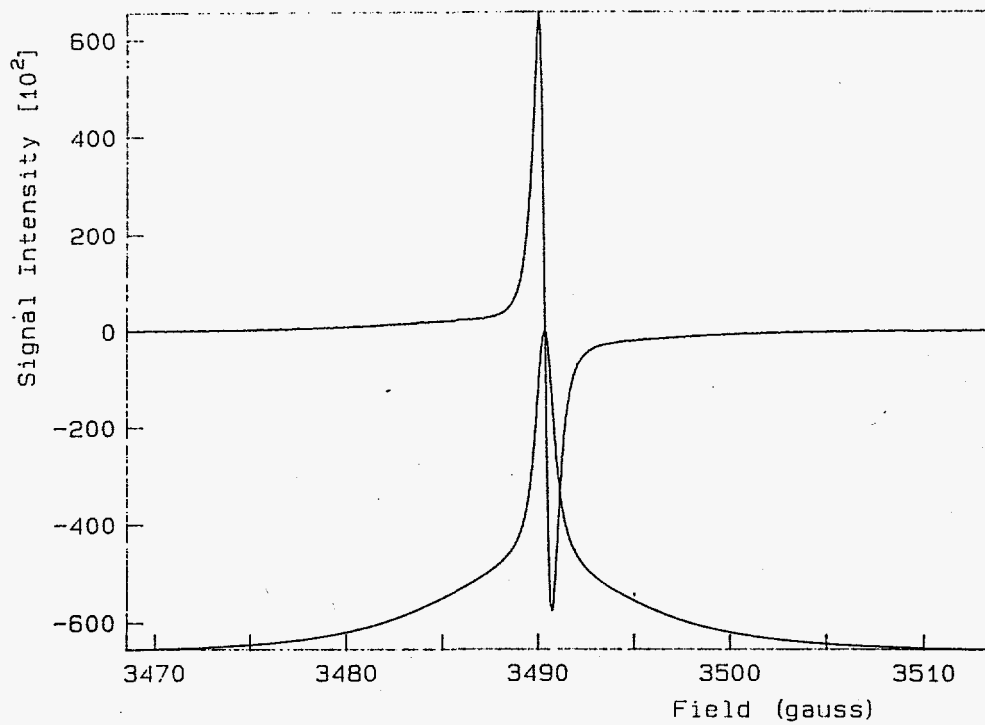


Figure 51. EPR Spectrum of Beulah-Zap Lignite Containing a 20% Loading of TCNQ. (based on PNA's)

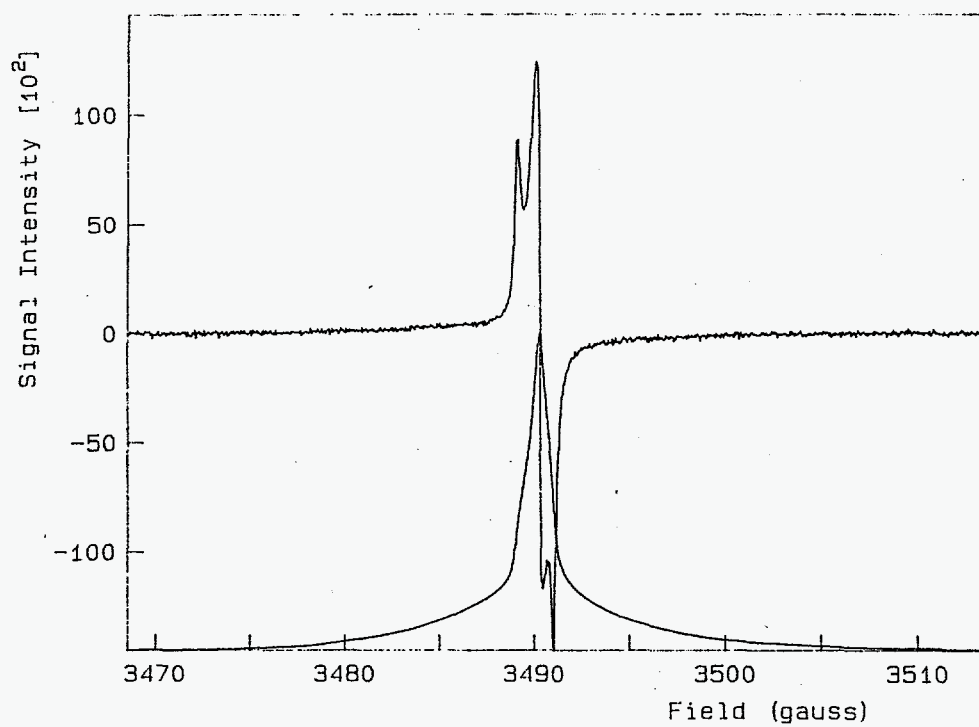


Figure 52. EPR Spectrum of Beulah-Zap Lignite Containing a 100% Loading of TCNQ. (based on PNA's)

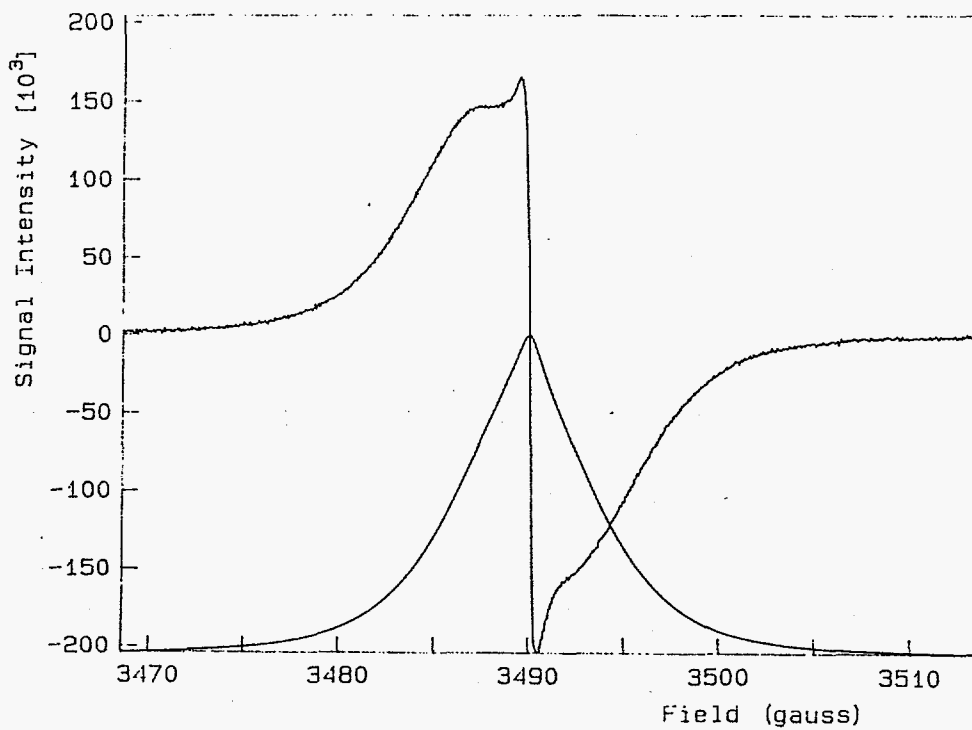


Figure 53. EPR Spectrum of Lewiston-Stockton Coal Containing a 3% Loading of TCNQ. (based on PNA's)

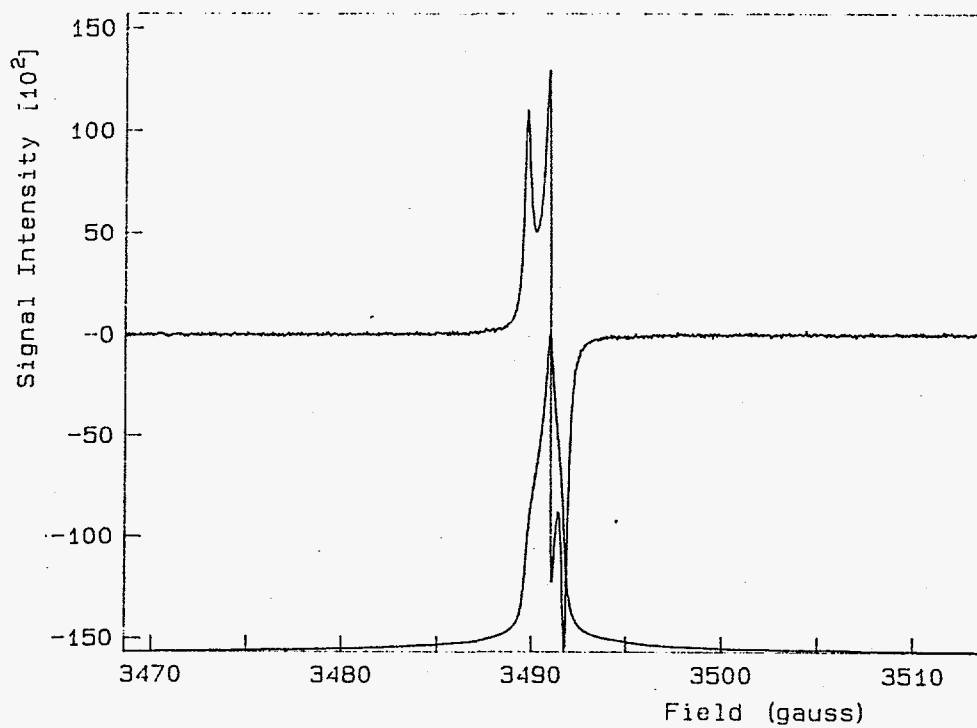


Figure 54. EPR Spectrum of Lewiston-Stockton Coal Containing a 100% Loading of TCNQ. (based on PNA's)

Chapter VIII

Summary and Conclusions

The purpose of the work performed in this thesis was to probe the single electron donor properties of coal. One aspect of this chemistry was the ability of coals to initiate reactions using its naturally occurring coal radicals. Another, perhaps more important, aspect of this chemistry is the ability of coals to donate an electron in a charge-transfer interaction, producing a radical cation in the donor and a radical anion in the acceptor. A summary of the results of this work is now presented:

1. The solid residues from a pyridine Soxhlet extraction of Pocahontas #3, Upper Freeport, Pittsburgh #8, Illinois #6 and Wyodak coals were exposed to 4-vinylpyridine vapors and swelled. All of the 4-vinylpyridine could not be removed under vacuum at 100 °C. Diffuse reflectance FTIR demonstrates the presence of poly-(4-vinylpyridine) in the Illinois #6 and Wyodak coals. EPR spectra display the loss of inertinite radicals in Upper Freeport, Illinois #6 and Wyodak residues after exposure to 4-vinylpyridine. There is little change in the vitrinite radical density or environment. Vitrinite radicals are unreactive and the inertinite radicals appear to be reactive. While the coincidence of inertinite

radical disappearance and polymerization does not demonstrate the radicals caused polymerization, it is a reasonable supposition.

2. The molecule N,N'-Diphenyl-p-phenylene diamine (DPPD) reacts with carbon radicals to give hydrocarbons and an imine product. The solid residues from a pyridine Soxhlet extraction of Pocahontas #3, Upper Freeport, Pittsburgh #8, Illinois #6 and Wyodak coals were exposed to DPPD dissolved in chlorobenzene. Diffuse reflectance FTIR failed to demonstrate the presence of the imine product from radical reaction with DPPD. EPR spectra display the loss of inertinite radicals in Upper Freeport and Wyodak residues. This part of the project was unsuccessful.

3. 7,7,8,8-Tetracyanoquinodimethane (TCNQ) and Tetracyanoethylene (TCNE) were deposited into coals in pyridine. FTIR indicates complete conversion of TCNQ to a material with a singly occupied LUMO. In TCNE the LUMO is about 30% occupied. TCNQ and TCNE were deposited into the pyridine extracts and residues of Illinois #6 and Pittsburgh #8 coals. Only a small amount of the TCNQ and TCNE displayed $C\equiv N$ shifts in the IR spectrum of a material with an occupied LUMO. Studies on model PNA's showed that individual molecules will not form the TCNQ radical anion. EPR radical population studies on coals

containing TCNQ was inconsistent with a high population of the TCNQ radical anion.

It has been concluded that TCNQ must be part of the aromatic stacks in coal and the TCNQ LUMO is part of an extended band. Furthermore, this behavior is a bulk property of the coal dependent on its solid structure which cannot be modelled using individual molecules.

List of References

1. Grimes, W.R. in "Coal Science, vol. 1" (eds. Gorbaty, M.L.; Larsen, J.W.; Wender, I.) Academic Press, New York, 1983, p. 21.
2. Van Krevelen, D.W. in "Coal: Typology-Chemistry-Physics-Constitution." Elsevier, Amsterdam, 1981.
3. Winans, R.E.; Crelling, J.C. Eds. in "Chemistry and Characterization of Coal Macerals" ACS Symposium Series 252; American Chemical Society: Washington, DC, 1984, p 3.
4. Blom, L. in "Analytical Methods in Coal Chemistry" Luijik, Eindhoven, 1960, 1.
5. Messenger, L.; Attar, A. Fuel, 1979, 58, 655.
6. Whitehurst, D.D. in "Organic Chemistry of Coal" (ed. Larsen J.W.) ACS Symposium Series 71; American Chemical Society: Washington, DC, 1978, p 1.
7. Meyers, R.A. "Coal Desulfurization" p. 3,4,18, Dekker, New York, 1977.
8. Attar, A; Dupuis, F. Am. Chem. Soc. Div. Fuel Chem, Prepr. 23, (2) 44, 1978.
9. Attar, A; Dupuis, F., Am. Chem. Soc. Fuel Div., Prepr., 24(1), 166, 1979.
10. van Krevelen, D.W. Fuel, 1966, 45, 229.
11. Green, T.; Kovac, J.; Brenner, D.; Larsen, J.W. in Coal Structure (ed Meyers A.) Academic Press, New York, 1982.
12. Larsen, J.W. Am. Chem. Soc. Div. Fuel Chem., Prepr. 1985, 30(4), 444.
13. Brenner, D. Fuel, 1985, 64, 167.
14. Shinn, J.H. Fuel, 1984, 63, 1187.
15. Retcofsky, H.L. In reference 1, p 50.
16. Austen, D.E.G.; Ingram, D.J.E.; Tapley, J.G. Trans. Faraday Soc., 1958, 54, 400.

17. Smidt, J.; van Krevelen, D.W. Fuel, 1959, 38, 355.
18. Toyoda, S.; Honda, H. Carbon, 1966, 3, 527.
19. Petrakis, L.; Grandy, D.W. Anal. Chem., 1978, 50(2), 303.
20. Elliot, M.A.; Yohe, G.R. in "Chemistry of Coal Utilization," 2nd Suppl. Vol., Elliot M.A. ed., John Wiley and Sons, New York, 1981, 4.
21. Wisr, W.H., Am. Chem. Soc., Div. Fuel Chem., Prepr., 1975, 20(2), 122.
22. Foster, R. in "Organic Charge-Transfer Complexes" (ed. Blomquist, A.T.) Organic Chemistry; Monograph Series 15; Academic Press, New York, 1969, p 1.
23. Howell, J.O.; Goncalves, J.M.; Amatore, C.; Klasinc, L.; Wightman, R.M.; Kochi, J.K. J. Am. Chem. Soc., 1984, 106, 3968.
24. Sankararaman, S.; Haney, W.A.; Kochi, J.K. J. Am. Chem. Soc., 1987, 109, 7824.
25. Uebersfeld, J.; Ettienne, A.; Combrisson, J. Nature (London) 1954, 174, 614.
26. Ingram, J.D.F.; Tapley, J.G.; Jackson, R.; Bond, R.I.; Murnaghan, A.R. Nature (London) 1954, 174, 797.)
27. Grandy, D.W.; Petrakis, L. Fuel, 1979, 58, 239.
28. Silbernagel, B.G.; Gebhard, L.A.; Dyrkacz, G.R. J. Am. Chem. Soc., Fuel Division Prepr., 28, 118, 1983.
29. Kevan, L.; Kispert, L.D. "Electron Spin Double Resonance Spectroscopy"; Wiley: New York, 1976, p 2.
30. Retcofsky, H.L.; Hough, M.R.; Maguire, M.M.; Clarkson, R.B. In Coal Structure; Gorbaty, M.L.; Ouchi, K., Eds; Advances in Chemistry Series 192; American Chemical Society: Washington D.C., 1981; pp 37-58.
31. Retcofsky, H.L.; Thompson, G.P.; Hough, M.R.; Friedel, R.A. in "Organic Chemistry of Coal," ACS Symp. Ser. 1978, 71, 142.

32. Schlick, S.; Narayana, P.A.; Kevan, L. J. Am. Chem. Soc., 1978, 100, 3322.
33. Elofson, R.M.; Schulz, K.F. Am. Chem. Soc. Fuel Division Prepr., 11, 513.
34. Schwager, I.; Yen, T.F. Am Chem. Soc. Fuel Division Prepr., 21, 199.
35. a) Yen, T.F. Fuel, 1973, 52, 93. b) Yen, T.F.; Young, D.K. Carbon, 1973, 11, 33.
31. Retcofsky, H.L.; Thompson, G.P.; Hough, M.; Friedel, R.A. In "Organic Chemistry of Coal" ACS Symp. Ser. 1978, 71, 142.)
36. Castellano, S.M.; Chisolm, W.P.; Sprecher, R.F.; Retcofsky, H.L. Anal. Chem., 1987, 59, 1726.
37. Ballester, M. Pure Appl. Chem., 1967, 15, 123.
38. Flowers, R.A.; Gebhard, L.A.; Larsen, J.W.; Silbernagel, B.G. unpublished results
39. Wertz, J.E.; Bolton, J.R. In "Electron Spin Resonance: Elemental Theory and Practical Applications", McGraw-Hill, New York, 1972, Ch. 7
40. Retcofsky, H.L.; Thompson, G.P.; Raymond, R., Friedel, R.A. Fuel, 1975, 54, 126.
41. Tschlamer, H.; De Ruiter, E. "Chemistry of Coal Utilization" Lowry, H. H. Ed.; Wiley: New York, 1963; Suppl. Vol., p. 78.
42. Petrakis, L; Grandy, D.W. Anal. Chem., 1978, 50, 303.
43. Silbernagel, B.G.; Gebhard, L.A.; Dyrkacz, G.R.; Bloomquist, C.A.A. In "Chemistry and Characterization of Coal Macerals," ACS Symp. Ser. 1984, 252, 121.
44. Segal, B.G.; Kaplan, M.; Fraenkel, G.K. J. Chem. Phys., 1965, 43, 4191.
45. Yen, T.F.; Sprang, S.R. Geochim. CosmoChim. Acta 1977, 41, 1007.
46. Keulen, D.J. Fuel, 1952, 31, 462.

47. Dyrkacz, G.R.; Horowitz, E.P. Fuel, 1982, 61, 3.
48. Silbernagel, B.G.; Gebhard, L.A.; Dyrkacz, G.R. In "Magnetic Resonance. Introduction, Advanced Topics and Applications to Fossil Energy; Petrakis, L. Fraissard, J.P. Eds.; Dordrecht, Netherlands, 1984
49. Schopf, J.M. Econ. Geol., 1948, 43, 207.
50. Terres, E.; Dahne, H.; Nandi, B.; Scheidel, C.; Trappe, K. Brennst.-Chem., 1956, 37, 269.
51. Petrakis, L.; Grandy, D.W. in "Free Radicals in Coal and Synthetic Fuels," 1983, Elsevier, Amsterdam p. 55.
52. Petrakis, L.; Grandy, D.W. Fuel, 1981, 60, 120.
53. Muntean, J.V.; Stock, L.M.; Botto, R.E. Energy and Fuels, 1988, 2, 108.
54. Silbernagel, B.G.; Gebhard, L.A.; Larsen, J.W.; Flowers, R.A. Accepted for publication in Energy & Fuels.
55. Fitzgerald, E.B.; Fuoss, R.M. Ind. Eng. Chem., 1950, 42(8), 1603.
56. Otake, Y.; Suuberg, E.M. Fuel, 1989, 68, 1609.
57. Kraus, G.; Collins, R.L. Rubber World, 1958, 139, 219.
58. Collins, R.L.; Bell, M.D.; Kraus, G. J. Appl. Phys., 1959, 30, 56.
59. Beitenbach, J.W.; Preussler, H. J. Polym. Sci., 1949, 4, 751.
60. Maron, S.H.; von Fischer, W.; Ellslager, W.M.; Savardi, G. J. Polym. Sci., 1956, 19, 29.
61. Symons, M.C.R. J. Chem. Soc., 1955, 4344.
62. Donnet, J. B.; Henrich, G. Compt. Rend., 1958, 266, 3230.
63. Hively, R.A.; Cole, J.O.; Parks, C.R.; Field, J.E., Fink, R. Anal. Chem., 1955, 27(1), 100.

64. Rotschova, J.; Taimr, L.; Pospisil, J. J. Chromatogr., 1981, 216, 151.
65. Taimr, L.; Pospisil, J. Angew. Makromol. Chem., 1980, 92, 53.
66. Bewick, A.; Serve, D.; Joslin, T.A. J. Electroanal. Chem., 1983, 154, 81.
67. Fuller, M.P.; Griffiths, P.R. Anal. Chem. 1978, 50, 1906.
68. Green, T.K. Dissertation, "The Macromolecular Structure of Coal." University of Tennessee, 1984.
69. Collins, C.J.; Hagaman, E.W.; Jones, R.M.; Raaen, V.F. Fuel, 1981, 60(4), 359-60.
70. Fuller, M.P.; Griffiths, P.R. Appl. Spectrosc., 1980, 34, 533.
71. Te Vrucht, M.L.E.; Griffiths, P.R. Appl. Spec., 1989, 43, 1492.
72. Kubelka, P.; Munk, F. Z. Tech. Phys., 1931, 12, 593.
73. Kubelka, P. J. Opt. Soc. Am., 1948, 38, 448.
74. Mulliken, R.S.; Person, W.B. in "Molecular Complexes" John Wiley & Sons, New York N.Y. 1969.
75. Solum, M.S.; Pugmire, R.J.; Grant, D.M. Energy & Fuels, 3, 187.
76. Soos, Z.G.; Klein, D.J. Charge Transfer in Solid State Complexes in "Molecular Association", Vol. 1 Ed. by R. Foster, Academic Press, New York, NY 1-109, 1981.
77. Dewar, M.J.S.; Lepley, A.R. J. Am. Chem. Soc., 1961, 83, 4560.
78. Whangbo, M.H. in J.S. Miller: Extended Linear Chain Compounds. Plenum, New York, 1982 p.127.
79. Briegleb, G.; Czekalla, J. Angew. Chem., 1960, 72, 401.
80. Shuler, K.E. J. Chem. Phys., 1952, 20, 1865.

81. Boeyens, J.C.A. J. Phys. Chem., 1967, 71, 2969.
82. Hubbard, J. Proc. Roy. Soc., Ser. A, 1963, 276, 238.
83. ibid. 1964, 277, 237.
84. ibid. 1964, 281, 401.
85. Van Vleck, J.H. In "Quantum Theory of Atoms, Molecules, and the Solid State" (ed. P.O. Lowdin), Academic Press, New York, 1966, p475-84.
86. Kittel, C. in "Introduction to Solid State Physics" 6th ed. Wiley, New York, 1986, p
87. Mott, N.F. Rev. Mod. Phys., 1968, 40, 677.
88. Ferraro, J.R.; Williams, J.M. in Practical Fourier Transform Infrared Spectroscopy, Ferraro, J.R. and Krishnan, K., Ed., Academic Press, San Diego, CA, 1990.
89. Hester, R.E. in Adv. in Infrared and Raman Spec., Vol 4, Eds. R.J.H. Clark and R.E. Hester, Heyden & Son Ltd., 1980, London U.K.
90. Andersen, G.R.; Devlin, J.P. J. Phys. Chem., 1975, 79, 1100.
91. Jeanmaire, D.L.; Van Duyne, R.P. J. Am. Chem. Soc., 1976, 98, 4029, 4043.
92. Suchanski, M.R.; Van Duyne, R.P. J. Am. Chem. Soc., 1976, 98, 250.
93. Girlando, A.; Bozio, R.; Pecile, C. Chem. Phys. Lett., 1974, 25, 409.
94. Bozio, R., Girlando, A.; Pecile, C. J. Chem. Soc. Faraday Trans., 1975, 2, 71, 1237.
95. Chappel, J.S.; Bloch, A.N.; Bryden, W.A.; Maxfield, M.; Poehler, T.O.; Cowan, D.O. J. Am. Chem. Soc., 1981, 103, 2442.
96. Stanley, J.; Smith, D.; Latimer, B.; Devlin, J.P., J. Phys. Chem., 1966, 70, 2011.
97. Jeanmaire, D.L.; Suchanski, M.R.; Van Duyne, R.P., J. Am. Chem. Soc., 1975, 97, 1699.

98. Moore, J.C.; Smith, D.; Youhne, Y.; Devlin, J.P. J. Phys. Chem., 1971, 75, 325.
99. Friedrich, H.B.; Person, W.B. J. Phys. Chem., 1966, 44, 2161.
100. Kamitsos, E.I.; Mattera, V.D.; Robinson, W.T.; Risen, W.M. J. Mol. Struct., 1986, 143, 211.
101. Becker, J.Y.; Bernstein, J.; Bittner, S.; Levi, N.; Shaik, S. J. Am. Chem. Soc., 1983, 105, 4468.
102. a) Tazuke, S.; Nagahara, H. Makromol. Chem., 1980, 181, 2207. b) Tazuke, S.; Nagahara, H.; Matsuyama, Y. Makromol. Chem. 1980, 181, 2199. c) Tazuke, S.; Sato, K.; Banba, F.; Matsuyama, Y. J. Polym. Sci., Polym. Lett. Ed., 1976, 14, 653. d) Ito, H.; Tazuke, S.; Okawara, M. Makromol. Chem., 1976, 177, 621. e) Matsuyama, Y.; Tazuke, S. Makromol. Chem., 1975, 176, 3167. f) Matsuyama, Y.; Tazuke, S. Makromol. Chem., 1975, 176, 1657.
103. Braun, A.M.; Cassidy, H.G.; Schulz, R.C.; Tanaka, H. Makromol. Chem., 1971, 146, 195.
104. Schulz, R.C. Pure Appl. Chem., 1972, 30, 239.
105. Grishna, A.D. Elektrokhimiya, 1973, 9, 961.
106. Grishna, A.D. Elektrokhimiya, 1974, 10, 291.
107. Kainer, H.; Otting, W. Chem. Ber., 1955, 88, 1921.
108. Matsunaga, Y., J. Chem. Phys., 1964, 41, 1609.
109. Matsunaga, Y., Nature, Lond., 1965, 205, 72.
110. Brown, J.K. J. Chem. Soc. (London), 1955, 744.
111. Davis, M.F.; Quinting, G.R.; Bronnimann, C.E.; Maciel, G.E. Fuel, 1989, 68, 763.
112. personal communication, Dr. Peter Hall and Patrick C. Wernett
113. Benesi, H.A.; Hildebrand, J.H. J. Am. Chem. Soc., 1949, 71, 2703.
114. Mulliken, R. S. J. Am. Chem. Soc., 1952, 74, 811.

115. Dewar M.J.S.; Thompson, C.C., Jr., Tetrahedron Suppl., 7, 97, 1966.
116. Bentley, M.D. Dewar, M.J.S. Tetrahedron Lett, 5043, 1967.
117. see reference 76, p. 2.
118. Merrifield, R.E.; Phillips, W.D. J. Am. Chem. Soc., 1958, 80, 2778.
119. Frey, J.E.; Andrews, A.M.; Ankoviac, D.G.; Beaman, D.N.; Du Pont, L.E.; Elsner, T.E., Lang, S.R.; Oosterbaan, Szart, M.A.; Seagle, R.E.; Torreano, L.A. J. Org. Chem., 1990, 55, 606.
120. personal communication, Peter Hall
121. Melby, L.R. in "The Chemistry of the Cyano Group" Z. Rappaport ed., Interscience, London, 1970, p. 639.
122. Bijl, D.; Kainer, H.; Rose-Innes, A.C. J. Chem. Phys., 1959, 30, 765.
123. Singer, L.S.; Kommandeur, J. Bull. Am. Phys. Soc., 1959, 4, 421.
124. Chestnut, D.B.; Phillips, W.D. J. Chem. Phys., 1961, 35, 1002.
125. Brown, I.M.; Jones, M.T. J. Chem. Phys., 1969, 51, 4687.
126. Bailey, J.C.; Chestnut, D.B. J. Chem. Phys., 1969, 51, 5118.
127. Chestnut, D.B.; Foster, H.; Phillips, W.D. J. Chem. Phys., 1961, 34, 684.
128. Jones, M.T.; Chestnut, D.B. J. Chem. Phys., 1963, 38, 1311.